Elsevier Editorial System(tm) for Gondwana Research
Manuscript Draft

Manuscript Number: GR-D-16-00192R3

Title: Insights from recent gravity satellite missions in the density structure of continental margins - with focus on the passive margins of the South Atlantic

Article Type: SI: Rifting to Passive Margins

Keywords: continental margins; satellite gravity missions; spatial resolution; omission error; interpretation gravity effects; interpretation gravity gradients.

Corresponding Author: Dr. Hans-Juergen Goetze, Prof. Dr.

Corresponding Author's Institution:

First Author: Hans-Juergen Goetze, Prof. Dr.

Order of Authors: Hans-Juergen Goetze, Prof. Dr.

Abstract: We focus on new gravity and gravity gradient data sets from modern satellite missions GOCE, GRACE and CHAMP, and their geophysical interpretation at passive continental margins of the South Atlantic. Both sides, South Africa and South America, have been targets of hydrocarbon exploration and academic research of the German Priority Program SAMPLE (South Atlantic Margin Processes and Links with onshore Evolution). The achievable spatial resolution, driven by GOCE, is 70 - 80 km. Therefore, most of the geological structures, which cause a significant gravity effect (by both size and density contrast), can be resolved. However, one of the most important aspects is the evaluation of the omission error, which is not always in the focus of interpreters. It results from high-frequency signals of very rough topographic and bathymetric structures, which cannot be resolved by satellite gravimetry due to the exponential signal attenuation with altitude. The omission error is estimated from the difference of the combined gravity model EIGEN-6C4 and the satellite-only model GOCO05S. It can be significantly reduced by topographic reductions. Simple 2D density models and their related mathematical formulas provide insights in the magnitude of the gravity effect of masses that form a passive continental margin. They are contrasted with results from satellite-only and combined gravity models. Example geophysical interpretations are given for the western and eastern margin of the South Atlantic Ocean, where standard deviations vary from 25 - 16 mGal and 21 - 11 mGal, respectively. It could be demonstrated, that modern satellite gravity data provide significant added value in the geophysical gravity data processing domain and in the validation of heterogeneous terrestrial data bases. Combined models derived from high-resolution terrestrial gravity and homogeneous satellite data will lead to more detailed and better constrained lithospheric density models, and hence will improve our knowledge about structure, evolution and state of stress in the lithosphere.

Response to Reviewers:

*Graphical Abstract

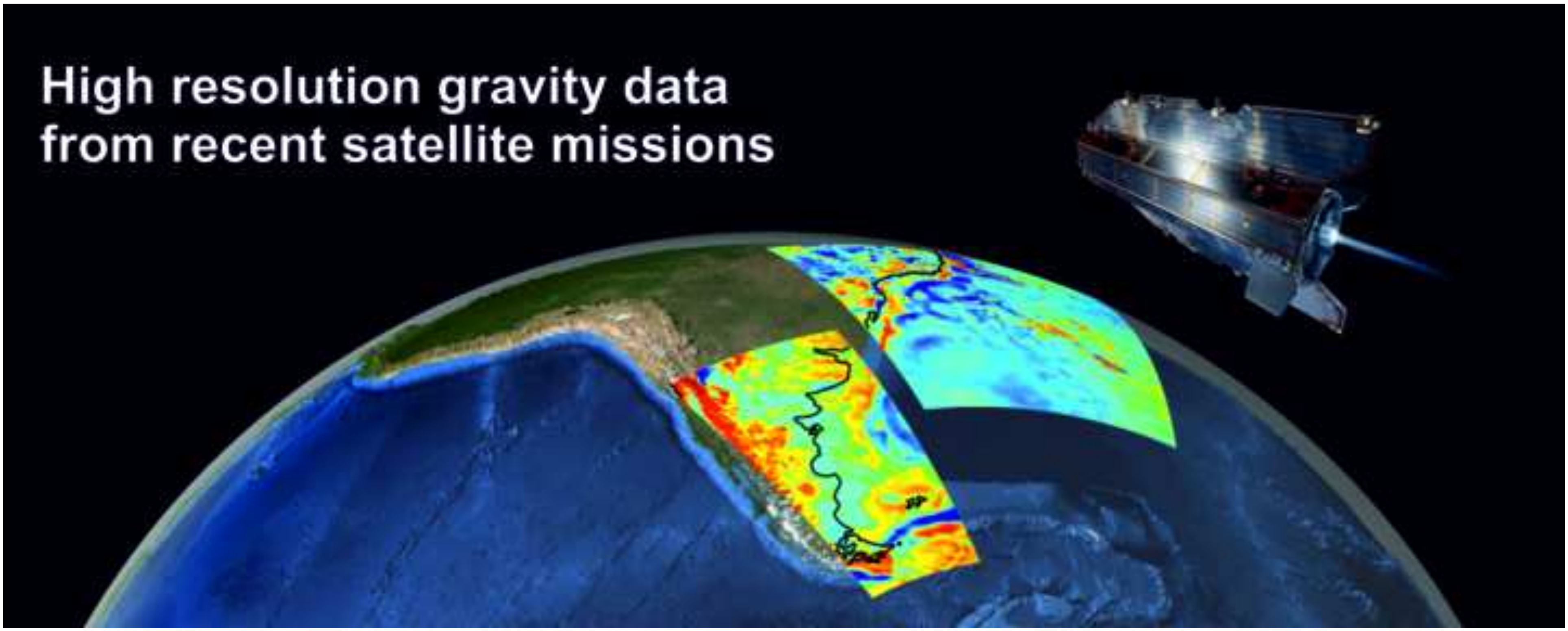

***Highlights (for review)**

- Combine terrestrial and satellite gravity to provide insights into passive margins.
- Satellite gravity and gradients were used to validate terrestrial gravity databases.
- 2nd derivations of satellite gravity can re-examine the continent-ocean boundaries.

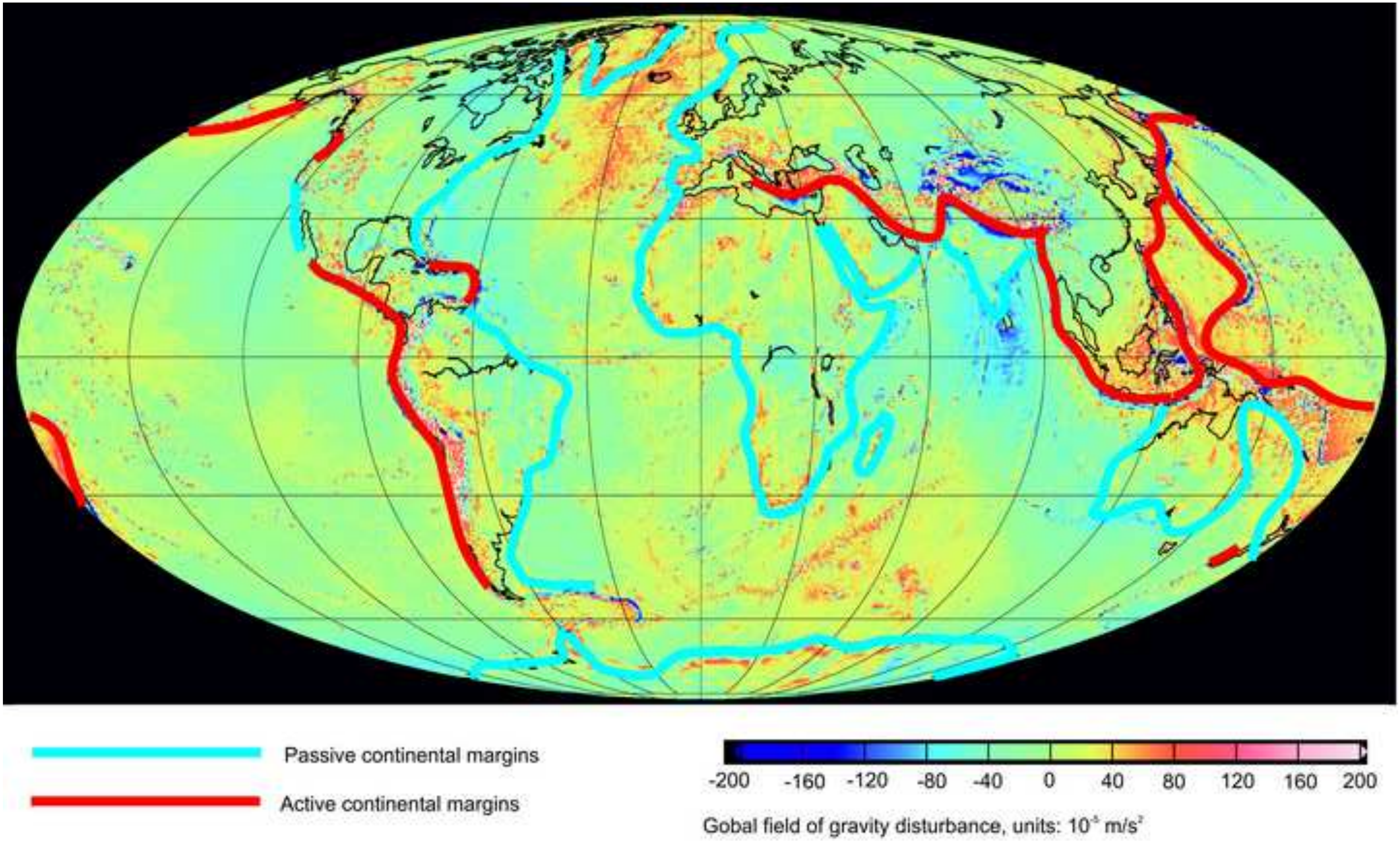
Passive continental margins
Active continental margins
-200
-160
-120
-80
-40
0
40
80
120
160
200
Gobal field of gravity disturbance, units: 10^{-5} m/s^2

Figure
Click here to download high resolution image

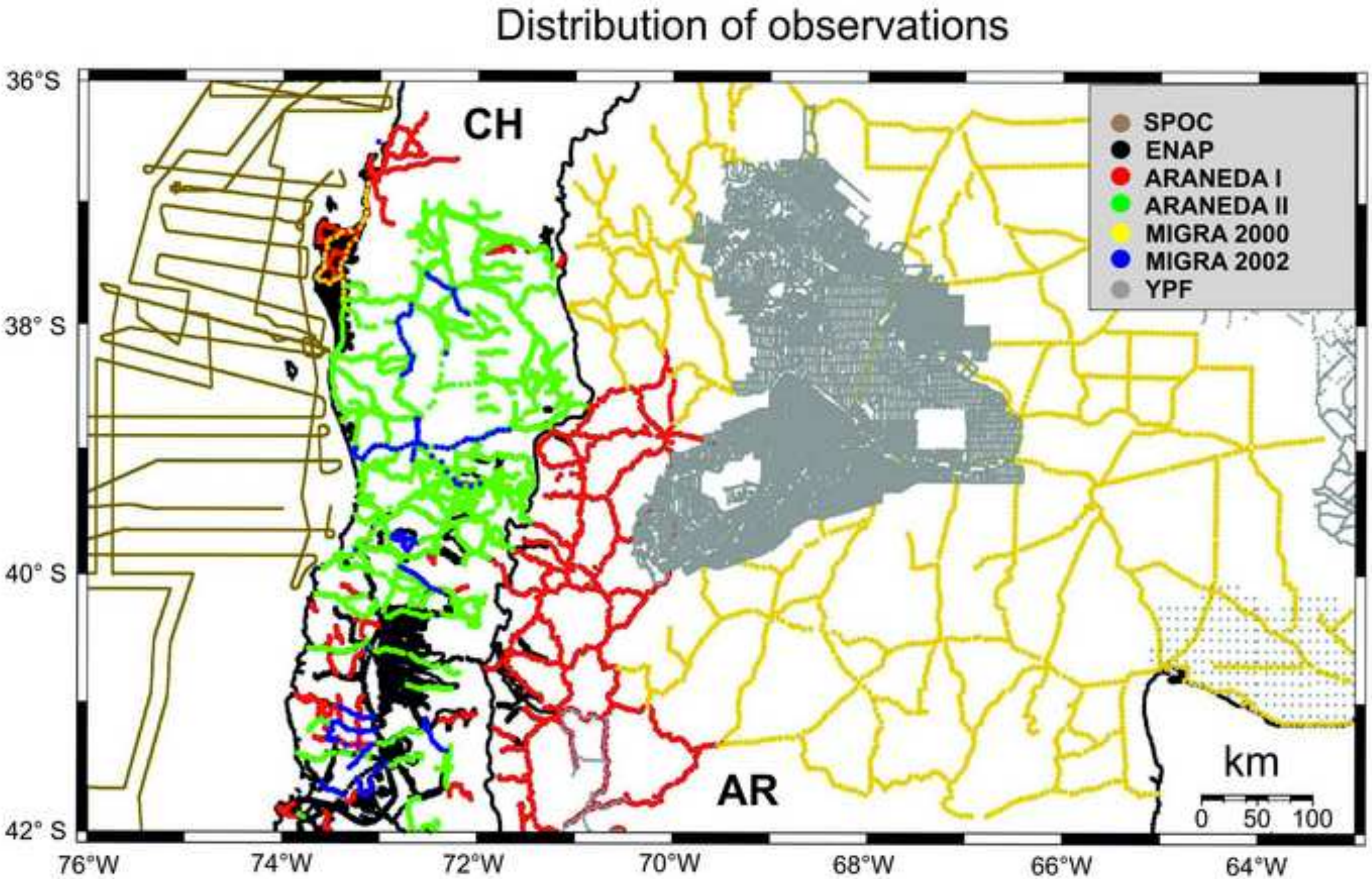

Figure

Click here to download high resolution image

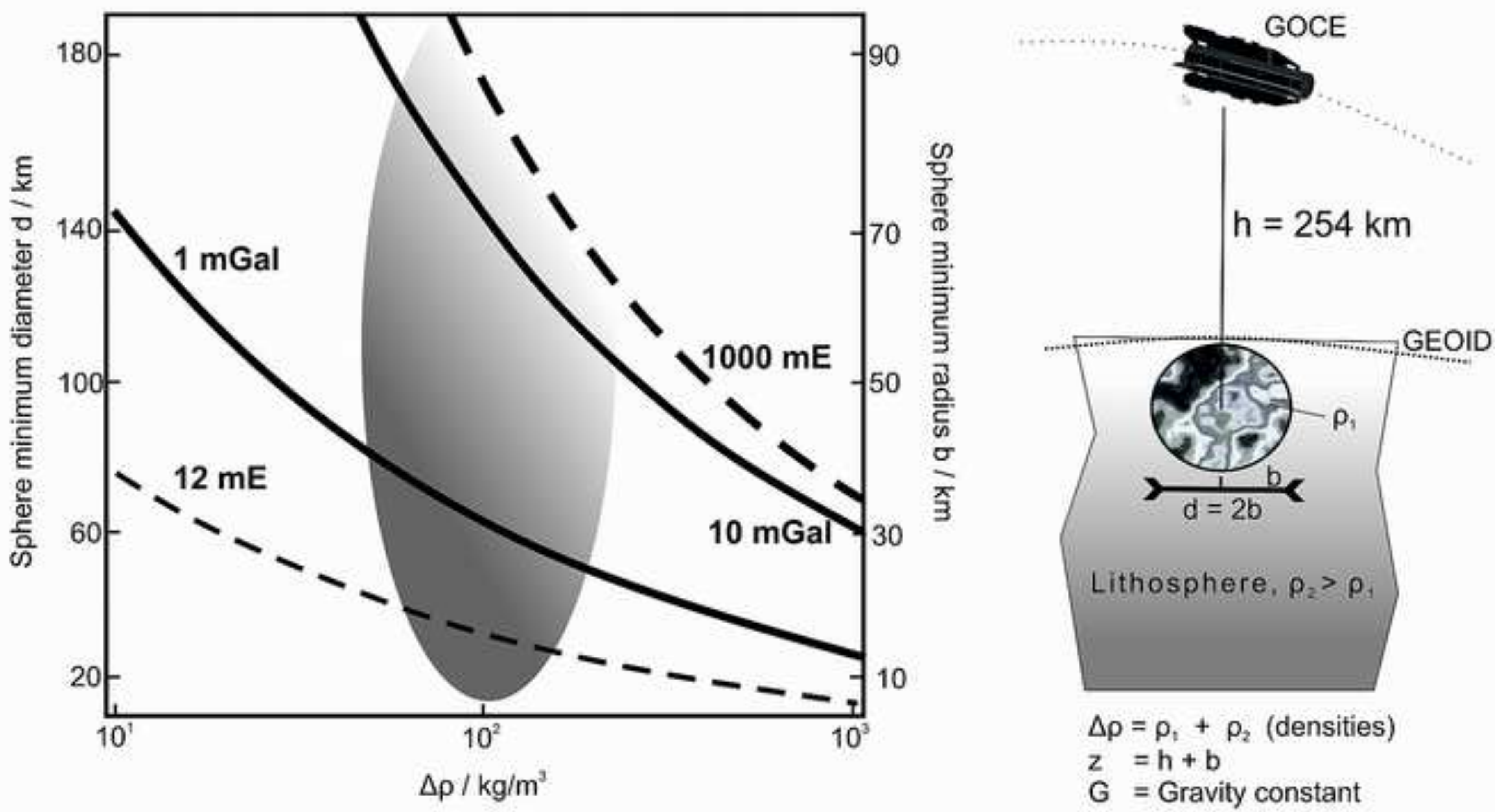

$$\Delta\rho(b) = \frac{3}{4}\cdot\frac{\Delta g_z}{\pi G}\cdot\frac{(h+b)^2}{b^3} \qquad |\Delta\rho(b)| = \frac{3}{8}\cdot\frac{\Delta g_{zz}}{\pi G}\cdot\frac{(h+b)^3}{b^3}$$

Figure
Click here to download high resolution image

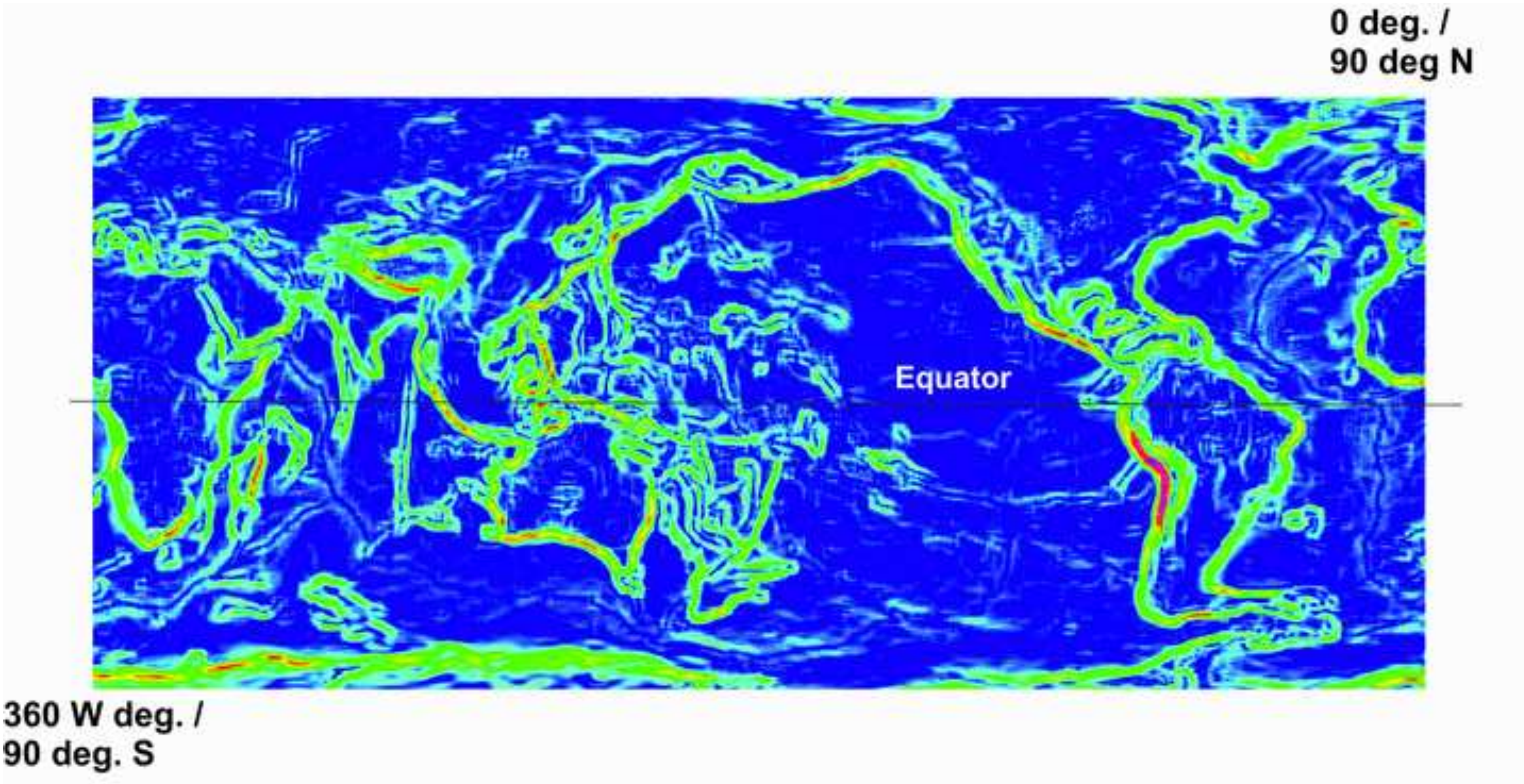

Figure
Click here to download high resolution image

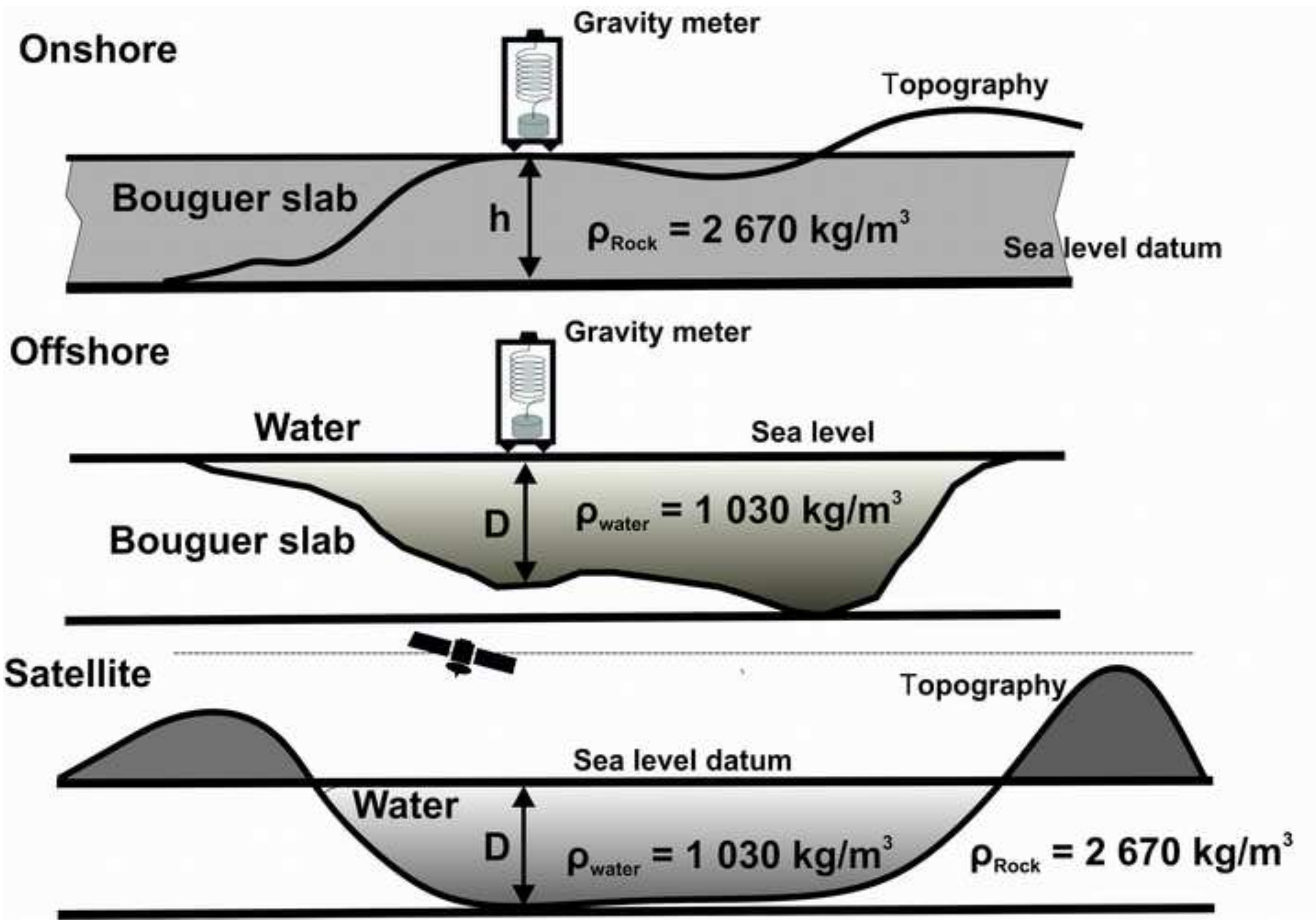

Figure
Click here to download high resolution image

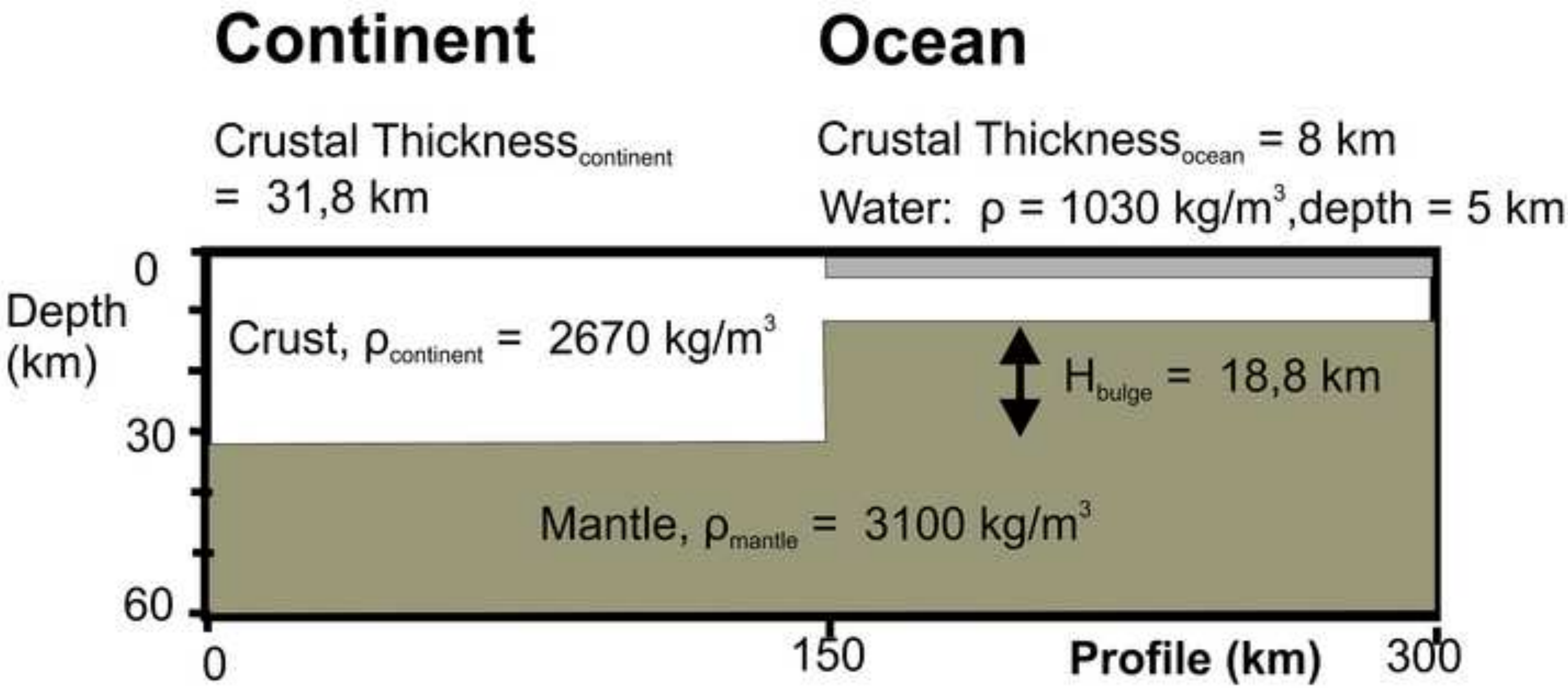

Figure
Click here to download high resolution image

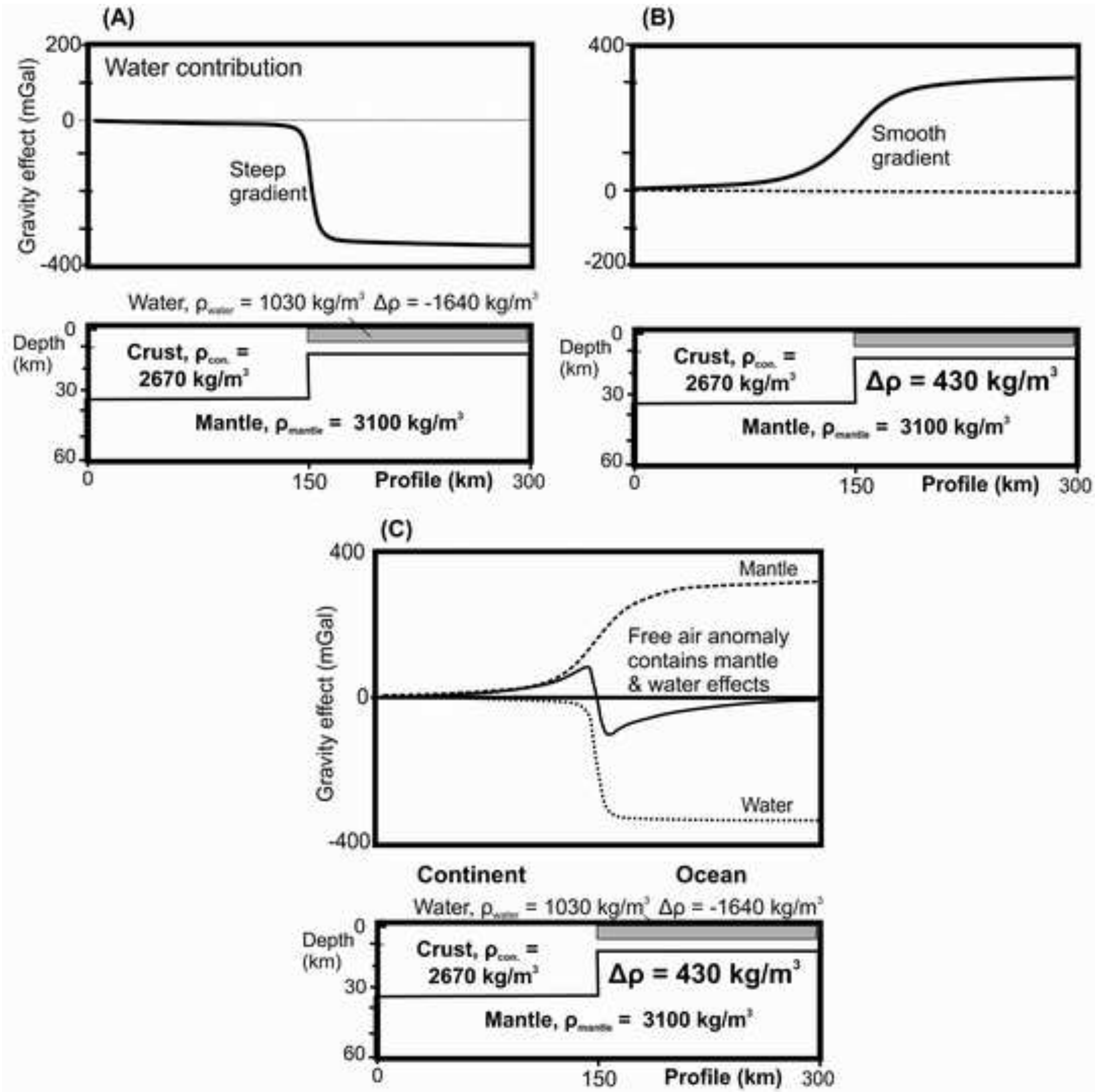

Figure

Click here to download high resolution image

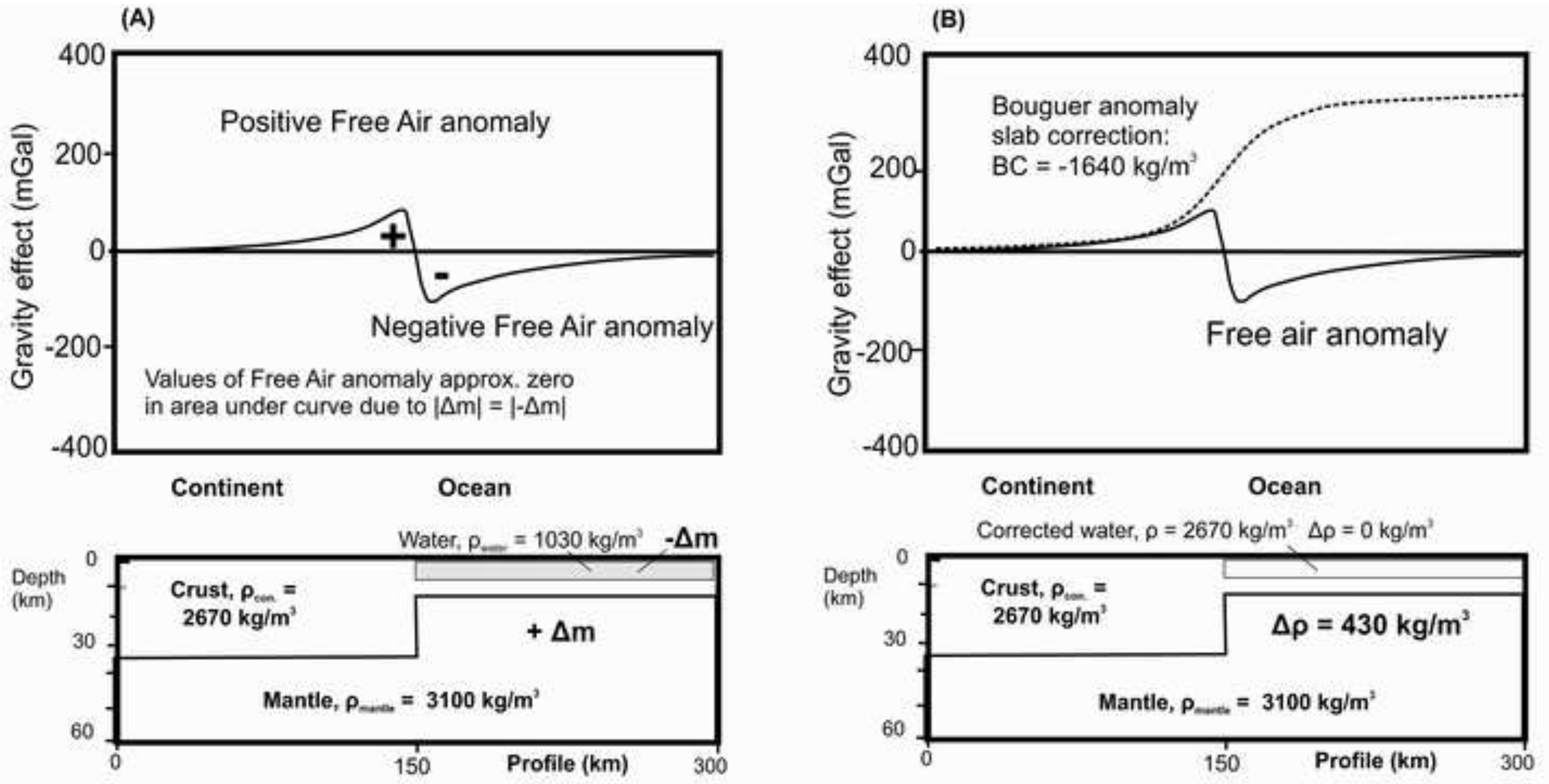

Figure
Click here to download high resolution image

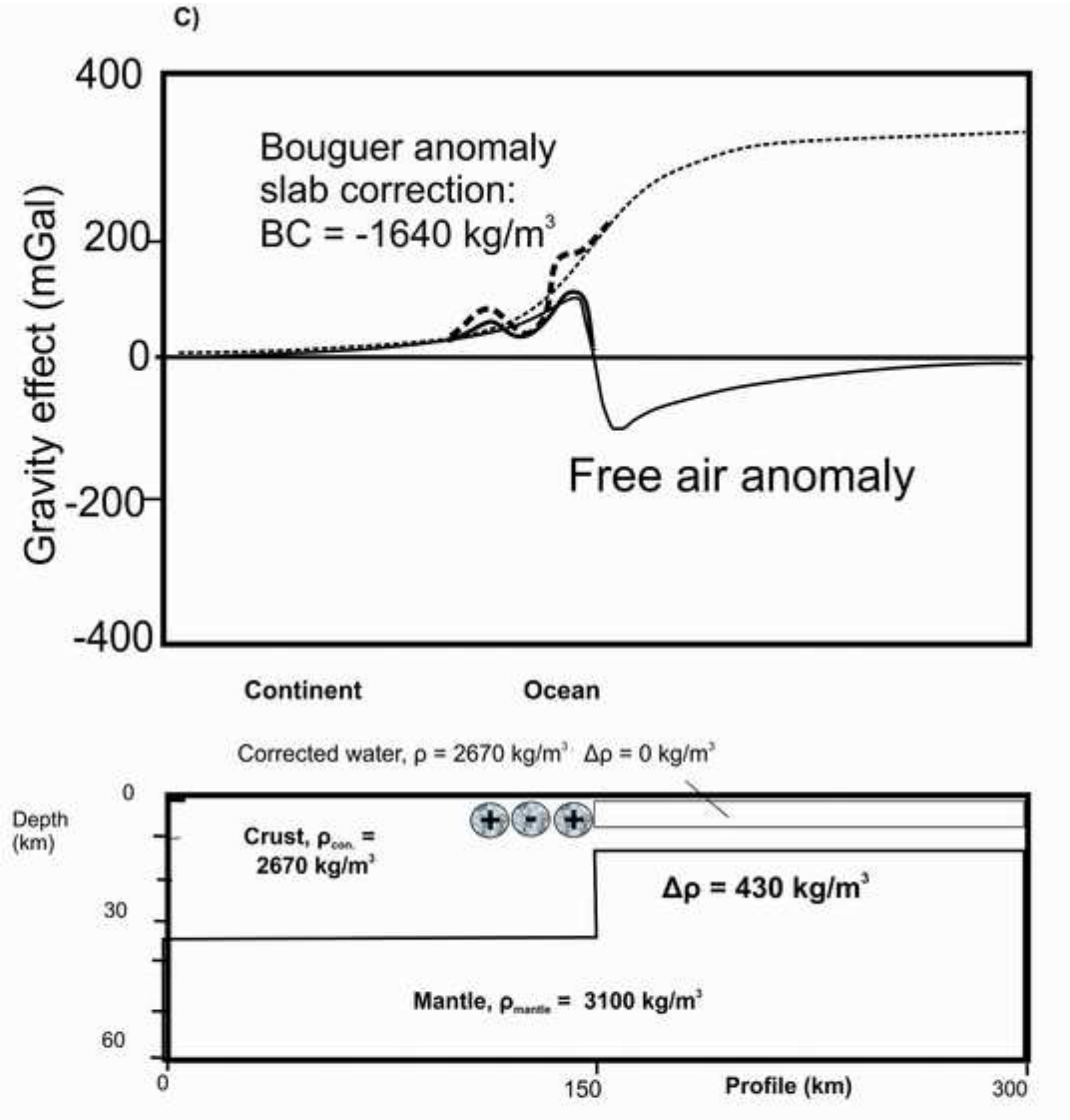

Figure
Click here to download high resolution image

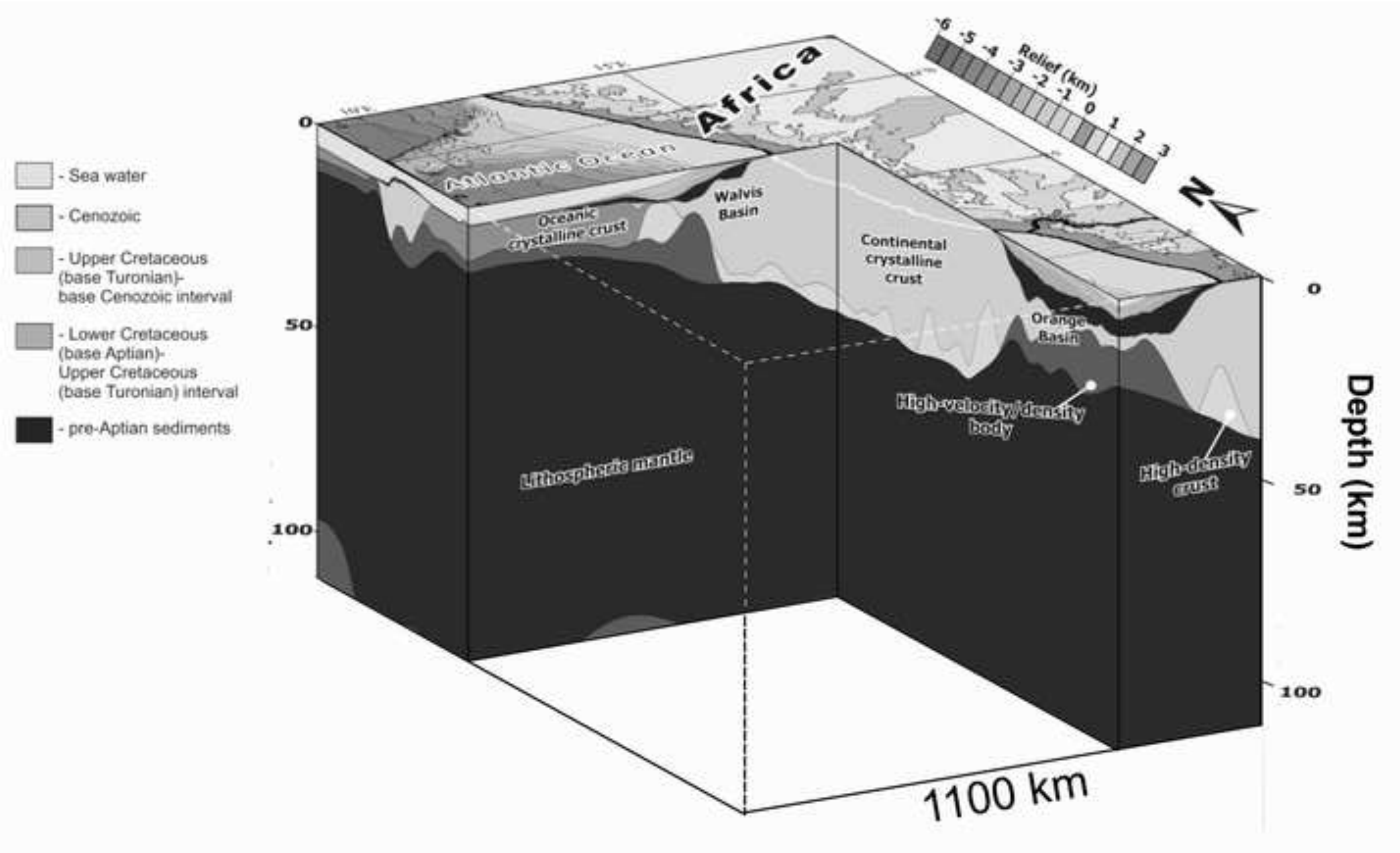

Figure
Click here to download high resolution image

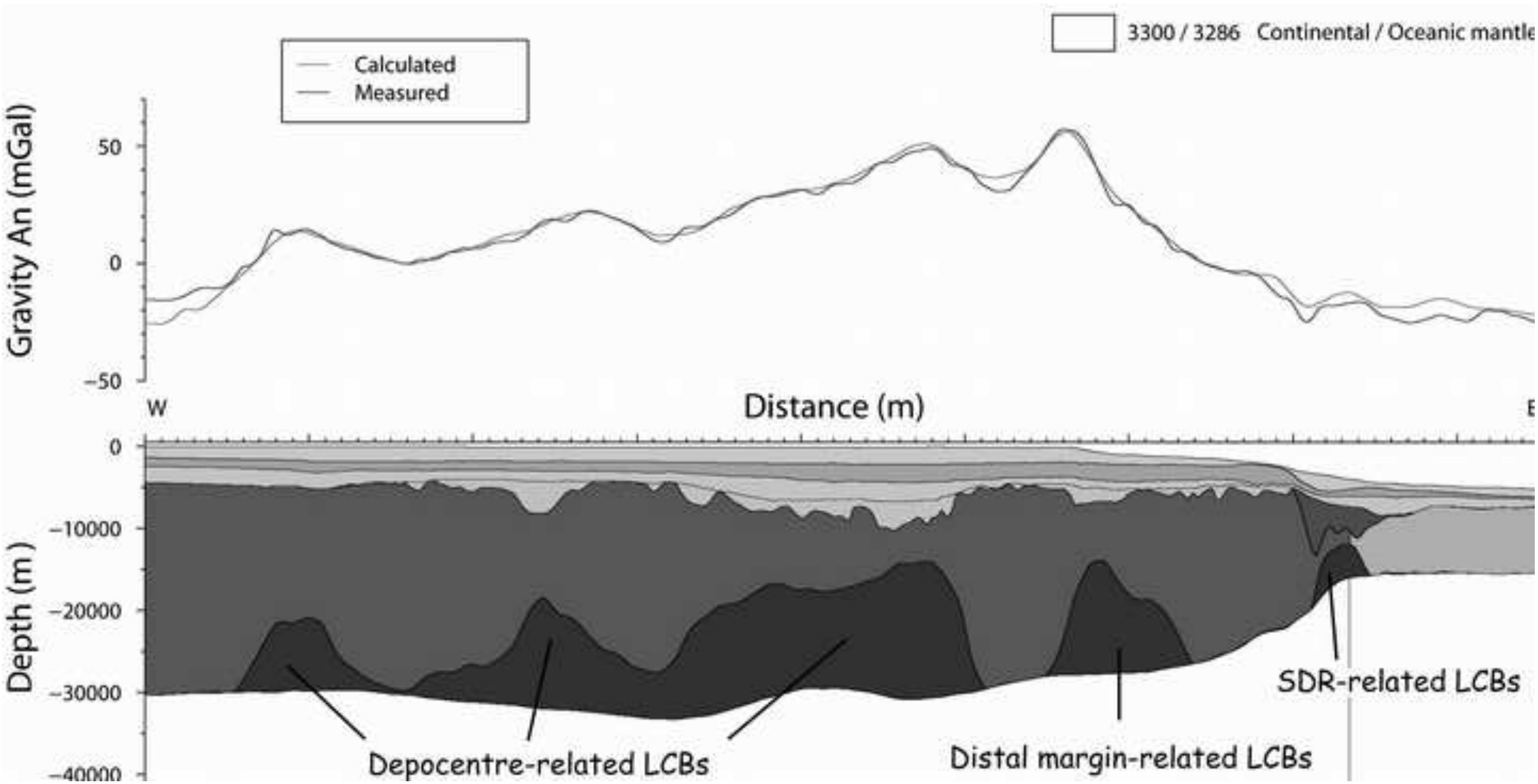

Figure
Click here to download high resolution image

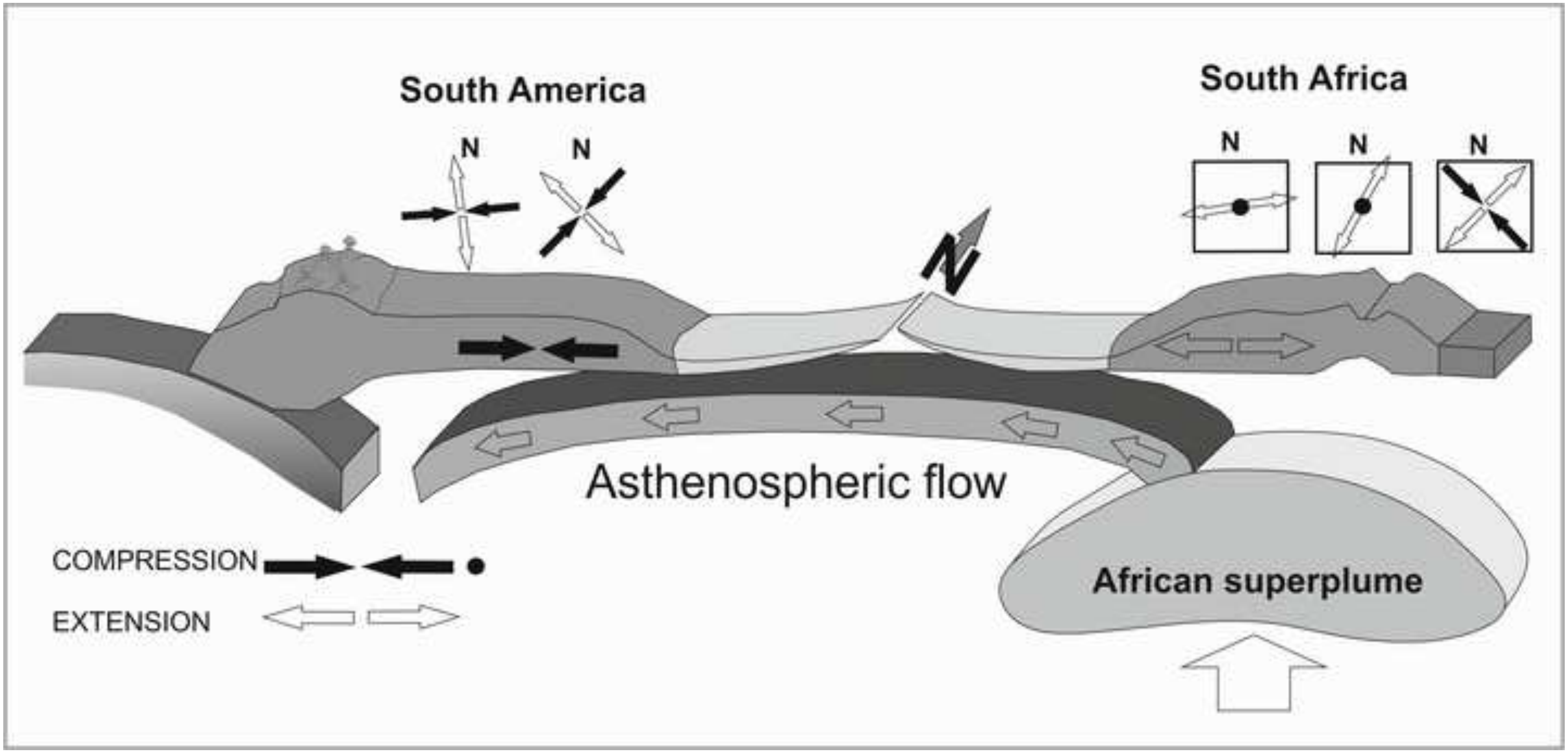

Figure
Click here to download high resolution image

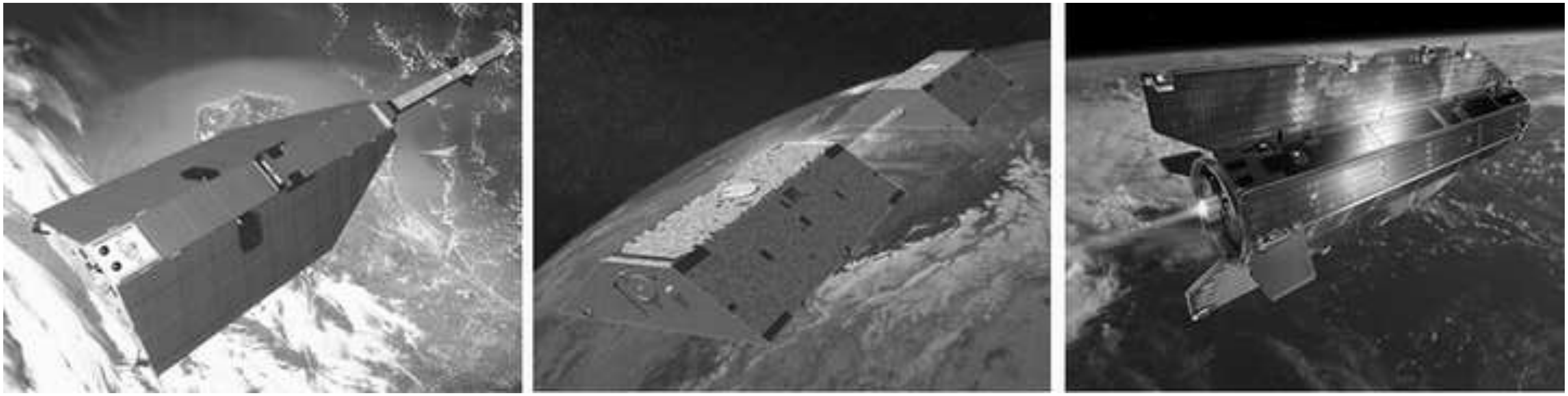

Figure
Click here to download high resolution image

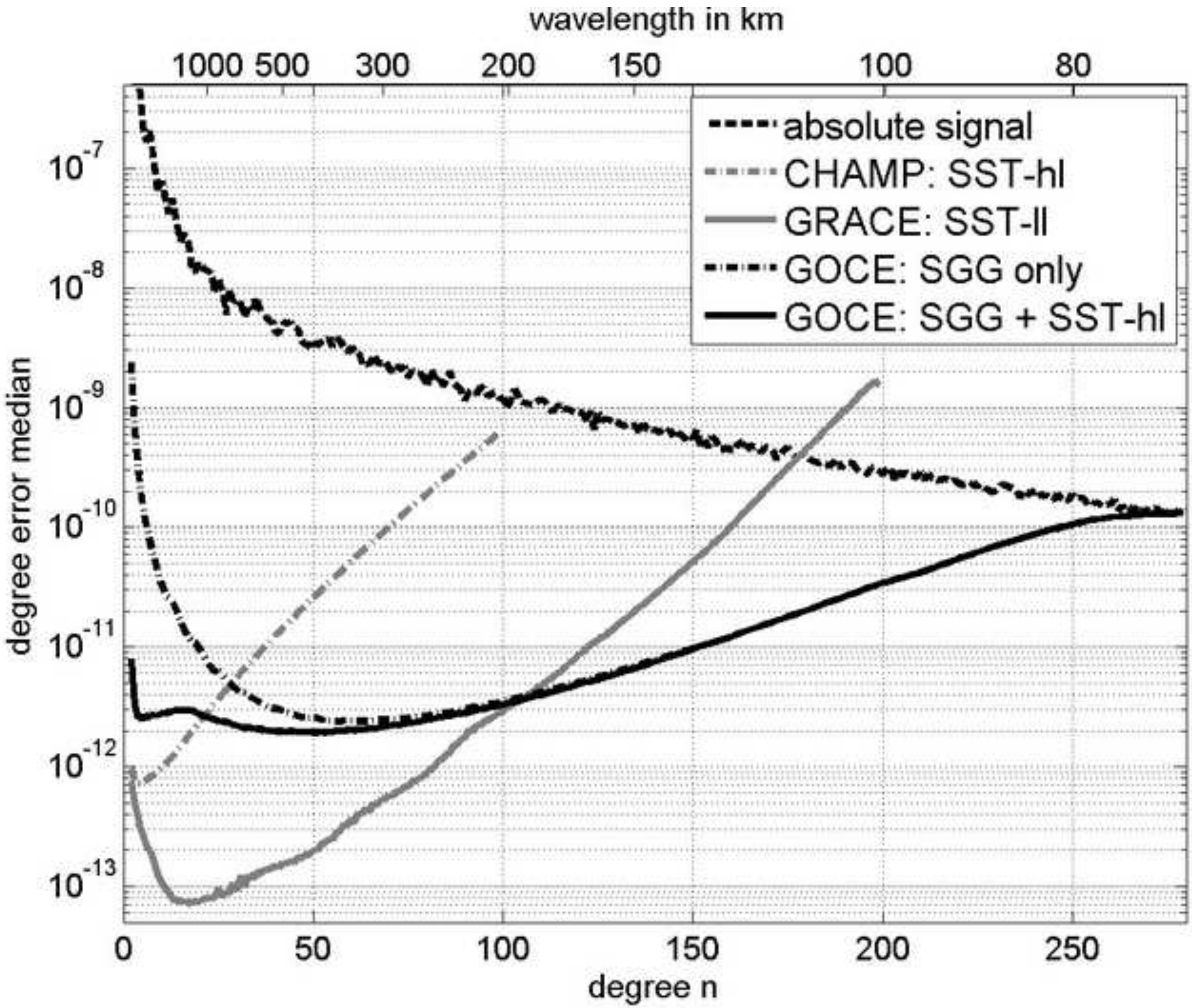

Figure
Click here to download high resolution image

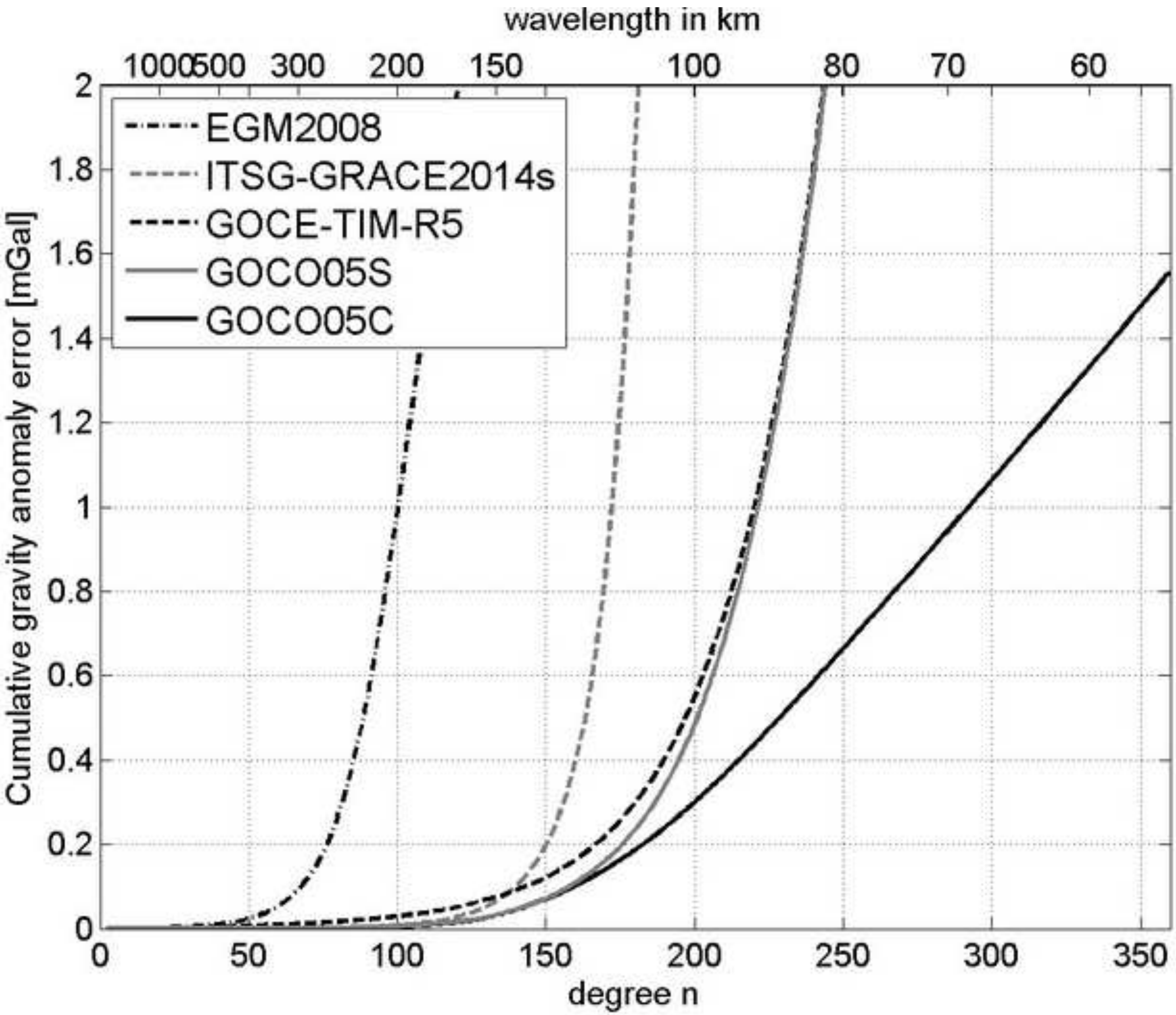

Figure
Click here to download high resolution image

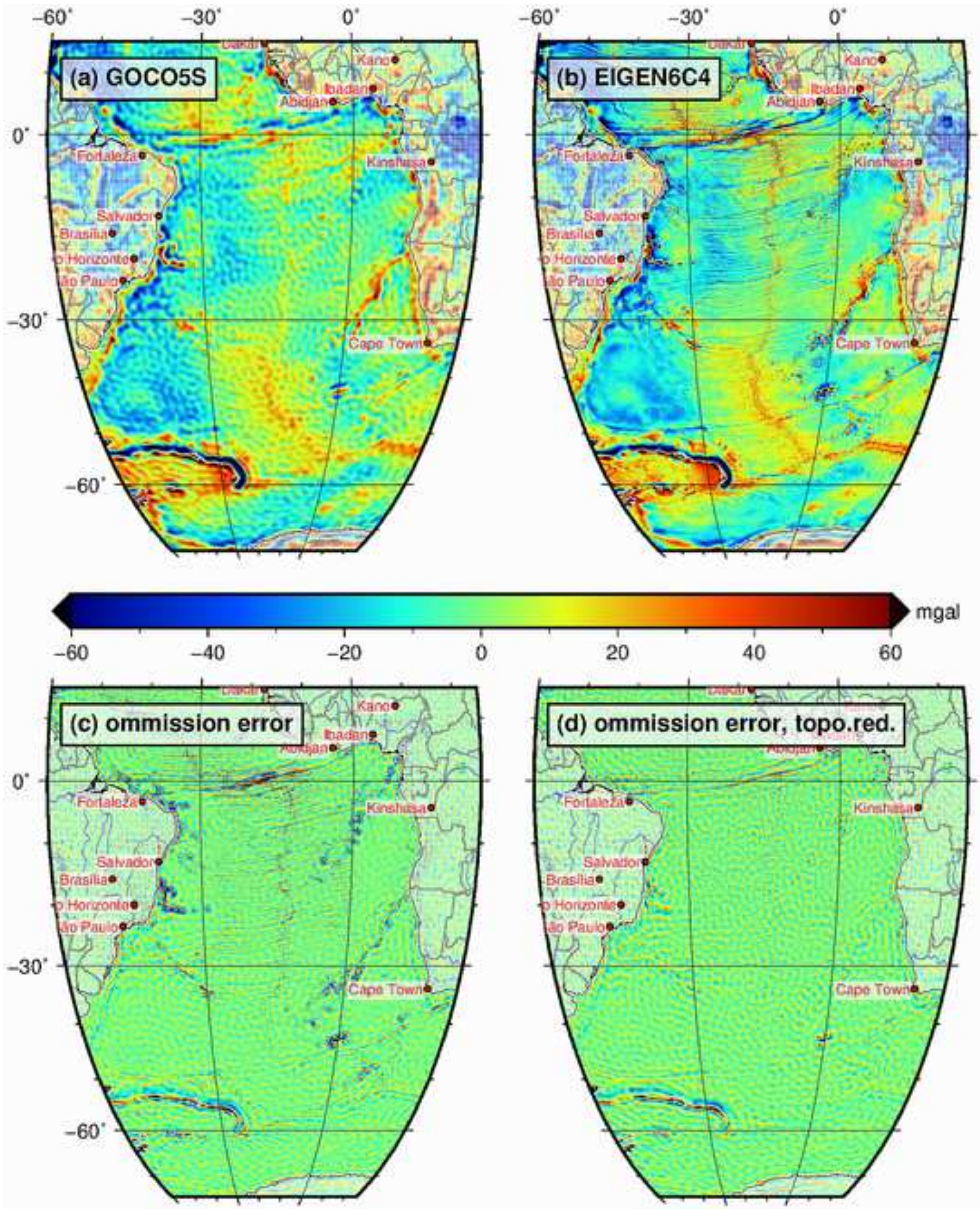

Figure
Click here to download high resolution image

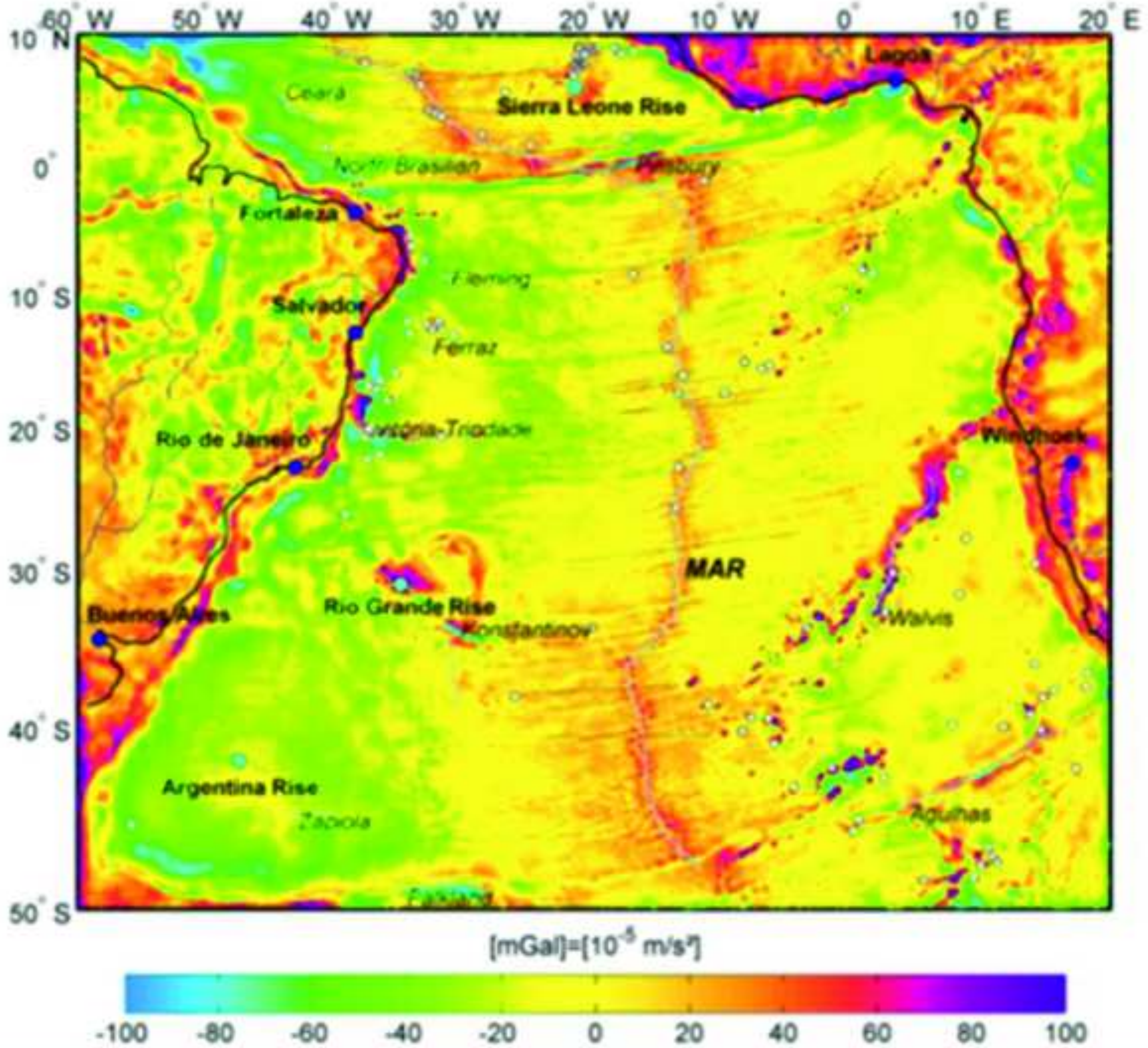

Figure
Click here to download high resolution image

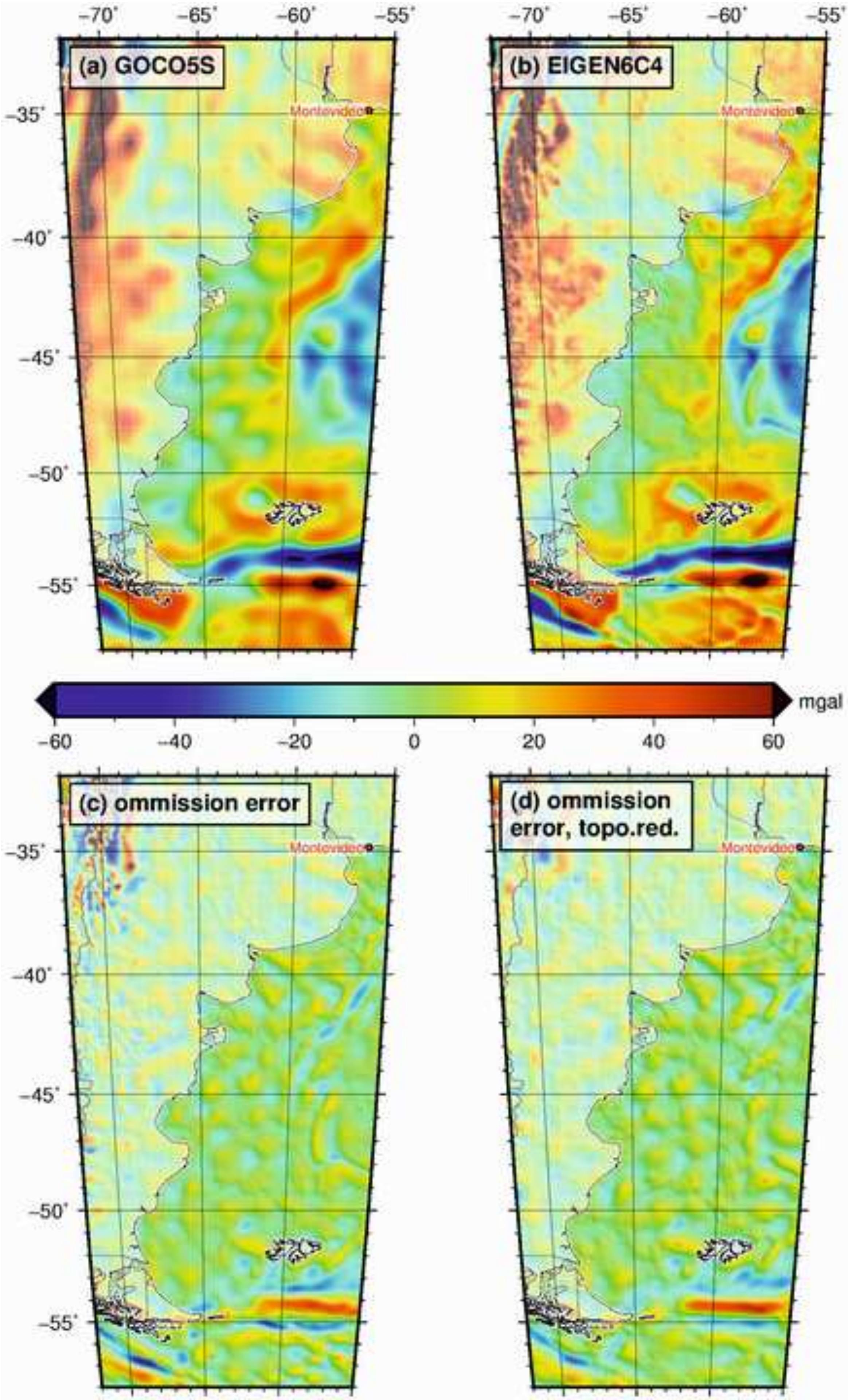

Figure
Click here to download high resolution image

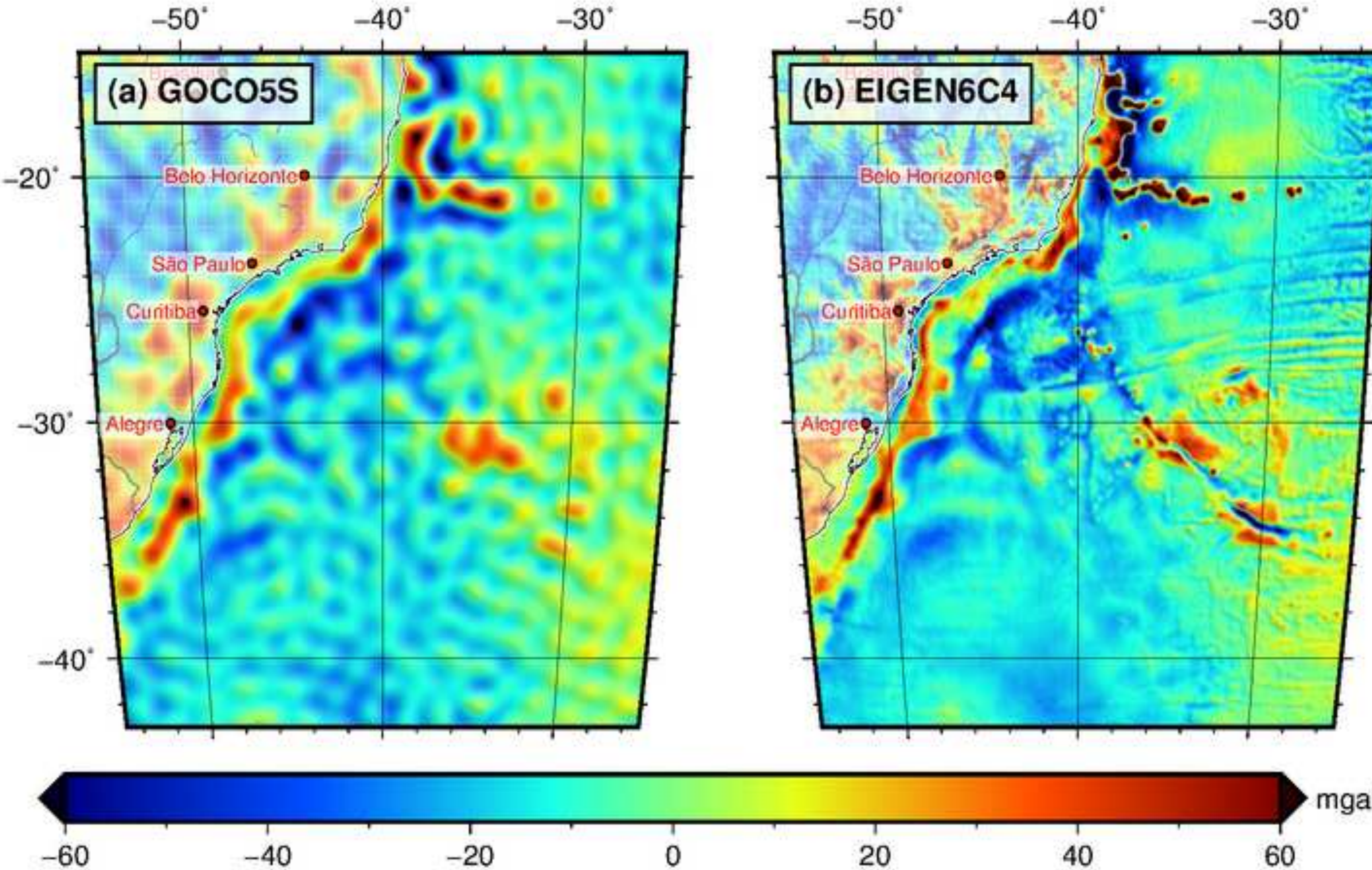

Figure
Click here to download high resolution image

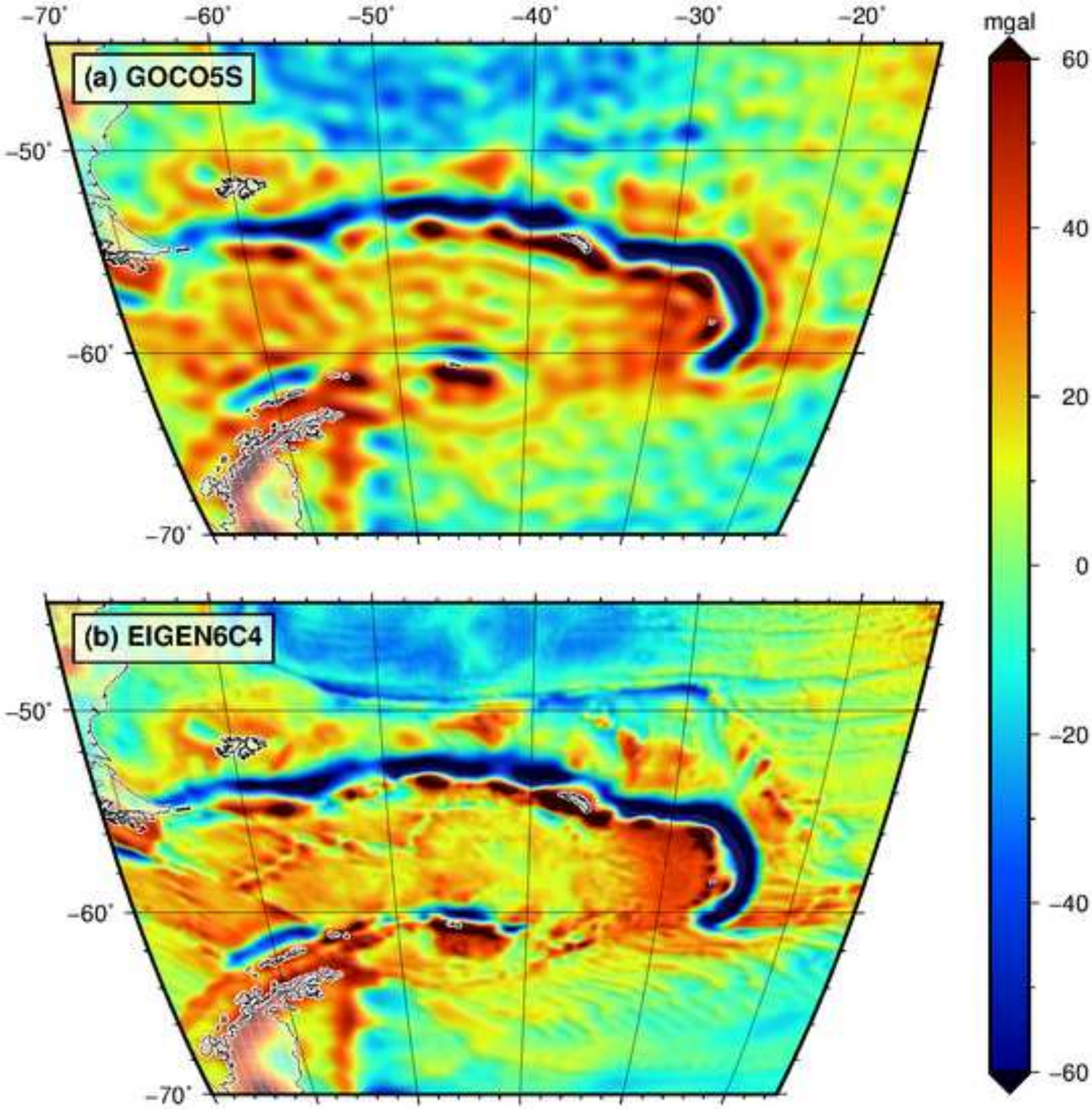

Figure
Click here to download high resolution image

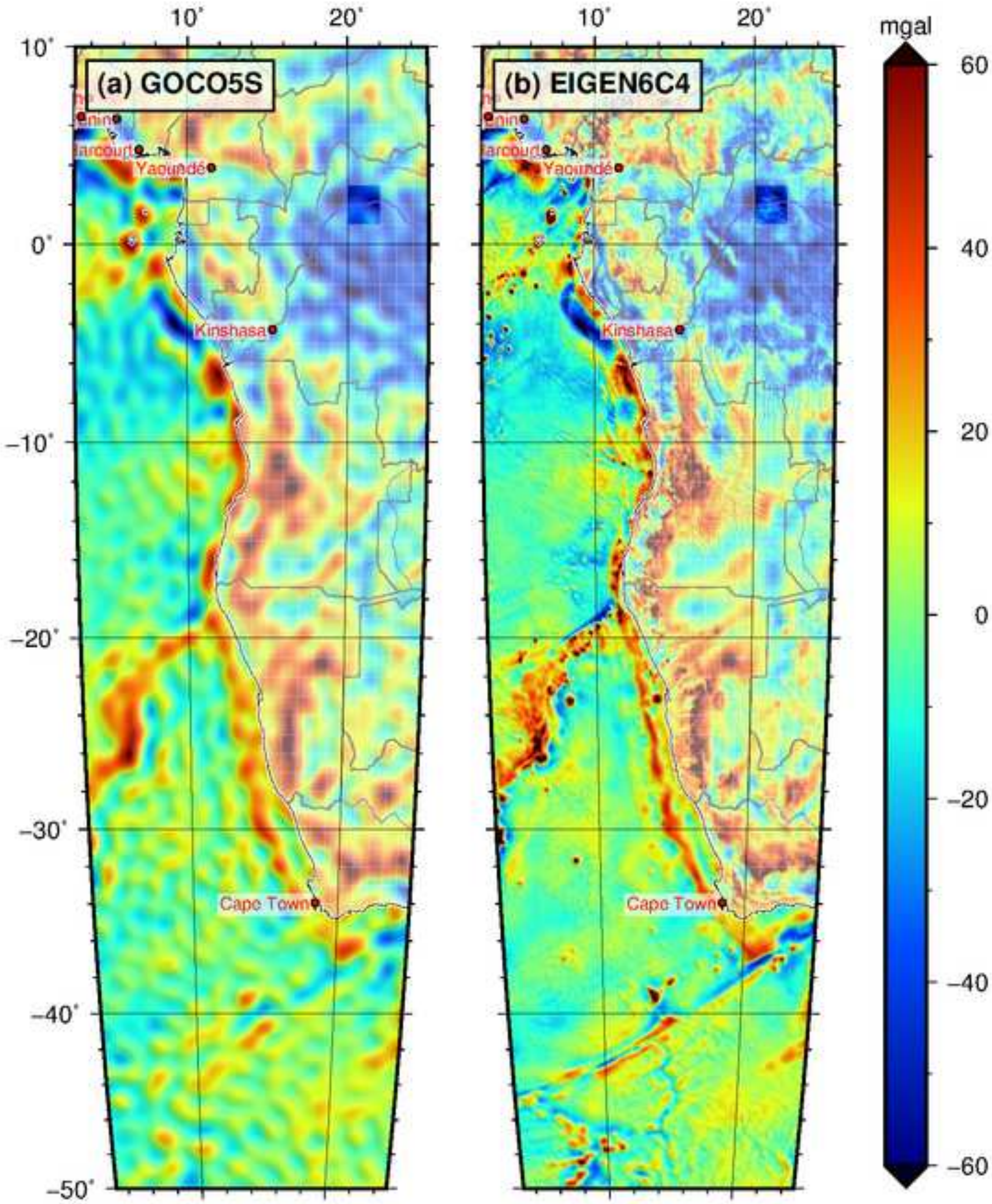

Figure
Click here to download high resolution image

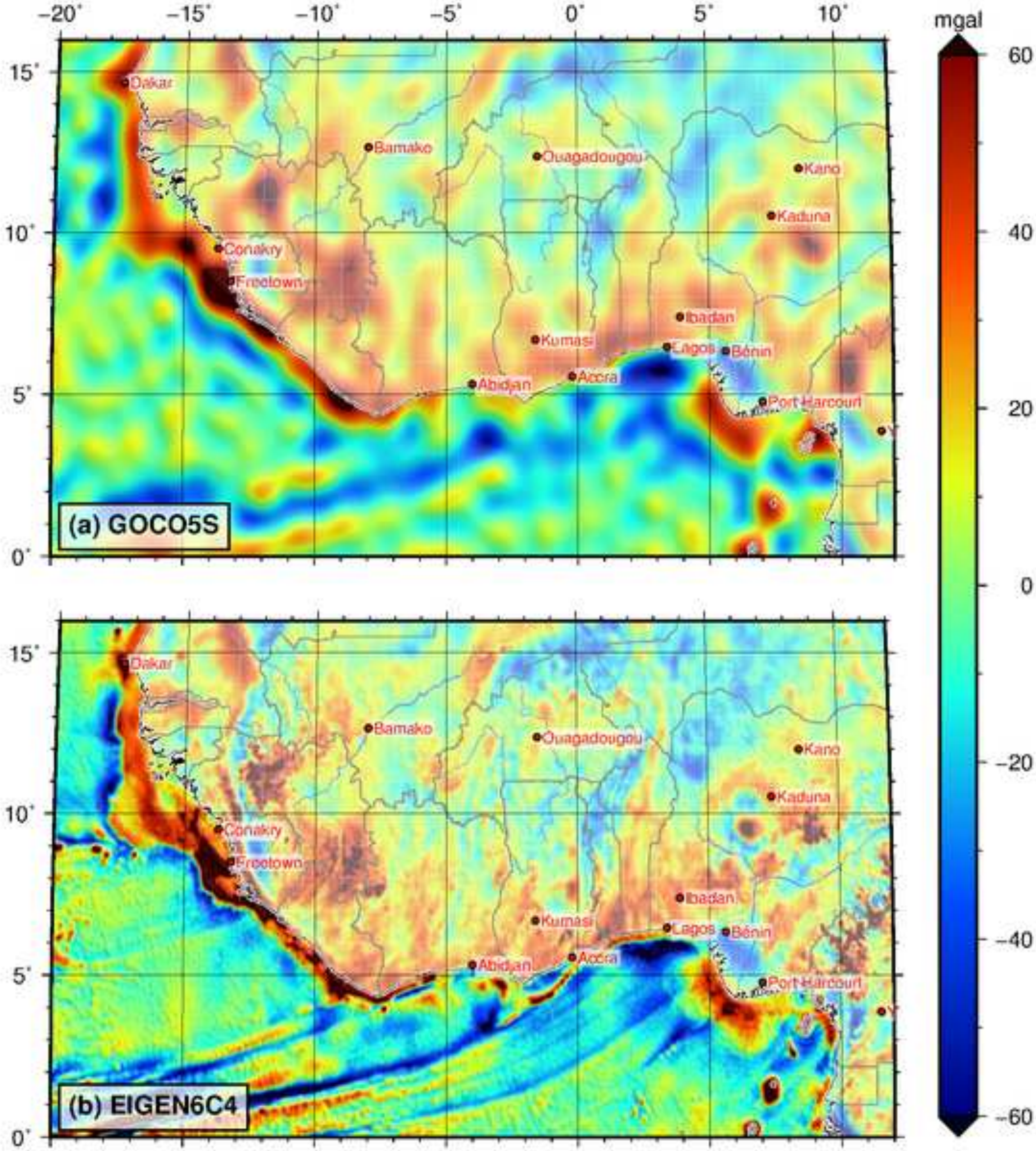

Figure

Click here to download high resolution image

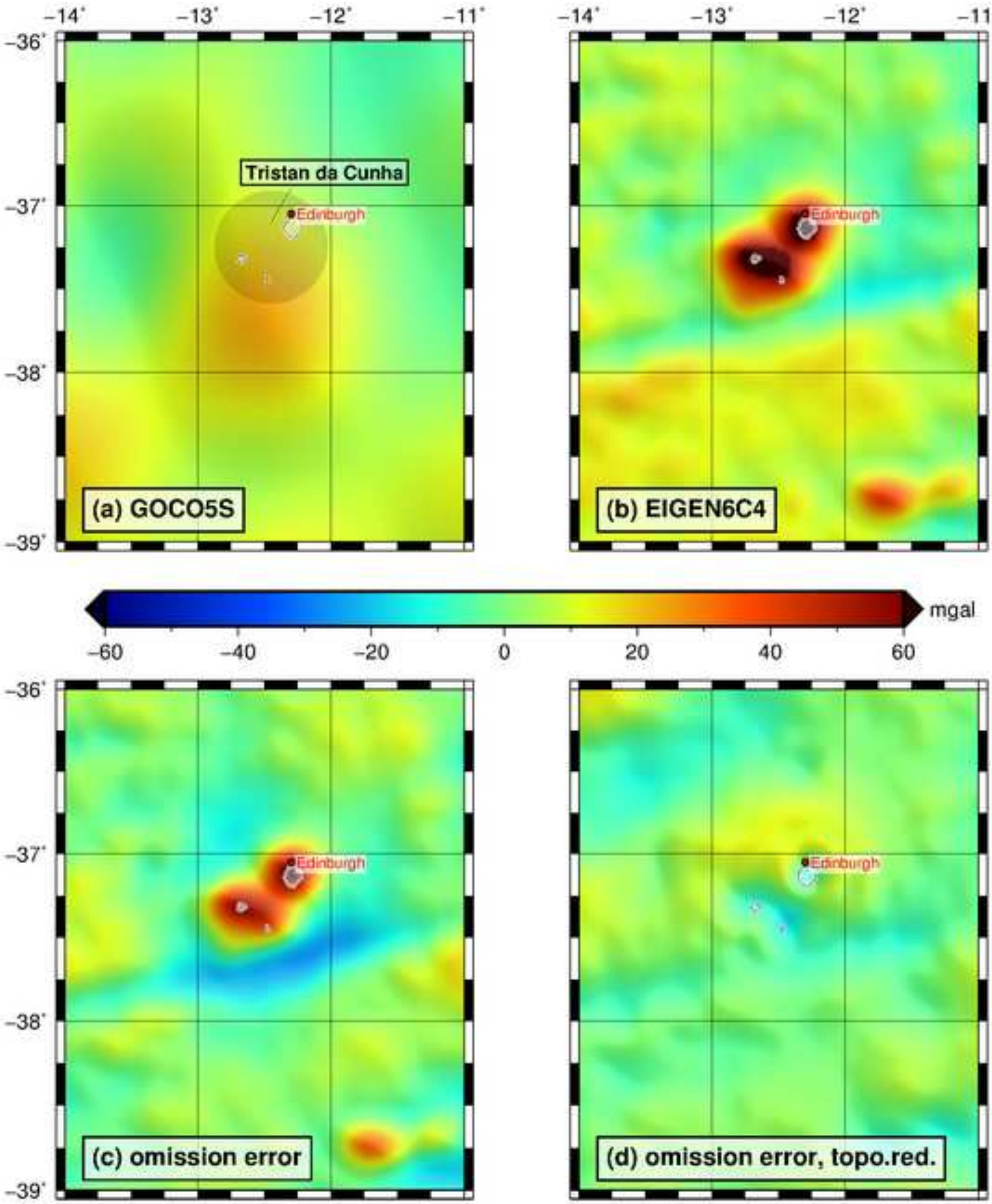

Figure
Click here to download high resolution image

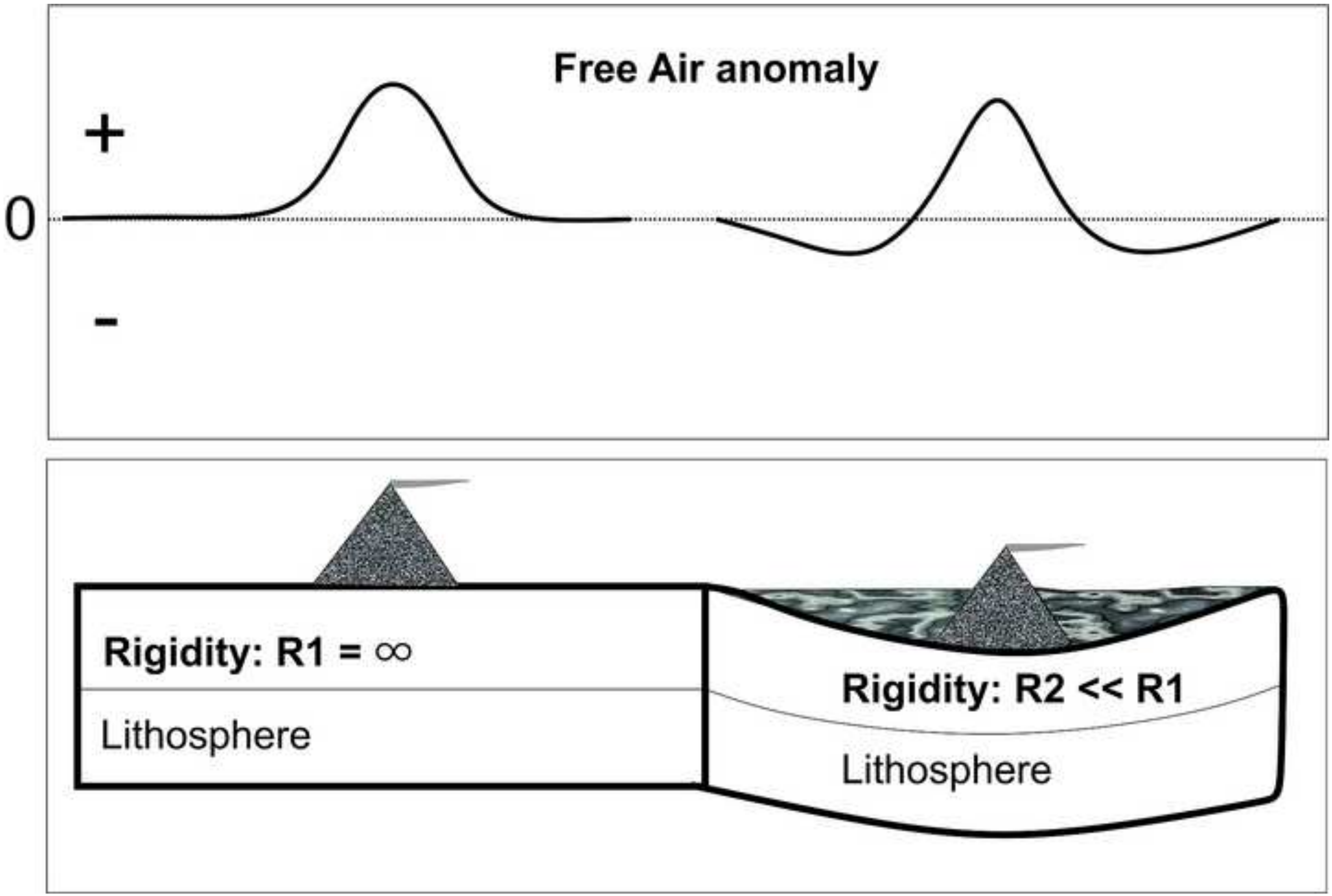

Figure

Click here to download high resolution image

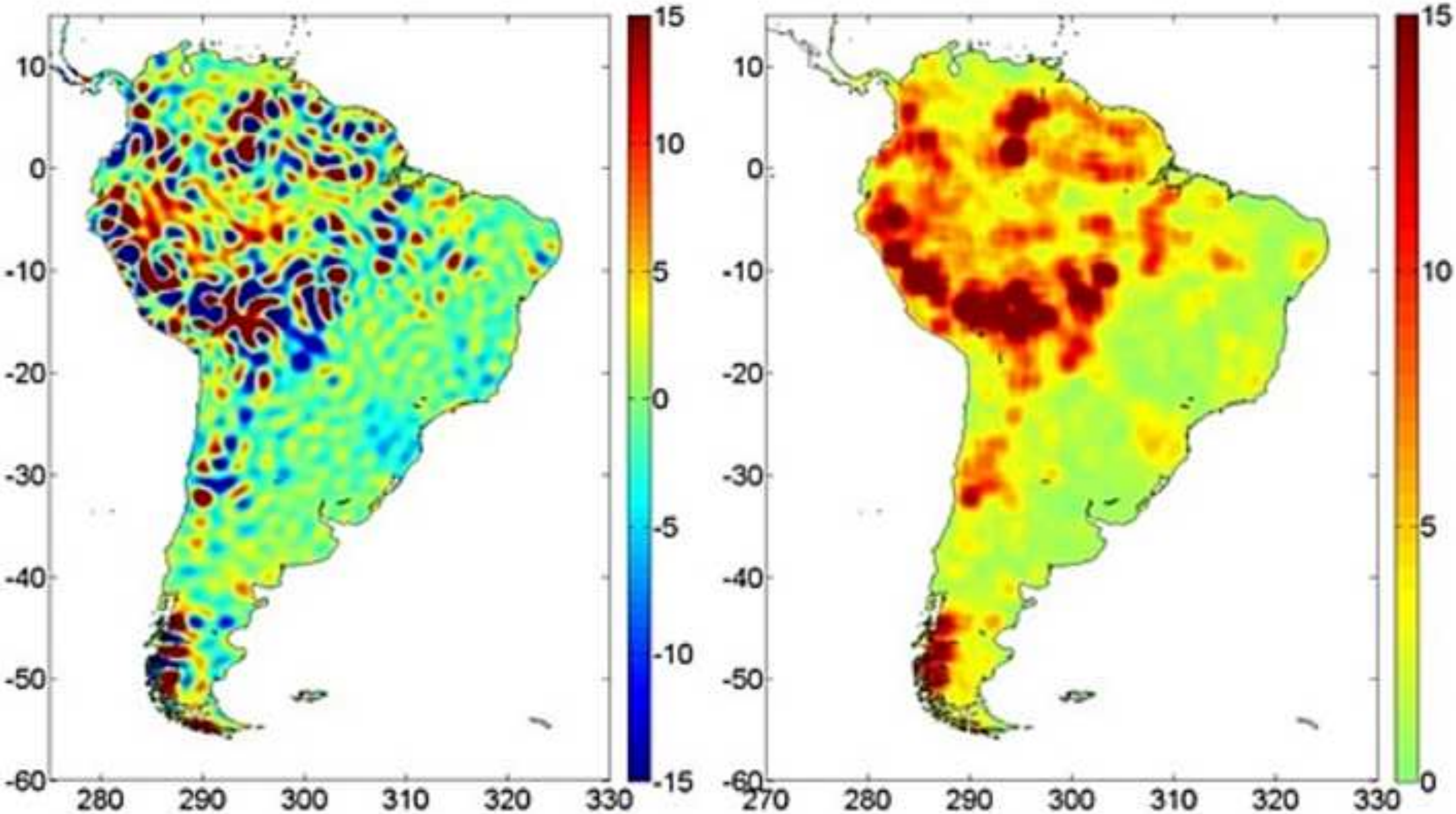

Figure
Click here to download high resolution image

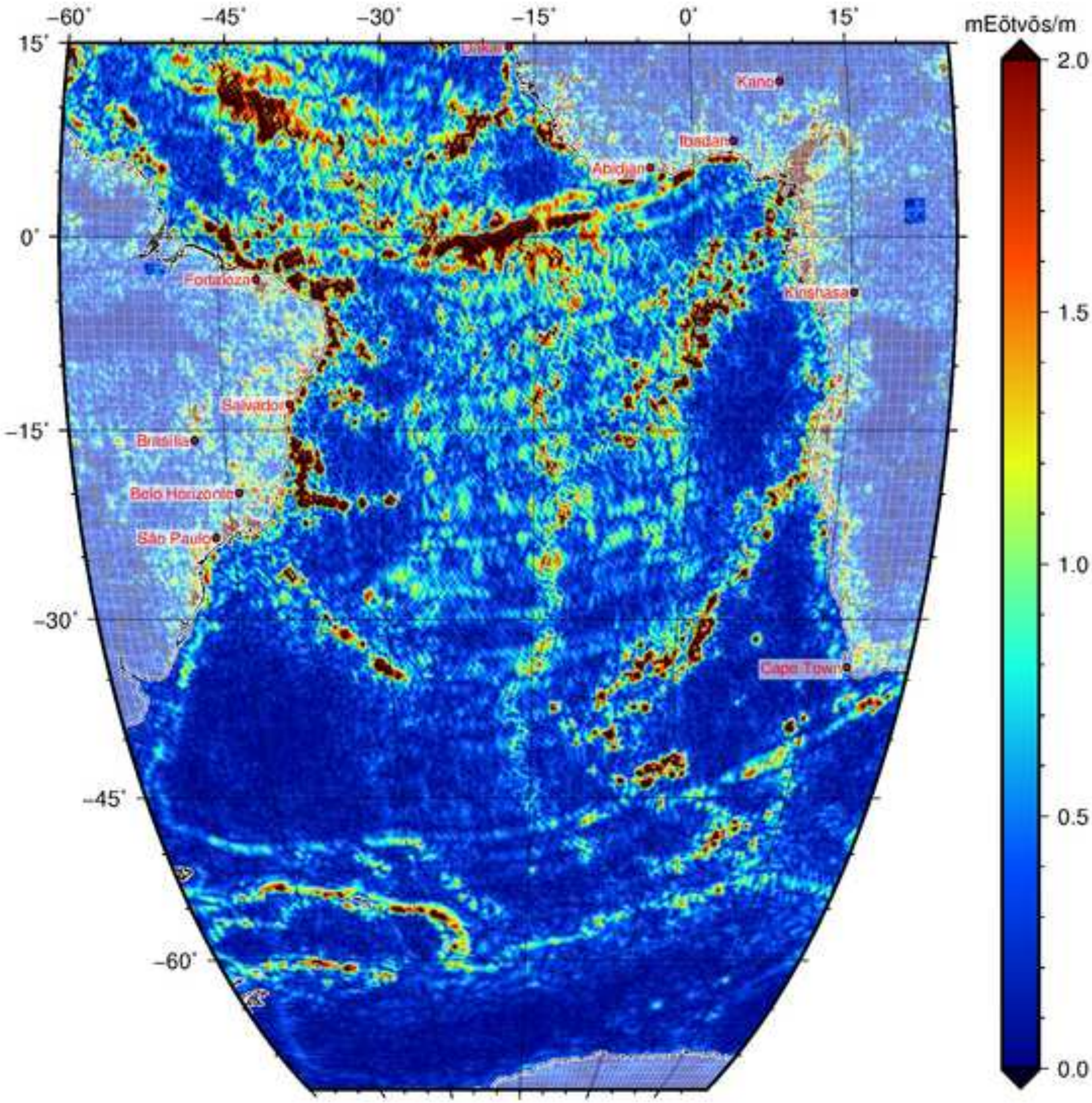

***Detailed Response to Reviewers**

Response to Reviewers/Editors

We corrected Line 324: „weak“ instaed of „week“.

We replaced in line 186 “Bocher et al.” and cited “Colli et al., 2016”

H.-J. Götze and R. Pail

Insights from recent gravity satellite missions in the density structure of continental margins – with focus on the passive margins of the South Atlantic

Abstract

We focus on new gravity and gravity gradient data sets from modern satellite missions GOCE, GRACE and CHAMP, and their geophysical interpretation at passive continental margins of the South Atlantic. Both sides, South Africa and South America, have been targets of hydrocarbon exploration and academic research of the German Priority Program SAMPLE (South Atlantic Margin Processes and Links with onshore Evolution). The achievable spatial resolution, driven by GOCE, is 70 - 80 km. Therefore, most of the geological structures, which cause a significant gravity effect (by both size and density contrast), can be resolved. However, one of the most important aspects is the evaluation of the omission error, which is not always in the focus of interpreters. It results from high-frequency signals of very rough topographic and bathymetric structures, which cannot be resolved by satellite gravimetry due to the exponential signal attenuation with altitude. The omission error is estimated from the difference of the combined gravity model EIGEN-6C4 and the satellite-only model GOCO05S. It can be significantly reduced by topographic reductions. Simple 2D density models and their related mathematical formulas provide insights in the magnitude of the gravity effect of masses that form a passive continental margin. They are contrasted with results from satellite-only and combined gravity models. Example geophysical interpretations are given for the western and eastern margin of the South Atlantic Ocean, where standard deviations vary from 25 – 16 mGal and 21 – 11 mGal, respectively. It could be demonstrated, that modern satellite gravity

data provide significant added value in the geophysical gravity data processing domain and in the validation of heterogeneous terrestrial data bases. Combined models derived from high-resolution terrestrial gravity and homogeneous satellite data will lead to more detailed and better constrained lithospheric density models, and hence will improve our knowledge about structure, evolution and state of stress in the lithosphere.

1. Motivation and the concept of Plate Tectonics

Geosciences are striving for an interdisciplinary perception to combine their basic findings in a world embracing synthesis to understand global processes in the Earth interior and at its surface. Most of these processes are generally geothermally driven, and it is easy to accept that their origin lies below the lithosphere, in the Earth's mantle (among others Stadler et al., 2010). Today, the theory of plate tectonics enables us to draw a coherent picture of the Earth´s lithosphere. Interactions between the plates at their plate boundaries are responsible for most of the earthquakes that occur here (among many other publications and websites: http://earthquake.usgs.gov/earthquakes/?source=sitenav, http://www.isc.ac.uk/about/ or http://geofon.gfz-potsdam.de/). This paper will review the status of satellite gravity missions and terrestrial data, as well as global gravity models, fields and gradients derived from them. It will focus on their accuracy, resolution and the omission error – which is out of focus of many earth scientists. It is structured as follows: Section 1 defines continent-ocean transitions and recalls some basics in the context of Plate Tectonics concept and passive margins in particular. For those readers who are not familiar with the interpretation of gravity anomalies at a continental margin in Section 2 the basic concepts are illustrated; this section can be skipped by experts. Further on the focus is set on the question how (satellite) gravity interpretations can help to explore these passive margins (Section 2.3). In the course of this paper we will notice later to what extent the new fields and gradients from recent satellite gravity missions can support research at the passive margins of the South Atlantic (Section 2.4).

In Section 3 we will demonstrate how this new information augmented our view on the density structures of the lithosphere particularly at passive margins of the South Atlantic. At last we describe the benefits for combined interpretations in Section 4, and merge information from both terrestrial and satellite gravity fields.

1.1 Short introduction to history of plate margins tectonics

Considering the history of the Plate Tectonic concepts in the early 1960s, Wegener´s view on the „the continental drift” (Wegener, 1920) began to be accepted after it was refined and confirmed by geophysical observations namely by early seismological studies on deep earthquakes (Wadati, 1929; Benioff, 1954), later by Isacks et al. (1968), Oliver and Isacks (1967) and paleo-magnetic shipborne observations (Hess, 1962; Vine and Matthews 1963 among others). Together with the techniques of radiometric dating (age determination) published first by Boltwood (1907) geophysicists were able to date the magnetic mid oceanic reversals by precise physical measurements. They helped to get the modern concept of “plate tectonics” fully accepted.

It provides the framework for the interpretation of structures, the history and composition of continental margins. Plate movements and the differences in density of oceanic and continental crust types led to the structural pattern of continental margins and result in a tectonic classification of coastlines as **active** or **passive** margins (among others Wefer et al., 2003). *Active margins* are typical units of the “Circum-Pacific Ring of Fire” in the Pacific where plates are converging and coincide with plate boundaries in a subduction zone. These margins are called *active* (e.g. Oncken et al., 2006; Lallemand, 2014) due to the big variety of tectonic, magmatic and metamorphic processes that occur here. If continental margins mark only the boundary to the oceanic portion of the same tectonic plate, they are called *passive margins*. Passive margins are typical of the Atlantic Ocean between Scandinavia and Greenland (Scheck-Wenderoth and Maystrenko 2008), Iberic peninsula and the East American coast or between Africa and South America (Blaich et al., 2011 and many papers within).

1.2 Passive Margins

Although we assume that most of the readers are familiar with the concept of plate tectonics we will recall briefly some basics. In particular *passive continental margins* are characterized by a transition of continental into oceanic crust within the same plate. It emerges from the splitting up of continents and the following divergent plate drift that forms new oceanic lithosphere by seafloor spreading at the divergent plate boundary. At the edges of the Atlantic geophysical investigations identify a laterally 10-15 km thick crustal transition between the thick crust of the continents and the thin oceanic crust. It is interpreted as relicts of thinned, mafic magmas which intruded into continental crust. In addition, passive continental margins are often stretched by intensive fault tectonics. They have a tectonically thinned continental crust, which is characterized by listric faults and tilted fault blocks. Tectonic crustal expansion starts at the time of installation of the continental drift rift system and refines the passive continental margin further (Blaich et al., 2011). These margins are marked by smooth relief due to tectonic inactivity and major sediment accumulation. This phenomenon is due to thermal cooling and sediment loading that led to conditions of subsidence and sediment accumulation, because the margins move away from the spreading center. Irregular subsidence and different sediment load often cause the accumulation of salt diapirs in the sediments of passive continental margins. The tectonic-sedimentary conditions are also favorable for the formation of hydrocarbon deposits and large salt deposits (Mohriak, 2014).

Modern passive margins (Fig. 1) border the oceans formed by the spreading caused by the break-up of the Gondwana supercontinent (e.g. Bond et al., 1984). From Figure 1 one can see that the margins of the South Atlantic Ocean (Cappelletti et al., 2011; Blaich et al., 2011; Mohriak, 2014), the western Indian Ocean, the Arctic and Norwegian seas (Scheck-Wenderoth and Maystrenko, 2008; Ebbing et al, 2006; Skogseid et al., 2000), the magma poor rifted margins of the North and Central Atlantic Ocean (Reston, 2009; Mohriak, 2014) and the margins of Antarctica are part of this system (Kalberg, 2016). A rising convection cell or a plume in the rifting area caused initial rifting and a regional uplift as well as volcanic activities above or below oceanic sea level after an initial period of crustal thinning and erosion. Basile (2015) describe another type of margin: “transform continental margins” by simple kinematic models of transform faulting which cause among two other types “passive transform margins”. The satellite gravity picture of the Equatorial Atlantic Ocean will be shown in Section 4.2, Fig. 20.

Figure 1: full page width

Fig. 1. Continental margins on Earth. Blue lines mark passive continental margins mainly surrounding the Atlantic Ocean, the Antarctic Seas, and Indian Ocean; red lines indicate active margins (subduction zones). Continental margins were taken from from Frisch und Meschede (2005).The underlying gravity field is the map of “gravity disturbance” calculated on base of the EIGEN-6C4 model (Förste et al., 2014). Gravity was calculated on a grid of 0.5° x 0.5°.

1.3 Volcanic passive margins

These margins present distinctive genetic and structural features, e.g., high-rate extension of the lithosphere is associated with catastrophic mantle melting responsible for the accretion of a thick igneous crust (Geoffroy, 2005). Typical rifted “magma-dominated” margins are characterized by large volumes of flood basalts which flow across the continental hinterlands during continental breakup (among others refer to: Hopper et al., 2004; Eldholm et al., 2000; Gernigon et al., 2006; White and Smith, 2009; O´Connor et al., 2012). Underlying the extrusive lavas at the continent-ocean transition zone, these margins exhibit high seismic velocities in the lower crust of some The deeper crust is characterized by two areas of high seismic velocity (7.2 to 7.4 km/s; Franke et al., 2010)., which are associated with voluminous igneous rocks intruded into the lower crust.

In recent time the question arose in the context of fixing international boundaries offshore of the continents due to economic interests because e.g. hydrocarbon exploration moved further offshore e.g. to explore deep water resources. Toward the definition of this “continent-ocean-boundary, COB” at passive margins one of the crucial questions is how to define these boundaries. Torsvik et al. (2009) described how COB for the South Atlantic margins at both sides can be defined: by the interpretation of seismic, gravimetric, magnetic, bathymetric and geological information. Any identification of the COB is also important for the definition of plate boundaries at the time of break-up which allows the reconstruction of geometry and earlier position of former continents - e.g. in the reconstruction of Pangaea. It is not the aim of this paper to recalculate COBs. However we trust that the processing of gravity field and its second derivatives for recalculation of COB (Torsvik et al., 2009) will benefit from the increase of high resolution satellite derived gravity fields. Later we will return to this point in the conclusion (Section 5) suggesting calculating the 2^{nd} derivative of satellite gravity (derivative of the gravity gradient).

2. Geophysical characteristics of margins

To investigate both active and passive continental margins almost all geophysical methods can help to discover their lithospheric structures: Seismic, potential, electro-magnetic and electrical fields. Recent studies (e.g. Torsvik et al. 2009) show that processes in the lithosphere are linked to the dynamic mantle and dynamic processes have an important influence on the evolution of lithospheric plates, which is manifested in the formation of dynamic topography (e.g. Flament et al., 2013; ~~Bocher et al., 2016~~Colli et al., 2016). A key example for this interaction is the opening history of the Atlantic, where asthenospheric material reaches the surface at the mid-ocean spreading center. The uplift of hot material of the asthenosphere leads to seafloor spreading which manifests itself in the spreading anomalies in the magnetic field. The spreading axes are expressed either by topographic (heights above sea level, e.g. Iceland) or bathymetric heights (below sea level e.g. Atlantic ocean ridge). The worldwide offshore stripe pattern of magnetic anomalies which are located parallel to mid-ocean ridges allow a temporal classification of developed oceanic crust. The EMAG2 total magnetic field model has a reasonable resolution of two arc-minutes (Maus et al. 2009). The model was compiled from ship-, air-borne and satellite data (CHAMP). For the purpose of interpolation of magnetic field anomalies the oceanic crust ages of Müller et al. (2008) were employed (Maus et al. 2009). Hydro-carboniferous exploration targeted most of the passive margins of the world with both refraction and/or reflection seismic.

Seismic onshore-offshore investigations of a passive continental margin aim to investigate the transition zone between the oceans and continents, e.g. SE Atlantic and the African continent (Franke et al., 2006; 2010; Bauer et al., 2000; Hirsch et al., 2009; Schnabel et al., 2008). These studies reveal the history and mechanisms of the break-up and its relation to the driving magmatic processes (plume – crust interactions) in the underlying mantle and lithosphere. The South American side of the southern Atlantic was target of multiple seismic investigations since many years (Mohriak, 2014; Blaich et al., 2011; Franke et al. 2006; Heit et al. 2007; Hinz et al., 1999 and many more) to investigate the shelf areas offshore, the continent-ocean transition and the seaward dipping reflectors (SDR) which are characterized by high seismic velocities and related high densities.

2.1 The role of gravity field interpretations and prerequisites

Remark:

> The units used for gravity field values and its gradients are given in mGal (Milligals) and E (Eötvös) – as it is still common use in Geophysics and Geodesy. Converting these units into SI-units, there are: 1 mGal = 10^{-5} m/s^2 and E = 10^{-9} s^{-2}.
>
> Rock densities are always given in kg/m^3.

First, the situation will be analyzed which was typical before the era of satellite missions which started in the year 2000 with the launch of the CHAMP satellite (refer to Chapter 4). Modelling and interpretation of the Earth´s gravity field and its derivatives often had to deal with a merge of data sets with rather different resolution, different age and quality, coverage and wavelength content. This has been documented in a long list of papers (among many others: Schaller et al., 2015; Bouman et al., 2014; Hosse et al., 2014; Gutknecht et al., 2014; Köther et al., 2012; Tašárová, 2007). These papers have shown that lithospheric models of study regions suffer mainly from two facts:

(1) Nearly all information for constrained gravity field modelling of the lithospheric is based on irregularly distributed profiles and

(2) large data gaps and partly low data quality due to very limited access and infrastructure.

The global gravity model EGM2008 (Pavlis et al. 2012) inherited – and still inherits - these problems related with available terrestrial databases. Pavlis et al. (2008) described the compilation of the EGM2008 gravity which consists of different sources: up to a spatial resolution of approximately 140 km GRACE (Gravity Recovery and Climate Experiment) data have been used, data from 140 km to approx. 10 km spatial resolution are derived from terrestrial and satellite altimetry and so called “fill-in” data (Section 4.2). Today we know that the relative weighting of GRACE with respect to the other datasets was too low, leading to a dominance of terrestrial data errors in spectral regions where better GRACE data would already have been available.

Figure 2: Full page width

Fig. 2. This figure portrays the terrestrial data inconsistency which is rather typical for gravity surveys in remote areas (here across the South American continent at a swath between 36°S – 42°S from the passive margin in the East

to the active margin in the West). As an example the different sources of gravity data of the Southern Central American continent are shown together with the visualization of big data gaps (Tašárová, 2007). The green and red points in Chile (CH) and Argentina (AR) are stations in the ARANEDA I and II (University of Chile) datasets; black points in southern Chile and the Arauco Peninsula are ENAP data (Chilean oil industry); the gray dense network in Argentina (AR) show the YPF data (Argentine oil company); yellow points: stations of the MIGRA 2000 dataset, and the MIGRA 2002 data (both measured by the gravity group at the University Kiel) are shown in blue. The brown lines offshore denote the ship-borne gravity data profiles from the German research vessel “Sonne”.

Fig. 2 shows the situation some 20 years ago at the central South American subcontinent. For a continental gravity field study the field had to be compiled from very different data sources often without any meta data information - e.g. for gravity data which were measured on behalf of oil companies (grey area in Fig. 2). In other areas, e.g., in the eastern part of Argentina (yellow dots in Fig. 2) data are missing due to difficult or impossible access.

At the end of this Section we will pose the question how large lithospheric structures and how big density differences to their surrounding have to be in order to cause a detectable signal at orbit height of a satellite. This consideration describes the situation at active and passive margins in an analogues manner. In Fig. 3 the effects of gravity and gradients are shown for a simple model. For density contrasts between the values $\Delta\rho = 10^1 - 10^3$ kg/m^3 Gutknecht et al. (2011) calculated gravity and gradients at the GOCE satellite orbit height of 255 km resulting from a sphere with minimum diameters between d = 20 – 200 km (b = 10 – 100 km, refer to Fig. 3) to be tangent to the Earth surface). Within the range of the assumed parameters the minimum diameter required to produce signal differences of 1×10^{-5} ms^{-2} and 12×10^{-12} s^{-2} at orbit height. This is rather close to the expected accuracies of the gravity and vertical gravity gradient of the GOCE mission (recent values are: 0.45 mE for GOCE-only, 0.2 mE for GOCE+GRACE models, cf. also Fig. 13). Fig. 3 conveys that a structure with a diameter of some 45 km and a density contrast of 240 kg m^{-3} could be detected in satellite gravity at orbit height. If the diameter of the model sphere increases to 90 km, its density contrast should not be less than 33 kg m^{-3}.

The simple model described above fits rather well the dimension of the Jurassic arc batholiths at the Northern Chilean continental margin with diameters of roughly 60 – 120 km (Sobiesiak et al., 2007). This supports the idea that batholithic structures e.g. intrusions at continental margins, can be detected using data of the modern satellite missions– both gravity and gradients.

Figure 3: one and a half page width

Fig. 3. Gravity and gradient signal caused by a minimum diameter of a sphere with given density contrast in the orbit height of 255 km (Gutknecht et al., 2011). The thick solid and dotted lines represent gravity signals of 1 and 10 mGal at orbit height. The thin dashed and dash-dotted lines represent gradients of 12 and 1000 mE, respectively. The grey shaded area shows results which are based on a possible combination of geometry and density parameters of the causing mass anomaly.

2.2 Gravity anomalies and isostasy

A first look at Fig. 4 provides already helpful information on the gravity gradients of the Earth at the continental margins. The figure bases on the evaluation of gravity field maps from the recent gravity missions. A complete Bouguer anomaly (corrected by the effect of elevation, spherical slab, topography both on- and offshore) was used to calculate the first derivative of the field – the dip curvature of gravity.

Figure 4: Full page width

Fig 4. Global horizontal gravity gradients. Deep blueish colors mark regions on Earth where the dip curvature (horizontal gradient) of the worldwide Bouguer gravity field (EIGEN-6C4) is small or even zero. The more reddish the colors are the steeper the gradients. The strongest gradients are observed at the active continental margin of Central South America. On the contrary at most of the passive continental margins (Fig. 1) the gradients are rather small.

Dark blueish colors indicate rather we~~e~~ak dip curvature which means that horizontal gravity gradients are small, on the contrary reddish tones point to strong dip curvature and therefore strong gradients. The active continental margins in the area of the Circum-Pacific are generally marked by reddish colors – strong gradients – which are related with extended density variations in crust and mantle in the transition from oceanic to continental margins. Mostly low gradients – light blueish colors - are typical for passive continental margins. In order to understand this relationship two questions arise:

(1) How was the gravity *anomaly* calculated and how big is its magnitude of the anomaly caused by the mass distribution (both topography/bathymetry and densities) at continental margins and

(2) How was the *field* observed and what is known about accuracy and homogeneity of gravity field observations?

With regard to the first question one has to consider that gravity observations at the Earth´s surface and the Earth near space vary from the theoretical ”normal” field value. Their magnitude is caused not only by the latitude effect but by elevation of observational points, the density of cap beneath the station in the underground and the topographic masses in the neighborhood. After correction of earth tidal effects and air pressure variations the remaining time invariable parts of the measured signal are:

Normal gravity	γ_0
Effect of topographic masses	δg_{TOP}
Bouguer slab	δg_{BPL}
Elevation effect (free air term)	δg_{NIV}
Effect of the crustal root	δg_R
Known mass inhomogeneities	δg_{GEOL}

Common representations of gravity measurements in maps and profiles depend on what has been calculated as stated in the table above and added as corrections to the measured gravity field values. From all measured gravity values the normal gravity (in the height and position of the observable) is subtracted, and therefore the term “gravity anomaly” is defined. This is simply the difference between the observable values to “normal” gravity. In Geophysics we distinguish mainly between three anomalies Free air- (FA), Bouguer- (BA) and isostatic anomaly (ISA) which define gravity in the height of the observation (e.g. Li and Götze, 2001; Hackney and Featherstone, 2003; Naudy et al., 1965; LaFehr, 1991 and many others).

With δg_R we describe the effect of a mountain root and define Free Air, Bouguer and isostatic anomalies such as:

$$FA = \Delta g'_0 = g_{obs} + \delta g_{NIV} \left[+ \delta g_{TOP} \right] - \gamma_0$$

$$BA = \Delta g''_0 = g_{obs} + \delta g_{NIV} + \delta g_{TOP} + \delta g_{BPL} - \gamma_0$$

$$ISA = \Delta g_{ISA} = g_{obs} + \delta g_{NIV} + \delta g_{TOP} + \delta g_{BPL} + \delta g_R - \gamma_0$$

Calculations of the individual correction terms depend on the objective of the survey and are variously complicated to handle. g_{obs} denotes the measured gravity field value. The calculation of the topographical reduction (δg_{Top}) requires precise knowledge of the terrain and surface near densities and today it is most likely calculated by the aid of digital elevation models (DEM), among others refer to (Holzrichter, 2013 and Szwillus and Götze, 2016); it requires the use of a computer and digital elevation data. The effect of topographic masses is normally calculated in a surrounding circular area of 50 km up to 167 km (e.g. La Fehr, 1991; Hinze et al., 2006). However, Mikuška et al. (2006), Szwillus and Götze (2016), Szwillus et al., (2016) point to “long distant relief effects” and propose the calculation of *all* topographic masses on Earth. The gravity effect of a Bouguer slab with a thickness which is defined by the difference between the physical station height and the reference level (normally the geoid) should always be calculated by a spherical cap (e.g. Baeschlin, 1948). For smaller areas (with a reduction radius R < 20 km) and moderate terrain roughness the Bouguer slab can easily be calculated by:

$$\delta g_{BPL} = -2 \pi G \rho (H_S - H_B)$$

with:

G	=	Gravitational constant ($6.672 \cdot 10^{-11}$ m^3 s^{-2} kg^{-1}),
ρ	=	crustal density (2 670 kg/m^3); offshore: rock-equivalent density
H_S	=	station height; offshore: ocean depth H_D,
H_B	=	reference height (usually it is referred to the geoid).

In the last step the free air effect δg_{NIV} is calculated by use of the “normal gradient” (0.3085 mGal/m):

$$\delta g_{NIV} = 0.3085 \cdot (H_S - H_B) \text{ mGal/m}$$

It has to emphasized that the above used constant gravity gradient for large scale investigations has to be replaced by equivalent values of derivation of closed mathematical expression of the normal gravity which is always latitude and height dependent. It was also recommended to calculate an “atmospheric correction” (Wenzel, 1985) in order to eliminate long wavelengths errors from the observed gravity field.

Note: the terms of “flat” Bouguer slab in δg_{BPL} and the “constant vertical gradient” in δg_{NIV} are in the above formulas are used here for simplification only. Modern satellite gravity field processing at large spatial scales requires a spherical cap calculation and the consideration of latitude and height dependent calculation of the vertical gradient.

Special emphasis has to be put on the situation in oceanic regions. If we assume that station heights are equal to geoidal heights (h = 0 m) Bouguer and Free Air anomaly is equal due to:

$$BA = FA + \delta g_{BPL} = FA + [-2 \pi G \rho (H_S - H_B)]$$

with: $H_s - H_B = 0$ m;

it follows that BA = FA, in case the FA is already corrected by δg_{TOP} which contains gravity effect of masses at the ocean floor.

In oceanic areas the slab density in the Bouguer slab correction term must be modified due to the known water depth “D” and the difference in water- and rock density (Fig. 5). If we assume a crustal rock density of 2 670 kg/m^3 and a water density of 1030 kg/m^3 the resulting density for calculations of offshore Bouguer anomalies is $\rho^* = -1\,640$ kg/m^3.

This results in:

$$BA = FA + \delta g_{BPL} = FA + 2 \pi G \rho^* (H_S - H_D)$$

Figure 5: Full page width

Fig. 5. Illustration for describing the calculation of Bouguer anomalies on continents (A), at the ocean (B) and from satellite (C). (A): On land the reduction density ρ is commonly taken as 2 670 kg m^{-3}. The effect of

topography is already removed. The thickness of Bouguer slab equals the station height (H_s). (B): In contrast the reduction density at sea is – 1 640 kg m^{-3}. It is the difference between the sea water density of 1 030 kg m^{-3} and the rock density of 2 670 kg m^{-3}; thickness of the slab now is equal to the different water depths (D). (C): Calculating a Bouguer anomaly in case of satellite gravity a "mass correction" is calculated: $\delta g_{Mass} = \delta g_{Top} + \delta g_{BPL.}$

2.3 Gravity at passive continental margins

In Fig. 6 a very simple Airy-Isostasy model of a passive continental margin is shown. The continental crust is much thicker than the oceanic crust and above the oceanic crust there is the water cover of a few 1000 meters. The specific geometry of the „crust – mantle – water cover" constellation plays an important role on the trend of the gravity field here. Because of the fact that in the example of Fig. 6 there is no topography, the continental margin remains in an isostatic equilibrium, and one can assume that no Free Air anomaly exists.

Figure 6: One and half page width

Fig. 6. Airy isostatic model at a continent – ocean transition. Notice the thick continental crust and the thin oceanic crust at a passive continental margin. Crust and mantle densities are simplified. Reasonable contrasts which cause large gravity anomalies are related to the water – continent density contrast

and crust – mantle density at the continent of approx. 430 kg m^{-3}. Refer to text for more information.

However, in Fig. 7 (A) strong gravity anomaly results from the same density model (Fig. 7C) which was shown in Fig. 6. The Fig. 7(A) shows the modelled anomaly only for water effect of gravity: related to a model of a “half-indefinite” plate the resulting anomaly is negative and is caused by a strong gradient. Fig. 7 (B) on the other side contains model results which have been done only for the oceanic mantle: now the anomaly is positive and it has a gentle increase because its position is far deeper. Finally Fig. 7(C) demonstrates how the total Free Air anomaly results from the superposition of both effects: the Free Air anomaly is zero in the continental area and over the ocean as well. However, exactly above the margin the gravity field is characterized by a maximum and a minimum that follows. This distribution is a so called „edge“ or boundary effect of the Free Air anomaly and is effected by the difference of the steep gradients in the model.

Figure 7: one and a half page width

Fig. 7. The principal effects on the gravity field at continental margins have equal gravity magnitudes but different gradients. In (A) the water effect causes a steep gradient and in (B) the density surplus of the oceanic mantle is a deeper seated effect which causes only a gentle gradient. In (C) it is explained that a Free Air anomaly at a continental margin is caused by both a negative

and positive “edge effect” due to the superposition of contributions that have equal magnitudes but different gradients.

The trends of a Free air and Bouguer anomalies are shown in Fig. 8. Here modelling again gets use of a „half indefinite“ thin plate for the offshore area (water). It is “zero” over the continent zero and over the oceanic area “positive” (ρ_w = 1030 kg/m^3). The half of the whole Free Air anomaly maximum is accomplished exactly over the edge of the continent.

Figure 8a-b: Full page width

Figure 8c: One and a half page width

Fig. 8. Free Air anomaly and Bouguer anomaly at continental margins which is also in an isostatic balance. (A) The absolute value of the excess mass $|+\Delta m|$ is equal to the absolute value of the deficient mass$|- \Delta m|$. Therefore the integral of gravity change with respect to the x-coordinate is zero: $\int \Delta g \, dx = 0$. (B) The Bouguer correction at the ocean (see Fig. 3) applied to the Free Air anomaly in (A) yields the general form of the Bouguer anomaly at passive continental margins. (C) The “geological” mass inhomogeneities at the continental margins (seaward dipping reflectors, magmatic remnants, salt structures etc.) cause rather local gravity anomalies which superimpose the regional gravity wavelengths – which are effected by the “simple” structures in (A) and (B).

The gravity fields in Figs. 7 and 8 are caused by the over simplified density structure at the “modelled margin” in Fig. 6. In the real world these margins show a rather complicated picture of gravity distribution due to mass inhomogeneities in the Earth´s crust and lithosphere (and even in the mantle) which are the results of the long-lasting history of the breakup of the Gondwana supercontinent. This becomes quite clear if looking at the processed gravity fields which are shown in the series of figures (Fig. 14 through 21) in Section 4. Their interpretation in terms of regional tectonic and distribution of rock densities will help to provide a rather detailed insight into the causing structure (geometry) and density distribution of the passive margins in the South Atlantic region.

Most aspects of the calculated anomalies, both Free Air and Bouguer, which were discussed before, are typical for nearly all of the continental passive and active margins on Earth. In the next Section the focus will be set on the situation in the Southern Atlantic between Africa and South America – the research area of the German Priority Program 1375 “SAMPLE” of the German Science Foundation – DFG (https://www.sample-spp.de/). The acronym stands for “**S**outh **A**tlantic **M**argin **P**rocesses and **L**inks with onshore **E**volution”. In this interdisciplinary project the primary research areas are the mantle dynamics and magmatic processes, the lithospheric structure, deformation processes and rifted margin formation, the post-rift topographic evolution and many more. In the following Section we will concentrate on this part of the world because a big variety of data and information is available to responds to one of the key questions – how modern satellite missions can contribute to the interpretations and to the understanding of the transition from continental to oceanic lithosphere.

2.4 Focus region: South Atlantic passive margins

To study deeper structures and the overall evolution of conjugate passive continental margins of the South African and South American continents 3D structural models have been designed and evaluated by SAMPLE scientists and their international partners: They constructed detailed density models at both sides of the Southern Atlantic Ocean and a rather preliminary density model for the oceanic part in course of a master thesis (Klinge, 2016). These models are constrained by information and data from boreholes, refraction and reflection seismic, seismological tomography and potential field data – mainly gravity field data. Geophysical fields and observations map geometry and distribution of physical properties of the transitional structures of both crust and lithospheric mantle. Model results (Fig. 9) show (Maystrenko et al., 2013; Autin et al., 2016) that basin centers at the western (Argentinean) side are oriented west-east and therefore oblique to the mid ocean rift axis while at the other (African) side basin centers extend parallel to the ocean rift in north-south direction.

Figure 9: One and a half page width

Fig. 9. For illustration this figure portrays a 3D density model of the SW African continental margin (left, modified after Maystrenko et al., 2013), and the density structure at the Argentinean side (right, Autin et al., 2016).

Apart from these structural differences both sides of the Southern Atlantic reveal similar distributions in temperature and density. Small thicknesses and density modifications in the lithospheric mantle point to small lateral variations of heat transfer into the overlaying crust. However, more relevant for the crustal heat field are lateral thickness changes of the crystalline crust which produce the bigger part of radiogenic heat. This contrasts observations and modelling results at passive continental margins in the area of the Northern Atlantic (Scheck-Wenderoth and Maystrenko, 2008). They found that the oceanic part of lithospheric mantle is much thinner and characterized by smaller densities which cause higher temperatures in the upper crust of the ocean.

To contrasting large scale paleostress fields on the correlating margins of the South Atlantic Salomon et al. (2014) point to in their studies of the South Atlantic. They asked themselves “how passive” continental margins across the globe currently are. Following the results of several other studies these margins experience a variety of stress states and undergo significant vertical movements, as they were deduced from studies of paleo-stresses at both sides of the Southern Atlantic. Here, the bounding continents consist of very different recent geological histories: Africa experiencing continental rifting whereas South America is influenced by subduction on the Pacific side. It is not clear to what extent the Atlantic continental margins are subject to the same stresses and vertical motions as the main continents. Their results show that the tectonic evolution of the continental margins of the South Atlantic is not only passive and that both margins vary significantly in structural style and stress fields, indicating that variable plate boundary forces play a major role in margin evolution. In Fig. 10 we show the situation at the S-American and S-African margin with reference of the paleo-stress field, as it was published by Salomon et al. (2014). Their findings demand careful modelling of both continental margins and a geophysical database which is able to resolve even very small modifications of physical parameters and their structures; refer also to Fig 9 (a) and (b) and the 3D density modelling of lithospheric by Maystrenko et al. (2013) and Autin et al. (2016).

Figure 10: Faull page width

Fig. 10. The sketch (Salomon et al., 2014) portrays an E-W cross-Section between South Africa and South America which summarize the situation of their obtained paleo stresses. It shows that the African margin is controlled by extension while compression characterizes the situation at the South American side. Salomon et al. (2014) explained the extensional state in the east by the existing “African superplume” and the compression in the west by the Andean subduction zone.

Novel satellite gravity missions aim at a breakthrough in recovering the Earth´s gravity and magnetic fields, their gradients as well as their temporal variation. Static anomalies in potential fields (refer to Figs. 14 through 21) are caused by irregular mass distribution on and within the Earth, temporal variations of the gravity field are associated with mass transport processes in the Earth system, such as dynamic processes on the Earth's surface, in lithosphere and upper mantle.

3. Modern satellite gravity missions

The launch of the first generation of satellite gravity missions (Fig. 11) has revolutionized our knowledge of the global Earth's gravity field and its temporal changes. The German CHAMP (Challanging Minisatellite payload; mission period 2000-2010; Reigber et al., 2002; http://op.gfz-potsdam.de/champ/) mission, the US/German GRACE (Gravity Recovery and Climate Experiment; mission period 2002-ongoing; Tapley et al., 2004; http://www.csr.utexas.edu/grace/) mission, and the European GOCE (Gravity field and steady-state Ocean Circulation Explorer; mission period 2009-2013; Drinkwater et al., 2003; http://www.esa.int/Our_Activities/Observing_the_Earth/The_Living_Planet_Programme/Earth_Explorers/GOCE/ESA_s_gravity_mission_GOCE) operated by the European Space Agency (ESA), improved significantly the coverage and availability of high resolution and precisely measured data. These gravity missions are the only measurement technique that can directly observe mass changes on a global scale, and thus they provide a unique observation system for monitoring mass transport in the Earth system. For modern magnetic field observation, apart from the CHAMP mission (2000-2010), with ESA's three SWARM satellites that have been successfully launched in November 2013 also gradients observations have become available (http://esamultimedia.esa.int/multimedia/publications/BR-302/).

Figure 11: Faull page width

Fig. 11. Satellite gravity missions CHAMP (left), GRACE (center) und GOCE (right). (Sources: CHAMP: GFZ Potsdam, GRACE: NASA, GOCE: ESA Medialab)

In these missions, three measurement concepts are implemented:

1. Observation of orbit perturbations of low-flying satellites due to the varying gravitational attraction, by Global Positioning System (GPS), with an accuracy of 2-3 cm. Non-gravitational forces acting on the satellite, such as drag of the residual atmosphere or solar radiation pressure, are measured by an accelerometer and corrected for in the frame of the gravity field modelling. This satellite tracking technique between a low Earth orbiter (LEO) and high-flying GPS satellites is called satellite-to-satellite tracking in high-low mode (SST-hl), and is implemented in all three missions CHAMP, GRACE and GOCE. It is the primary measurement technique of CHAMP.

2. Observation of orbit differences (ranges) and their temporal change (range rates) between two LEO satellites. This satellite-to-satellite tracking in low-low mode (SST-ll) concept is realized by the GRACE mission. It consists of two identical satellites following each other on the same orbit with an average distance of 200 km. The inter-satellite ranging is performed by means of a K-band microwave system with micrometer accuracy, and shall be done by laser interferometry in future gravity missions in order to further increase the ranging accuracy.

3. Observation of acceleration differences on very short baselines (satellite gravity gradiometry, SGG), representing second order derivatives of the gravitational potential *V* in all three spatial directions. This concept was

applied by the GOCE mission. Its core measurement, the gravity gradiometer, was composed of 6 accelerometers fixed on 3 orthogonal axes symmetrically around the center of mass of the satellite, measuring acceleration differences on very short baselines of only half a meter in all three spatial dimensions.

The achievable performance of satellite gravity missions depends mainly on the observation technique and the orbit altitude. Fig. 12 shows the performance of different mission concepts in terms of the degree error median, which describes the average signal or noise amplitude at a certain degree *n* of the spherical harmonic series expansion of the gravitational potential *V* in spherical coordinates (with radius *r*, co-latitude ϑ, longitude λ):

$$V(r,\vartheta,\lambda)=\frac{GM}{R}\sum_{n=0}^{N_{\max}}\left(\frac{R}{r}\right)^{n+1}\sum_{m=0}^{n}\bar{P}_{nm}(\cos\vartheta)\left[\bar{C}_{nm}\cos(m\lambda)+\bar{S}_{nm}\sin(m\lambda)\right]$$

where *G* is the gravitational constant, *M* the mass of the Earth*, R* the mean Earth radius, $\bar{P}_{nm}$ the fully normalized Legendre polynomials of degree *n* and order *m*, and $\{\bar{C}_{nm},\bar{S}_{nm}\}$ the corresponding (Stokes) coefficients (e.g Torge, 2001). Therefore, the degree error median describes the achievable gravity field accuracy at a certain spatial (half) wavelength λ. The wavelength λ is linked to the harmonic degree *n* by

λ = 20 000 km/*n*

As an example, a harmonic degree of n = 200, which was the minimum target resolution for the GOCE mission, corresponds to a spatial wavelength of λ = 20 000 km/*n* = 100 km.

As a reference, the stippled black curve in Fig. 12 shows the gravity field signal itself. Correspondingly, the cross-over point of a mission performance curve with the black stippled curve indicates at which harmonic degree the signal-to-noise ratio is ‘1’.

Figure 12: One and a half page width

Fig. 12. Absolute gravity signal and error estimates of different observation concepts as a function of the harmonic degree *n* (bottom axis) and spatial wavelength λ (top axis).

From the orbit information (SST-hl) only the long-wavelength features of the gravity field can be extracted. Although this observation type is not a direct gravity field functional, it can be interpreted as disturbing acceleration acting on the orbit, and thus the first order spatial derivative of the gravitational potential $\partial V/\partial x_i$. As a representative of this measurement concept, the grey dot-and-dashed line curve shows the performance of the CHAMP-only model AIUB-CHAMP 03S (Prange, 2011), which is based on 8 years of CHAMP kinematic orbit data.

The grey curve shows the performance of the recent GRACE-only model ITSG-Grace2014 (Mayer-Gürr et al., 2014), which is based on almost 11 years of K-band inter-satellite ranging data following the SST-ll concept (and supported by SST-hl in the very low degrees). Compared to CHAMP, the superior measurement principle of SST-ll results in a significantly better accuracy in the low to medium degree range as well as a higher spatial resolution. This can be explained by the fact that the SST-ll concept can be interpreted as a measurement of acceleration differences on long baselines of about 200 km. The excellent performance of GRACE in this spectral range makes this mission sensitive to the tiny temporal variations of the Earth’s gravity field, which are 4 - 5 magnitudes smaller than the static signal.

The black solid curve shows the performance of GOCE, represented by the GOCE-only model GOCE-TIM-R5 (Brockmann et al., 2014). It is mainly based on the measurement technique of SGG and again SST-hl in the low degrees, because SGG alone (green curve) is weak in this spectral range due to the specific noise characteristics of the gravity gradiometer instrument. Measuring acceleration differences on very short baselines of about half a meter, which approximate second order derivatives of the gravitational potential $\partial^2 V/(\partial x_i\, \partial x_j)$, enables a further increase of sensitivity for high-frequency signals. GOCE starts to become superior over GRACE approximately at degree n = 115.

3.1 Global Gravity Field Models

Gravity field models including GOCE data from the complete mission period are meanwhile available. While the model GOCE-TIM-R5, which is based on the time-wise approach (Pail et al., 2011), is based purely on GOCE data, GOCE-DIR-R5, which is based on the direct method (Bruinsma et al., 2014), contains also GRACE and satellite laser ranging (SLR) data. Further satellite-only models are, e.g., EIGEN-6S2 (Rudenko et al., 2014), or the S-models of the GOCO series (Pail et al., 2010). The maximum degree of expansion of these models is driven by the resolution of GOCE, and varies from n = 280 to 300, corresponding to about 70 km spatial wavelength. This makes clear that all medium scaled geological structures at continental margins and elsewhere in the world which cause a significant gravity effect can be detected (resolved) in the GOCE gravity field.

Combination models (notice the “C” in the field identifier) including also terrestrial, air- and shipborne as well as altimetric gravity are, e.g., the already mentioned pre-GOCE model EGM2008 (Pavlis et al. 2012), EIGEN-6C4 (Förste et al., 2014), and GOCO05C (Fecher et al., 2013, 2016). These models extend the spatial resolution beyond degree 2000 (which corresponds to 10 km wavelength). However, it should be noticed that there are many regions with sparse and/or low-quality terrestrial data, where it has to be questioned if such a high resolution is justified. This holds for many areas worldwide, e.g., the Central Andes in South America and also for the passive continental margins of the South Atlantic.

3.2 Products for use in Earth sciences interpretation

Specifically regarding GOCE-related data, modelers and other users have the choice among basically three representations of gravity field products:

3.2.1 Spherical harmonic coefficients

The most commonly used representation of the global gravitational potential *V* is its series expansion into spherical harmonics (Section 3). There corresponding fully normalized spherical harmonic (Stokes) coefficients $\{\bar{C}_{nm}, \bar{S}_{nm}\}$ represent the model parameters, and are usually the target quantity when deriving the model from the original gravity field data. The advantage of using this representation is that it can be considered as a weighted average of the original measurement data, so that the original noise level is significantly reduced due to this averaging. Based on the set of spherical harmonic coefficients any arbitrary gravity anomaly can be derived at the Earth's surface or at any height in outer space. All the global gravity models discussed above are given in this parametrization.

3.2.2 Original gravity gradients along the satellite's orbit

In principle, also the gravity gradient time series for all six tensor components measured along GOCE's satellite orbit can be used for geophysical modelling (refer e.g. to Fig. 3). They represent the most original measurements. However, it has to be considered that they are measured in a rotating reference frame, the so-called "gradiometer reference frame" (GRF), which means that tensor rotations of the base functions have to be applied to exploit them to the best possible extent. Additionally, they are affected by the colored noise characteristics of the GOCE gradiometer (Pail et al., 2011), so that a single point-wise gravity gradient observation is affected by large instrument noise, and therefore by itself has a low signal-to-noise ratio. All these drawbacks make it difficult to use this data type directly for geophysical modelling.

3.2.3 Gravity gradient grids

A reasonable compromise between the use of spherical harmonics and original gravity gradients (see above) results in the use of *gravity gradient grids*, which are usually defined in a well-oriented radial (North-East-up) frame at a constant altitude. They are computed from the original gravity gradients defined in the GRF by means of regional gravity processing methods. In fact, they are the spatial equivalent of the spherical harmonic representation, but much easier to use and interpret. Pure GOCE gravity gradient grids result from the space-wise method (Gatti and Reguzzoni, 2015). In the frame of the ESA project GEOExplore global grids of all six components of the gravity gradient tensor, based on a combination of GOCE and GRACE data, and defined in a radial Earth-fixed reference frame at two altitudes of 225 km and 255 km, have been derived (Bouman et al., 2015). Since these grid values are products of “averaging” original gradient data, the error level should be similar as that of gradients synthesized from global spherical harmonic models.

There is an ongoing discussion whether the gradient data contain more (high-frequency) signal than global gravity models that have been derived from them. The answer to this question lies in the constraints applied to these models. Constraints applied to global gravity models are usually designed to optimize the signal-to-noise ratio on a global scale. This means that in regions of very rough topography and therefore high-frequency gravity signals there is the tendency to constrain the system too strongly. Regional gravity solutions techniques, which are usually applied to generate gridded gravity gradient products, allow for regionally optimized constraints, but on the cost of global homogeneity. In Pail et al. (2015b) it could be shown, that compared to global models the gravity gradient grids are affected by a higher noise level.

The achievable accuracy and sensitivity of current gravity field models or corresponding gravity (gradient) grids can be expressed by cumulative quantities, which describe the estimated cumulative error at a certain harmonic degree (or the corresponding spatial wavelength). Fig. 13 shows cumulative gravity anomaly errors (a), as well as cumulative vertical gravity gradient errors at GOCE satellite altitude of 250 km (b), and ground level (c), for the GRACE models ITSG-GRACE2014s, the pure GOCE model GOCE-TIM-R5, the combined satellite-only model GOCO05S and the combined models EGM2008 (pre-GOCE) and GOCO05C (including GOCE data).

From Fig. 13 we can learn which geological structure at passive continental margins (or elsewhere) can be resolved by the different gravity model types. Assuming that the geological structure/mass anomaly generates a *gravity anomaly* with a certain spatial wavelength on the Earth's surface, Fig. 13a then provides the accuracy in mGal with which this anomaly can been captured. (The connection from the size of a disturbing body to the resulting gravity signal is made in Fig. 3.). As an example, a gravity signal with 100 km spatial wavelength at the Earth's surface could be measured by satellites with an accuracy of about 0.5 mGal (black dashed and solid grey curves). It can clearly be seen that the accuracy for shorter wavelength signals dramatically decreases, and is already larger than 2 mGal for gravity signals with approx. 80 km spatial wavelength. Beyond this resolution, satellites cannot significantly contribute anymore, and high-accuracy terrestrial information, as it was included, e.g., in

Figure 13: Full page width

Fig. 13. Cumulative gravity anomaly errors in (mGal) (a); vertical gravity gradient errors in (mE) at 250 km (b), and ground level (c). This figure shows the generally dramatic increase of the gravity gradient errors at ground level as a result of downward continuation.

GOCO05C (solid black curve), is necessary to resolve smaller-scale geological structures. This becomes immediately clear if looking at the series of Figs. 14 through 21: most of the anomaly sizes at the margins of the South Atlantic are smaller than 80 km. On the other hand we state that the regional gravity field caused at the ocean-continent transition can satisfyingly be resolved by satellite only models (S models). Fig. 13a also shows the major step forward due to satellite missions compared to pre-GOCE models such as EGM2008 (black dot-and-dashed line) especially in the long to medium wavelengths for gross interpretations at a continental scale.

Fig. 13b shows a similar representation when using *gravity gradients* at satellite altitude as basis information for geophysical modelling of geological structures. Pure GOCE-only models such as GOCE-TIM-R5 (dashed black curve) provide gravity gradients at satellite altitude with standard deviations of 0.45 mE for gravity signals with a spatial resolution of 100 km. These values can be decreased further to 0.25 mE by combination with GRACE information, as it was done, e.g., in the GOCO05S model (solid grey curve). Evidently, GRACE alone (dashed grey curve) results in very high error amplitudes in the higher degrees, demonstrating the dominant impact of GOCE at shorter wavelengths. Modern combined gravity models such as GOCO05C (solid black curve) further increase the performance in the short-wavelength range by complementing the satellite data by ground data over the continents and satellite altimetry over the oceans. Also here the improvement compared to pre-GOCE combined models such as EGM2008 (black dot-and-dashed line curve) is significant. Recently gradients of the satellite gravity field came into the focus for modelling purposes which can support interdisciplinary interpretations (Ebbing et al., 2013; Schaller et al., 2015; Götze, 2015).

In Fig. 13b a very interesting feature is the flat curve of the combined gravity model GOCO05C beyond degree 250. This results from the fact that beyond this degree the signal amplitude of gravity gradients is already below the mE level, i.e., due to signal attenuation with altitude there is no significant gradient signal left in orbit altitude beyond this degree, because most parts have been “filtered out” due to upward continuation. Inversely, this also means that GOCE has captured 97% of the amplitude of the gradient signal that exists in orbit altitude.

The picture changes completely (Fig. 13c) when continuing the gradient information down to ground level. Here the GOCE model (black dashed curve) and the GOCE+GRACE combination (solid grey curve) perform practically identical, again showing the dominance of GOCE compared to GRACE at shorter scales. However, also here for gravity signals with spatial scales below 80 - 100 km a combination with terrestrial/airborne gravity information is necessary to achieve acceptable accuracies (solid black curve), so that the gravity field information can be used for local geophysical modelling of short-scale density structures.

3.3 Not always in focus: the omission error

In order to perform a complete evaluation of the impact of modern satellite missions for deriving density structure of continental margins, one of the most important aspects is the evaluation of the *omission error*. It results from high-frequency signals, which cannot be resolved by satellite gravimetry due to the exponential signal attenuation with altitude. These missing signals of satellite-only models are an important issue for the determination of near-surface density variations, but also shallow lithospheric structures.

Fig. 14 shows gravity anomaly fields for the South Atlantic region. Fig. 14 a is based on the GOCO05S model resolved up to its maximum resolution of degree *n* = 280 (~ 70 km), while Fig. 14 b displays the free-air gravity anomalies based on EIGEN-6C4 with its maximum resolution of degree *n* = 2160 (10 km). Comparing these two figures, the current limits of satellite-only models regarding their spatial resolution becomes evident, and can only be coped with by combination with complementary data sources from terrestrial/airborne/shipborne gravimetry, and satellite altimetry over the oceans, as it was done in EIGEN-6C4. An estimate of the omission error (Fig. 14 c) for satellite gravity models is given by the difference of EIGEN-6C4 and GOCO05S, being equivalent to the difference of the Figs. 14 a and b. Evidently, very rough topographic and bathymetric structures, generating high-frequency gravity field anomalies and steep slopes, cannot be resolved by the satellite data. However, usually these topographic features are not the main focus of geophysical modelling and interpretation, but rather sub-surface lithospheric structures. Therefore, a topographic reduction was applied, using the RWI_TOPO_2015 topographic potential model (Grombein et al., 2015) and thus taking away the effect of topographic masses up to zero level: $\delta g_{TOP} + \delta g_{BPL}$. The so called "mass reduction effect" was already introduced in Fig. 6. The result is a significantly reduced omission error (Fig. 14 d).

This difference field in Figs. 14 c and d can be considered as errors made when computing Bouguer anomalies from pure satellite models, which are then further used for lithospheric modelling. Table 1 gives an overview of the main statistical parameters of the gravity anomaly fields shown in Fig. 14.

Figure 14: Full page width

Fig. 14. Free-air gravity anomalies (mGal) of the South Atlantic region based on satellite-only model GOCO05S (a) resolved up to degree 280 , combined gravity model EIGEN-6C4 (b) resolved up to degree 2160, omission error of a satellite-only model (c) and omission error after reduction of topographic signals (d).

Table 1: Main statistical parameters of gravity fields of the South Atlantic region.

Gravity field	Figure	min (mGal)	max (mGal)	std.dev. (mGal)
GOCO05S (d/o 280)	14 a	-199.8	116.1	18.8
EIGEN-6C4 (d/o 2160)	14 b	-227.7	453.8	21.3
GOCO05S omission error	14 c	-166.7	415.1	10.8
GOCO05S omission error, topo-reduced	14 d	-143.1	112.8	7.1

4. Benefits for combined interpretations

However, in relation with the two key questions asked in Section 2.3 (processing, quality and secondly availability for interpretations at continental margins) we have to respond to them in the light of interpretations of solid Earth structures. For example a precise geoid can be used to identify global and deep anomalies related to mantle lithosphere and deeper structures. Gravity anomalies, being first order radial derivatives of the gravitational potential, are sensitive to gravity effects of the entire lithosphere, and in particular to the crustal and upper crustal structures and density variations e.g. at active and passive continental margins. As it has been shown above (Fig. 14), each combination of satellite gravity data with terrestrial gravity data can be used for all interdisciplinary interpretations techniques, e.g., “back stripping” in basin modelling at the African continental margin (Dressel et al. 2015) which also includes thermal subsidence in the reconstruction of the passive margins through time or 3D modelling of Moho undulations. The new database was also used to reconstruct the Gondwana continent (Braitenberg, 2015). Fig. 15 refers to the isostatic residual anomaly in the Southern Atlantic. It was calculated by Klinge (2016) on base of the corresponding formula for “ISA” in Section 2.3 and the EIGEN-6C4 model also portrayed in Fig. 14 (b).

Both anomaly maps are rather similar and caused by the main tectonic features of the South Atlantic: the “highs” which are caused by the Mid Atlantic ridge, the extended “lows” of the four basins in front of South America (Argentinean and Brazilian basins) and South Africa (Cape and Angola basins). The hotspot trail (e.g. Torsvik et al., 2009 among others) is visible in the structure of the SW-NE trending Walvis Ridge offshore South Africa and the corresponding trace of the Rio Grande Rise at the western side. To the North of the Romanche Fracture Zone between Fortaleza in the west and Lagos in the East the Sierra Leone Rise is located. Even the regions of salt deposits offshore Brazil and West Africa (blueish colors indicating low gravity values) and the magmatic margins at both sides of the margins (reddish colors and high gravity values) can be distinguished in the satellite derived fields. The very short wavelengths in the gravity field correspond to masses that are located in the crust and lithosphere – they were already mentioned in the sketch of Fig. 8 and mark places of different density contrast at the margins. Other examples were given in Bouman et al. (2014), Gutknecht et al. (2014), and Hosse et al. (2014).

Figure 15: one and a half page width

Fig. 15. The isostatic residual field was calculated by Klinge (2016) in the framework of his MSc thesis. Reference depth T_0 = 30km and T_e = 20 km (elastic thickness

which was kept constant over the entire area). The figure shows the residual gravity field in the Southern Atlantic Ocean of the combined EIGEN-6C4 model (Förste et al., 2014). It correlates well with bathymetric/topographic structures e.g. the Mid Atlantic Rift (MAR) and portrays also the effect of geological bodies: the positive anomalies in the area of Windhoek and Buenos Aires. Along the Mid-ocean rift axes positive anomalies of up to 40 mGal exist. MAR = Mid Atlantic rift.

4.1 The continental margins of the South Atlantic

New light can be shed on the gravity structures of South Atlantic oceanic margins at regional (Figs. 16, 17, 19 and 20) and more local scales (Figs. 18 and 21). By the help of these new compiled maps we will show that modern satellite gravity fields described in Section 4 can support (1) interpretations of the lithospheric structures in the South Atlantic and its passive margins and (2) provide much more details in the gravity field than it was showed along the oversimplified profiles of Figs. 7 and 8.

With reference to the Fig. 14, the following sequence of Figs. (16 – 21) contains always the same information for comparative reasons: the two gravity fields based on the “satellite only” model GOCO05S (a) and the “combined model” EIGEN-6C4 (b), and additionally Figs. 18 and 19 include the omission errors *without* (c) and *with* (d) calculated topographic reductions.

Table 2 provides a summary of the standard deviations of the gravity fields shown in these figures. **d**/**o** refer to the spherical harmonic analysis: to **d**egree and **o**rder of the expansion.

Table 2: Standard deviations (mGal) of the gravity fields shown in Figures 16 to 21.

Region	Figure	GOCO05S	EIGEN-6C4	GOCO05S	GOCO05S

		(d/o 280)	(d/o 2160)	omission error	omission error, topo-reduced
Argentinean coast	16	22.4	24.6	9.8	7.1
Brazilian coast	17	15.9	18.8	10.8	6.3
Falkland Bank	18	24.4	25.3	7.3	5.9
African coast	19	19.3	21.5	10.6	7.3
Equatorial African margin	20	19.3	23.9	14.3	9.8
Tristan da Cunha isle	21	6.9	12.3	10.3	4.8

Continental gravity edge effects indicate a fast change from positive to negative anomalies as it is normal for the transition from oceanic to continental crust. In Fig. 16 the positive anomalies indicate in the offshore area the seaward dipping reflectors (SDR) which are of magmatic origin (e.g. Blaich, 2011; Franke et al. 2006; Section 2). The negative anomalies (greenish and blueish colors) offshore are caused by the sedimentary infill of the margin basins e.g. Colorado and Salado (e.g. Autin et al., 2013; 2016). Onshore positive anomalies follow W-E trending topographic features (Salado and Colorado Basin) and in the western continental part of the maps the topography of the Southern Central Andes.

Figure 16: Full page width

Fig. 16. Detailed picture of the free-air gravity field along the Argentinean coast compiled by the GOCO05S (a) and the EIGEN-6C4 (b) models. The lower two

figures indicate the omission errors without (c) and with topographic correction (d). For more information refer to manuscript. The continental areas are marked by transparent overlays.

In general the series of the following figures will portray similar gravity anomalies (both magnitude and trend of anomalies). It is no wonder that all EIGEN-6C4 compilations consist of more structural details than the GOCO05S models which base on data in the orbit height of some 250 km where small local gravity anomalies are not detectable.

Figs. 17 (a) and (b) shows that the “central Atlantic segment” is dominated by high density rocks which cause positive anomalies. The positive gravity offshore between 40° - 30° longitude is caused by the “Rio Grande High” which marks the most western edge of the hot spot trace which starts at the position of the Tristan da Cunha hotspot area. The negative gravity anomalies close to the Brazilian coast are caused by negative densities of salt accumulation here (Mohriak, 2014). The SDRs with their high rock densities (Section 2.2) of the southern segment are not documented here with high resolution; they are too small to be resolved *in detail* as we show already in Fig. 3. However, at a larger scale the belt of positive gravity marks the area of SRDs quite well.

Figure 17: Full page width

Fig. 17. The gravity fields (a) GOCO5S and (b) EIGEN6C4 along the Brazilian coast and offshore regions of the “central segment” of the southern Atlantic. Figures content is equal to Figs. 14 and 16. However the omission errors are not portrayed here.

The resolution of gravity anomaly in the off-shore area of the *Falkland Bank* and the Scotia Plate with the Eastern Sandwich trench allows the separation of subduction related trench lithosphere, the eastern border of the Sandwich Plate, and the southern rim with the Antarctic Plate (low gravity corresponding to blueish colors in Fig. 18) from high density rocks of the Scotia Plate and Sandwich Isles (yellow and reddish colors in Fig. 18 (a and b). Exactly here in a region with rather complex interplay of different plates the resolution of gravity fields before the era of the modern satellite missions was extremely low and often hindered a tectonic interpretation of lithosphere at medium scale. The Scotia Plate in the center (reddish colors in Fig. 18) is clearly separated from the other plates of the region (South American plate to the North, Antarctic plate to the South, Scotia plate to center.

Figure 18: One and a half page width

Fig. 18. The gravity field of the Falkland bank and the Scotia plate with the eastern South Sandwich trench after the processing of new satellite gravity (GOCO5S: (a) and EIGEN6C4: (b). Figures content is equal to Fig. 14.

Due to the symmetry of evolution of the South American and South African margins also the gravity field of the western African margin shows the same general features as it was exemplified for the South American margin: in the southern segment the magma dominated structures cause small positive gravity anomalies and North of the Walvis Ridge the area of salt layers is characterized by negative anomalies (blueish colors) in Fig. 19. The SW – NE trending Walvis Ridge separates the domains of magmatic material from salt layers. Positive gravity anomalies of the ridge clearly indicate the Tristan da Cunha hotspot trace – as it was already explained for the western part of the Southern Atlantic. More to the South at the South African tip of the Cape a second ridge (Agulhas Ridge) can be identified.

Onshore at the African continent close to the equator the extended gravity low (-50 mGal) of the Congo Basin with its thick sediments dominates the gravity picture.

Figure 19: full page width

Fig. 19. The gravity field of the African margin in the central and southern segment (Fig.15) after the GOCE gravity (a) and the EIGEN-6C4 data (b) processing. The series of maps correspond to the displayed formats of figures before; transparent overlay mark continental area.

One of the most spectacular fracture zones in the Equatorial and Northern South Atlantic connecting Africa and South America is illustrated in Fig. 20 (a and b). Fairhead and Wilson (2005) explain the formation of the fracture system with processes which were related with the opening of the Central and South Atlantic. They state that a differential motion between plate segments was absorbed in the Caribbean and West and Central African rift systems. The fracture system developed due to the temporal different opening phases of the northern and southern Atlantic. Then the two independent spreading centers joined a major shear zone developed between West Africa and the northern margin of Brazil. The maps of satellite gravity image impressively this major shear zone. The gravity map of the EIGEN6C4 model provides a clear and sharp picture of the fractures zones.

Figure 20: One a a half page width

Fig. 20. The two gravity fields (GOCO5S (a) and EIGEN (b)) of the Equatorial Atlantic Ocean map major transform structures offshore the African margin. Sequence of maps corresponds with displayed formats of figures before; transparent overlay mark continental area.

The limits of resolution of modern satellite only gravity fields (S models) can nicely be demonstrated by the gravity field of the Tristan da Cunha Isle, whose gravity field signal is at the edge of the spatial resolution of current satellite gravity missions. Fig. 21 shows that although GOCE is able to detect the gravity field signal of this island, it is significantly damped. It should be emphasized, that a constraint has been applied to the GOCO05S model in the frame of the gravity modelling procedure in order to improve the signal-to-noise ratio at higher degrees, i.e. noise is filtered out at the cost of damping also the signal. As already discussed in Section 3.2, the strength of constraining the solution was optimized on a global scale. Therefore, it is not tailored to small regions with strong gravity field signal, where a weaker constraint would be preferable due to a larger signal-to-noise ratio in this region compared to the global average. If the satellite gravity solution were optimized for this specific region, it can be expected that in such a regionally tailored solution slightly more signal could be retained. The series of Figs. 21 (a) – 21 (d) shows that the satellite gravity fields of both GOCE and EIGEN-6c4 are mainly caused by the topography of the island. Perfectly seen is the “ring” of negative anomalies in Fig. 21 (b) which can be explained by the flexure of oceanic lithosphere due to isostatic response of the loaded isle masses. After calculating a topographic correction (Fig. 21 (d)) an anomaly of some 20 mGal appears. One may speculate if this negative anomaly is caused by a mass deficit which is related to the hot spot or to crustal thickening..

The statistics in Table 2 shows that for such rather small-scale structures the amplitude of the omission error can be larger than the signal captured by GOCE. However, Fig. 21d shows that significant parts of this high-frequency gravity signal result from topography.

Figure 21: one a half page width

Fig. 21. The Free Air gravity field of the Tristan de Cunha area after the GOCE (a) gravity and EIGEN-6C4 (b) data processing. Sequence of the four maps corresponds with displayed formats of figures before; omission error without (c) and (d) with topographic correction. The limits of resolution of satellite observations can nicely be demonstrated by these gravity fields.

Figure 21a: Small column size

Fig. 21a. In addition to what we interpret in Fig. 21 this sketch can explain the typical negative ring around the positive anomaly in the last figure: the central mass causes the positive anomaly while the sediments around the central mass cause a symmetrical gravity low. The extent of deformed crust below the mass crust depends on the rigidity of the surrounding crust: the left situation (rigidity R1) demonstrates a case with extreme high rigidity, on the right a lower crustal rigidity R2 was assumed.

4.2 Validation of terrestrial gravity by GOCE data

The GOCE mission provided not only new geoid and gravity fields, but also gravity gradient data. Representing the second derivatives of the gravitational potential, they are more sensitive to the density structures of the upper crust than gravity data normally are. Additionally, gravity gradients provide a better resolution of flanks of geological structures, faults, lineaments or even large intrusions at continental margins. Gradient data from satellite missions have the potential to identify the extent of different structures with varying densities even in the lower crust (e.g. Ebbing et al., 2013). Panet et al. (2014) even identify correlations of certain components of the gravity gradient tensor with lower mantle structures.

For gravity interpretations at larger wavelengths the new satellite gravity database will help to identify a density zonation and segmentation in horizontal and vertical directions in the lithosphere. As shown in Section 3.2, GOCE satellite-only gradient data provide a spatial (horizontal) resolution in the range of less than 100 km. However, for many structures - in particular for offshore studies of Applied Geophysics - this spatial resolution is not yet sufficient, because smaller crustal structures cause anomalies with smaller spatial wavelengths. Therefore, terrestrial and airborne gravity measurements have not become obsolete even in the modern satellite era, but on the contrary they complement satellite observations on the short-wavelength scale where satellite data lack sensitivity.

In addition to their very high accuracy in the long to medium wavelength range, modern satellite gravity data definitely provide significant added value in the geophysical gravity fields processing domain, especially for:

a) Validation of heterogeneous terrestrial gravity data bases and identification of outliers;

b) Fill-in of regions with sparse terrestrial data coverage or even data gaps.

As an example of the first task (a), Fig. 22 a shows the difference between a terrestrial gravity data base of South America and GOCO05S, resolved up to degree 200. To bring them to the same spatial resolution, the terrestrial data have been expanded as part of a global 0.25° × 0.25° terrestrial gravity anomaly grid into a spherical harmonic series to degree 720, and then have been cut at degree 200. Fig. 22 a clearly indicates systematic differences, which can be attributed to errors of the terrestrial data, because of the globally homogeneous accuracy of less than 1 mGal for the satellite model. Based on this result, the terrestrial database can be further screened for outliers and suspicious observations (either of the gravity value itself or the attached height information, Hosse et al., 2014). This information can then be used to derive empirical error estimates of the terrestrial dataset, which can be further used for a spatially depending weighting scheme in the frame of a combined solution with satellite data (Fecher et al., 2013, 2016). The implicit assumption is that the data quality of a terrestrial observation is already reflected in its long-wavelength component. By means of this procedure, satellite data get a higher weight in regions where a lower accuracy of terrestrial data is suspected.

Figure 22: Full page width

Fig 22. (a) Gravity anomaly differences (mGal) between a South American terrestrial database (kindly provided by the US National Geospatial-Intelligence Agency) and GOCO05S, consistently resolved up to degree 200; b) empirical error estimates (mGal) derived from the difference field (after: Fecher et al. (2015), modified).

It should be emphasized, that this validation procedure can be applied in any region on Earth. Thereby, a globally uniform satellite gravity model provides the chance to estimate a-posteriori the accuracy and reliability even of historical gravity data bases (terrestrial, ship- and air-borne), for which only incomplete or even no meta-information about the measurement process and conditions is available.

Also Bomfim et al. (2013) describe how gradients of the GOCE mission can help to estimate systematic errors in terrestrial gravity data in the cratonal basins (e.g. Amazon and Parnaiba Basins) in Brazil. Here they calculate an average value of terrestrial gravity anomaly and compare its long- and medium-wavelength content of the terrestrial gravity with the GOCE gravity field. The analysis shows that where terrestrial data are sparse and therefore require an improvement in data coverage, satellite data can be substituted in order to represent the gravity field correctly. The method they proposed can be used directly to control other gravity databases and constitutes as a tool for the quality assessment of terrestrial gravity observations, both on- and offshore.

The second task (b) also addressed the heterogeneity of terrestrial gravity data. There are many regions worldwide where terrestrial data are of very bad quality or not available/accessible at all (refer to Fig. 2). In these regions, data from satellite gravity missions are the only available data source.

These examples demonstrate, that although satellite missions provide (only) long to medium wavelength gravity field data, they are able to provide new gravity field information especially in regions where up to now the gravity field has been practically unknown. This regional model can then been used as constraint for an improved lithospheric density model and the derivation of the state of stress of the subduction zone (Gutknecht et al., 2014), clearly demonstrating the added value of GOCE especially in these data-critical onshore regions.

5. Conclusions and outlook

The resolution of “satellite only data” up to now does not fall below a resolution of 80 - 100 km. This is still the borderline for studies presented in the above mentioned Sections. In summary we have to say that rather small complex structures related e.g. to the “seaward dipping reflectors at passive continental margins (SDR)” with small size and density contrast cannot be resolved as separated anomalies in the orbit heights of recent satellite missions (e.g. Schaller et al. 2015). For this purpose terrestrial gravity data have to be combined with satellite data in gravity models e.g. GOCO5C. The interpretations of Section 4.1. showed that gravity and its gradients from the modern satellite missions support interpretations at a medium scale – at passive continental margins and elsewhere.

Modelers of lithospheric structures at continental margins hope that medium scale gravity data from the recent and future satellite missions (GRACE and/or GOCE; GRACE follow on) can support combined interpretation together with seismological and gravity studies. For rather local models (wavelengths of gravity anomalies are smaller than 20 km) both resolution and quality of satellite only gravity data have to be seen still reluctant until today. However, there is no doubt that combinations with terrestrial gravity data bases and satellite gravity with a spatial resolution of 10 – 20 km can provide detailed insight in the structural behavior of continental margins.

For modelling at continental scales Fig. 2 demonstrated that terrestrial databases often are of inhomogeneous distribution (e.g. in South America), just if gravity data are sampled over long time-consuming field campaigns with big human efforts: there remain big gaps in the data base. They are mainly caused by limited access to the terrain in remote areas of the world – high mountains, deserts, swamps and jungle. Even more field procedures and technical instrumentation varied over time and together with missing other metadata a homogeneous data base can be established only with big effort and high costs. Here the new data bases already helped in a spectacular way: Hosse et al. (2014) and Gutknecht et al. (2014) replaced the incomplete terrestrial gravity data base by homogeneously measured satellite gravity and gravity gradient data for lithospheric modelling. New data were applied to the calculation of GPE (gravity potential energy), stress distributions and combined interpretation of complex geologic structures. Satellite gravity information was also used for validation and cleaning of inhomogeneous gravity databases taking the benefit of very homogeneous error characteristics and accuracy of global satellite gravity data (Hosse et. al, 2014; Bomfim et al., 2013). The high spatial resolution of terrestrial gravity *combined* with the homogeneous lower-orbit satellite data leads to more detailed and better-constrained lithospheric density models, and hence improves our knowledge about structure, evolution and state of stress in the lithosphere basing on the consistency in the long-to-medium wavelengths, down to 10 – 50 km.

At the beginning (Section 1.1) we mentioned the calculation/recalculation of the COB from an integrated interpretation of gravity, magnetic, seismic, electrical methods and geology (Torsvik et al., 2009). We did not deal with the calculation of COB, however, we think that the combined satellite fields can successfully replace the terrestrial gravity data which have to be used in former times. Because we analyzed Free Air gravity from the GOCE mission, in Fig. 23 topographic features on- and offshore are enhanced. These enhancements indicate clearly the slopes of the continental shelf regions of the Southern Atlantic.

Figure 23: Full page width

Fig. 23. The third derivations of the gravitational potential and the resulting total gradient of the vertical gravity gradient were calculated from the GOCO5C model (expansion to degree 720). It provides already good insight into local gravity field structures particularly at the margins by the derivations of the vertical gradient (V_{zz}).

In the near future complementary information from seismic and magnetics could be included in a joint inversion for lithospheric modelling also at passive continental margins. ESA's magnetic field mission *Swarm* was successfully launched in November 2013 and provides valuable information of the long to medium wavelength Earth's magnetic field and its temporal variations with an accuracy on the nT- (nano tesla) level (http://esamultimedia.esa.int/multimedia/publications/BR-302/). The value of the mission for the determination of the crustal remanent magnetic field will increase in the future, because the three satellites will continuously lower their orbit altitudes during mission lifetime, thus also increasing their sensitivity for detail magnetic field structures. However, a joint interpretation of remanent magnetic and gravity field is only possible in the case of common sources, i.e. similar contrasts in density and magnetization. In this case Poisson's equation can be applied, which links the magnetic and gravity potential fields. Swarm is already now a very valuable tool to determine the electric conductivity of the Earth's mantle and thus provides very important information on the thermochemical and compositional structure of the Earth.

Several concepts for future satellite mission constellations to explore the Earth's potential fields are under development and investigation. A strong need by the user communities was expressed in terms of a joint IUGG resolution adopted at the IUGG General Assembly 2015 (IUGG, 2015). The science requirements and user needs for a future gravity field mission constellation were consolidated (Pail et al., 2015a) also under active participation of the geophysical user community. In addition to an improved temporal resolution for the detection of co- and post-seismic deformation, an increased spatial resolution together with an improved accuracy will shift the capabilities to use satellite-based gravity observations for geophysical interpretation in passive continental margins, and elsewhere, to even more small-scale structures.

Acknowledgements

The research partly described here in this paper was part of the Priority Program SAMPLE (**S**outh **A**tlantic **M**argin **P**rocesses and **L**inks with onshore **E**volution). It is financed by the Deutsche Forschungsgemeinschaft (DFG), Bonn which is thankfully acknowledged. HJG thanks M. Scheck-Wenderoth and members of her research team at GeoForschungsZentrum Potsdam for their continuous interest and many fruitful discussions over the last years. The satellite part of the paper was elaborated in a second DFG Priority Program “Mass Transport and Mass Distribution”. HJG and RP are deeply grateful to their research teams at the Christian Albrechts Universität Kiel, Technische Universität München and Friedrich-Schiller-Universität, Jena. We thank Reiner Rummel and Jörg Ebbing for their intensive “test reading” and fruitful suggestions. Carla Braitenberg, Bruno Meurers and an anonymous reviewer improved an earlier version of the paper by their careful reviews.

References

Autin, J., Scheck-Wenderoth, M., Loegering, M.J., Anka, Z., Vallejo, E., Rodriguez, J.F.,Dominguez, F., Marchal, D., Reichert, C., di Primio, R., Götze, H.-J., 2013. Colorado Basin 3D structure and evolution, Argentine passive margin. Tectonophysics 604, 264–279, doi:10.1016/j.tecto.2013.05.019

Autin, J., Scheck-Wenderoth, M., Götze, H.-J., Reichert, Ch., Marchal, D., 2016. Deep structure of the Argentine margin inferred from 3D gravity and temperature modelling, Colorado Basin. Tectonophysics 676, pp. 198-210, doi.org/10.1016/j.tecto.2015.11.023.

Baeschlin, C. F., 1948. Lehrbuch der Geodäsie. Verlag Orell Füssli, Zürich.

Bauer, K., Neben, S., Schreckenberger, B., Emmermann, R., Hinz, K., Fechner, N., Gohl, K., Schulze, A., Trumbull, R.B., Weber, K., 2000. Deep structure of the Namibia continental margin as derived from integrated geophysical studies. Journal of Geophysical Research 105, pp. 25 829 - 25,853.

Basile, C., 2015. Transform continental margins - Part 1: Concepts and models. Tectonophysics, Elsevier, no. 661, pp.1-10. 10.1016/j.tecto.2015.08.034

Benioff, H., 1954. Orogenesis and deep crustal structure – additional evidence from seismology, Bulletin of the Seismological Society of America, 66, 385–400.

Blaich, O. A., Faleide, J. I., Tsikalas, F., 2011. Crustal breakup and continent-ocean transition at South Atlantic conjugate margins, Journal of Geophysical Research. 116, B01402, doi:10.1029/2010JB007686.

~~Bocher, M., Coltice, N., Fournier, A. and Tackley, J.P., 2016. A sequential data assimilation approach for the joint reconstruction of mantle convection and surface tectonics. Geophysical Journal International, 204, pp. 200-214.~~

Boltwood, B., 1907. The Ultimate Disintegration Products of the Radio-active Elements. Part II. The disintegration products of uranium. American Journal of Science series, 4, 23, 77–88. doi:10.2475/ajs.s4-23.134.78.

Bomfim, E.P., Braitenberg, C. and Molina, E.C., 2013. Mutual evaluation of global gravity models (EGM2008 and GOCE) and terrestrial data in Amazon Basin, Brazil. Geophysical Journal International, 14 pages, doi: 10.1093/gji/ggt283.

Bond, G.C., Nickelson, P.A., Kominz, M. A., 1984. Breakup of supercontinent between 625 Ma and 55 Ma, New evidence and implicationes for continental histories. Earth and Planetary Science Letters, 70, 325-345.

Bouman J., Ebbing J., Meekes S., Fattah R.A., Fuchs M., Gradmann S., Haagmans R., Lieb V., Schmidt M., Dettmering D., Bosch W., 2015. GOCE gravity gradient data for lithospheric modeling. International Journal of Applied Earth Observation and Geoinformation 35(A): 16-30, Elsevier, 10.1016/j.jag.2013.11.001.

Bouman, J., Fuchs, M., Lieb, V., Schmidt, M., Ebbing, J., Holzrichter, N., Gradmann, S., Abdul Fattah, R., Meekes, S., Novak, P., Sebera, J., 2014. GOCE+ GeoExolore - Final Report ESA, RP-GOCE+-DNT-11, 2.1, 1 – 443.

Braitenberg, C., 2015. Exploration of tectonic structures with GOCE in Africa and across continents. International Journal of Applied Earth Observation and Geoinformation, 35, pp. 88-95.

Brockmann, J.M., Zehentner, N., Höck, E., Pail, R., Loth, I., Mayer-Gürr, T., Schuh, W.-D., 2014. EGM_TIM_RL05: An independent Geoid with Centimeter Accuracy purely based on the GOCE Mission. Geophysical Research Letters, Wiley, doi: 10.1002/2014GL061904.

Bruinsma, S.L., C. Foerste, O. Abrikosov, J.M. Lemoine, J.C. Marty, S. Mulet, M.H. Rio und S. Bonvalot. 2014. ESA's satellite-only gravity field model via the direct approach based on all GOCE data. Geophysical Research Letters, 41(21), 7508–7514, DOI: 10.1002/2014GL062045.

Cappelletti, A., Salvi, F., Meda, M., Cavozzi, C., Chowdhury, B.R., Nestola, Y., Argnani, A., Tsikalas, F., Magistroni, M., Dalla, S., Roveri, M., Bevilacqua, N., 2011. Tectono-Stratigraphic Evolution of South Atlantic Extensional Rifted Margins: Constraints from Sandbox Analogue Modeling. Search and Discovery Article, no. 30204.

Colli, L., Ghelichkhan, S. and Bunge, H. -P., 2016. Geophysical Research Letters, Volume 43 Issue 6, pp. 2510-2516.

Dressel, I., Scheck-Wenderoth, M., Cacace, M., Lewerenz, B., Götze, H.-J., Reichert, Ch., 2015. Reconstruction of the southwestern African continental margin by backward modeling. Marine and Petroleum Geology, 67, DOI: 10.1016/j.marpetgeo.2015.06.006.

Drinkwater, M.R., Floberghagen, R., Haagmans, R., Muzi, D., Popescu, A., 2003. GOCE: ESA’s first Earth Explorer Core mission. In Beutler, G., Drinkwater, M.R., Rummel, R., von Steiger, R. (eds.), Earth Gravity Field from Space – From Sensors toEarth Sciences, Space Sciences Series of ISSI, vol. 17. Kluwer Academic Publishers,Dordrecht, The Netherlands, S. 419–432, ISBN: 1-4020-1408-2.

Ebbing J., Bouman J., Fuchs M., Lieb V., Haagmans R., Meekes J.A.C., Fattah R.A., 2013. Advancements in satellite gravity gradient data for crustal studies. Leading Edge, 32 (8), pp. 900-906.

Ebbing, J., Lundin, E., Olesen, O., Hansen, E.K., 2006. The mid-Norwegian margin: A discussion of crustal lineaments, mafic intrusions, and remnants of the Caledonian root by 3D density modelling and structural interpretation. Journal of the Geological Society, 163, 47-60.

Eldholm, O., Gladczenko, T.P, Skogseid, J., Planke, S., 2000. Atlantic volcanic margins: a comparative study. In: Nøttvedt, A., Larsen, B.T., Olaussen, S., Tørudbakken, B., Skogseid, J., Gabrielsen, R.H., Brekke, H.,Ø. Birkeland (eds.), Dynamics of the Norwegian Margin. Geological Society of London, Special Publication 167, 411-428.

Formatted: English (United States)

Formatted: English (United States)

Formatted: English (United States)

Formatted: English (United States)

Formatted: English (United States)

Formatted: German (Germany)

Fairhead, J.D. and Wilson, M. 2005. Plate tectonic processes in the South Atlantic Ocean: do we need deep mantle plumes? In: G.R. Foulger, J.H. Natland, D.C. Presnall, D.L. Anderson (Eds.), Plates, Plumes, and Paradigms, Geological Society of America Special Paper, 388, pp. 537–553.

Fecher T., Pail R., Gruber T., 2013. Global gravity field modeling based on GOCE and complementary gravity data. International Journal of Applied Earth Observation and Geoinformation, doi: 10.1016/j.jag.2013.10.005.

Fecher T., Pail R., Gruber T. 2016. GOCO05c - A new combined gravity field model based on full normal equations and regionally varying weighting. Surveys in Geophysics, in review.

Fecher T., Pail R., Gruber Th., Holmes S., 2015. Validation of South American Terrestrial Gravity Anomalies by GOCE. Geophysical Research Abstracts, 17, EGU2015-4859-1 European Geosciences Union General Assembly 2015, Vienna, 14.04.2015.

Flament, N., Gurnis, M. and Müller, R.D., 2013. A review of observations and models of dynamic topography, Lithosphere, vol. 5, no. 2, pp. 189-210. doi: 10.1130/L245.1

Förste, C., Bruinsma, S. L., Abrikosov, O., Lemoine, J.-M., Marty, J. C., Flechtner, F., Balmino, G., Barthelmes, F., Biancale, R., 2014. EIGEN-6C4 The latest combined global gravity field model including GOCE data up to degree and order 2190 of GFZ Potsdam and GRGS Toulouse. GFZ Data Services. http://dx.doi.org/10.5880/icgem.2015.1

Franke, D., Neben, S., Schreckenberger, B., Schulze, A., Stiller, M., and Krawczyk, C.M., 2006. Crustal structure across the Colorado Basin, offshore Argentina. Geophys. J.Int., 165, 850 – 864.

Franke, D., Ladage, S., Schnabel, M., Schreckenberger, B., Reichert, C., Hinz, K.,Paterlini, M., de Abelleyra, J., Siciliano, M., 2010. Birth of a volcanic margin off Argentina, South Atlantic. Geochemistry, Geophysics, Geosystems 11,Q0AB04.

Frisch, W. und Meschede, M., 2005. Plattentektonik. Kontinentverschiebung und Gebirgsbildung. Primus Verlag GmbH, 208 Seiten. ISBN-10: 3896785257.

Gatti, A., Reguzzoni, M., 2015. Comparison of the space-wise grids with other GOCE solutions. Geophysical Research Abstracts, Vol. 17, EGU2015-11112, EGU General Assembly 2015.

Geoffroy, L.C.R., 2005. Volcanic passive margins. Geoscience 337, 1395 –1408. doi:10.1016/j.crte.2005.10.006.

Gernigon, L., Lucazeau, F., Brigaud, F., Ringenbach, J.-C., Planke, S., Le Gall, B., 2006. A moderate melting model for the Vøring margin (Norway) based on structural observations and a thermo-kinematical modelling: Implication for the meaning of the lower crustal bodies. Tectonophysics 412 (3-4), 255-278.

Götze, H.-J., 2015. Potential Methods and Geoinformation Systems. In: Freeden, W., Nashed, M.Z., Sonar, T. (Eds.): Handbook of Geo-Mathematics. Berlin, Heidelberg, Springer Verlag, S. 1-21. - ISBN 978-3-642-27793-1, (doi>10.1007/978-3-642-27793-1_52-2)

Grombein, T.; Seitz, K.; Heck, B. 2015. RWI_TOPO_2015: An update of the Rock-Water-Ice topographic gravity field model of the Earth, available from http://www.gik.kit.edu/rwi_model.php

Gutknecht, B.D., Götze, H.-J., Jahr, T., Jentzsch, G., Mahatsente, R., Zeumann, S., 2014. Surveys of Geophysics, 35, 1417–1440. DOI 10.1007/s10712-014-9296-9.

Gutknecht, B.D., Köther, N., Mahatsente, R., Götze, H.J., 2011. Utilisation of Gravity Gradients and Invariants for 3D Density Modelling. Proc. General Assembly of the International Union of Geodesy and Geophysics (IUGG), Melbourne, Australia.

Hackney, R. I. and Featherstone, W. E., 2003. Geodetic versus geophysical perspectives of the 'gravity anomaly'. Geophysical Journal International 154 (1), 35-43. doi: 10.1046/j.1365-246X.2003.01941.x

Heit, B., Sodoudi, f., Yuan, X., Bianchi, M., Kind, R., 2007. An S- Receiver Function Analysis of the Lithospheric Structure in South America, Geophyical. Resarch Letters, 34, L14307, doi:10.1029/2007GL030317.

Hess, H. H., 1962. History of Ocean Basins. In A. E. J. Engel, Harold L. James, and B. F. Leonard. Petrologic studies: a volume in honor of A. F. Buddington. Boulder, CO: Geological Society of America. pp. 599–620.

Hinz, K., Neben, S., Schreckenberger, B., Roeser, H.A., Block, M., Goncalves de Souza, K., Meyer, H., 1999. The Argentine continental margin north of 48°S: sedimentary successions, volcanic activity during break-up. Mar. & Petrol. Geol.,16, 1 - 25.

Hinze, W.J., Aiken, C., Brozena, J., Coakley, B., Dater, D., Flanagan, G., Forsberg, R., Hildenbrand, T., Keller, G.R., Kellogg, J., Kucks, R., Li, X., Mainville, A., Morin, R., Pilkington, M., Plouff, D., Ravat, D., Roman, D., Urrutia-Fucugauchi, J., Véronneau, M., Webring, M., Winester, D., 2006. New standards for reducing gravity observations: The Revised North American Gravity Database: http://paces.geo.utep.edu/research/gravmag/PDF/Final%20NAGDB%20Report%20091403.pdf

Hirsch, K.K., Bauer, K., Scheck-Wenderoth, M., 2009. Deep structure of the western South African passive margin e results of a combined approach of seismic, gravity and isostatic investigations. Tectonophysics 470, 57 - 70. http://dx.doi.org/10.1016/j.tecto.2008.04.028.

Holzrichter, N., 2013. Processing and interpretation of satellite and ground based gravity data at different lithospheric scales. Dissertation, 126 pages. Christian-Albrechts-Universität zu Kiel. Fakultät für Mathematik und Naturwissenschaften.

Hopper, J.R., Funck, T., Tucholke, B.E., Larsen, H.C., Holbrook, W.S., Louden, K.E., Shillington, D., Lau, H., 2004. Geological Society of America. Geology, 32, (1), 93 - 96. DOI 10.1130/G19694.1.

Hosse, M., Pail, R., Horwath, M., Holzrichter, N., Gutknecht, B.D., 2014. Combined Regional Gravity Model of the Andean Convergent Subduction Zone and Its Application to Crustal Density Modelling in Active Plate Margins. Surveys in Geophysics, 35, (6), 1393-1415.

Isacks, B., Oliver, J.,Sykes, L. R., 1968. Seismology and the New Global Tectonics. Journal of Geophysical Research, 73, (18), 5855.

IUGG, 2015. Resolutions adpoted by the IUGG Council at the XXVI General Assembly, Prague, Czech Republic, 22 June – 2 July 2015; http://www.iugg.org/resolutions/IUGGResolutions2015.pdf

Kalberg, T., 2016. Interpretation tektonomagmatischer Prozesse basierend auf 3D Potentialfeldmodellierungsergebnissen. Dissertation 185 pages. Fachbereich für Geowissenschaften, Universität Bremen.

Klinge, L., 2016. Gravitational potential energy (GPE) und Stress im südlichen Atlantik (in German). Master Arbeit, 89 pages. Institut für Geowissenschaften, Mathematisch-naturwissenschaftliche Fakultät der Christian-Albrechts-Universität Kiel.

Köther, N., Götze, H.-J., Gutknecht, B.G., Jahr, T., Jentzsch, G., Lücke, O.H., Mahatsentea, R., Sharma, R., Zeumann, S., 2012. The seismically active Andean and Central American margins: Can satellite gravity map lithospheric structures? Journal of Geodynamics, 59– 60, 207– 218.

LaFehr, T.R., 1991. An exact solution for the gravity curvature (Bullard B) correction: Geophysics, 56, (8), 1179–1184, doi: 10.1190/1.1443138.

Lallemand S., 2014. Active continental margin. In Encyclopedia of Marine Geosciences, Springer Science, Eds.: Harff, J., Meschede, M., Petersen, S. and Thiede, J., 7 pages, DOI 10.1007/978-94-007-6644-0_102-2.

Li, X. and Götze, H.-J., 2001. Ellipsoid, Geoid, Gravity, Geodesy, and Geophysics - A Tutorial. Geophysics, vol. 66, no. 6, 1660-1668.

Maus, S., Barckhausen, U., Berkenbosch, H., Bournas, N., Brozena, J., Childers, V., Dostaler, F., Fairhead, J.D., Finn, C., von Frese, R. R. B., Gaina, C., Golynsky, S., Kucks, R., Lühr, H., Milligan, P., Mogren, S., Müller, R.D., Olesen, O., Pilkington, M., Saltus, R., Schreckenberger, B., Thébault, E. and Caratori Tontini, F., 2009. EMAG2: A 2-arc min resolution Earth Magnetic Anomaly Grid compiled from satellite, airborne, and marine magnetic measurements. Geochemistry, Geophysics, Geosystems, vol. 10, no. 8. doi: 10.1029/2009GC002471.

Mayer-Gürr, T., Zehentner, N., Klinger, B., Kvas, A., 2014. ITSG-Grace2014: a new GRACE gravity field release computed in Graz. Presented at GRACE Science Team Meeting (GSTM), Potsdam, 29.09.2014.

Maystrenko, Y.P., Scheck-Wenderoth, M., Hartwig, A., Anka, Z., Watts, A.B., Hirsch, K.K, Fishwick, S. 2013. Salt as a 3D element in structural modeling – Example from the Central European Basin System. Tectonophysics, doi:10.1016/j.tecto.2012.06.030

Mikuška, J., Pašteka, R., Marušiak, I., 2006. Estimation of distant relief effect in gravimetry. GEOPHYSICS, 71, (6), J59–J69, doi: 10.1190/1.2338333.

Mohriak, W., 2014. Birth and development of continental margin basins: analogies from the South Atlantic, North Atlantic and the Red Sea. Search and Discovery article, [http://www.searchanddiscovery.com/pdfz/documents /2014/41502mohriak/ndx_mohriak.pdf.html](http://www.searchanddiscovery.com/pdfz/documents/2014/41502mohriak/ndx_mohriak.pdf.html)

Müller, R. D., Sdrolias, M., Gaina, C. and Roest, W.R., 2008. Age, spreading rates, and spreading asymmetry of the world's ocean crust. Geochemistry, Geophysics, Geosystems, vol. 9, no. 4., 19 pages, doi: 10.1029/2007GC001743.

Naudy, H. and Neumann R., 1965. Sur la définition de l'anomalie de Bouguer et ses

conséquences pratiques, Geophys. Prosp., vol 13, 1-11O’Connor, J.M., Jokat, W., le Roex, A.P., Class,C., Wijbrans,J.R., Keßling, S., Kuiper, K.F. and Nebel, O., 2012. Hotspot trails in the South Atlantic controlled by plume and plate tectonic processes. Nature Geoscience 5, pp. 735–738, doi:10.1038/ngeo1583.

Oliver, J., Isacks, B., 1967. Deep earthquake zones, anomalous structures in the upper mantle, and the lithosphere. Journal of Geophysical Research, 72 (16), pp. 4259-4275.

Oncken, O., Chong, G., Franz, G., Giese, P., Götze, H.-J., Ramos, V., Strecker, M. and Wigger, P., (Eds), 2006: The Andes - Active Subduction Orogeny., Frontiers in Earth Sciences, 1, Springer Verlag, pp. 570.

Pail R., Fecher T., Rexer M. 2015b. Validation of GOCE gravity gradient grids for geophysical applications. Geophysical Research Abstracts, Vol. 17, EGU2015-1652, Poster presented at EGU General Assembly 2015, Vienna.

Pail, R., Bingham, R., Braitenberg, C., Dobslaw, H., Eicker, A., Güntner, A., Horwath, M., Ivins, E., Longuevergne, L., Panet, I., Wouters, B. 2015a. Science and User Needs for Observing Global Mass Transport to Understand Global Change and to Benefit Society. Surveys in Geophysics, 36(6): 743-772, Springer Netherlands, doi: 10.1007/s10712-015-9348-9.

Pail, R., Goiginger, H., Schuh, W.-D., Höck, E., Brockmann, J. M., Fecher, T., Gruber, T., Mayer-Gürr, T., Kusche, J., Jäggi, A., Rieser, D. 2010. Combined satellite gravity field model GOCO01S derived from GOCE and GRACE. Geophysical Research Letters, Vol. 37, L20314, doi:10.1029/2010GL044906.

Pail, R., S. Bruinsma, F. Migliaccio, C. Förste, H. Goiginger, W.-D. Schuh, E. Höck, M. Reguzzoni, J. M. Brockmann, O. Abrikosov, M. Veicherts, T. Fecher, R. Mayrhofer, I. Krasbutter, F. Sansò, and C. C. Tscherning 2011. First GOCE gravity field models derived by three different approaches, Journal of Geodesy, 85(11), 819-843, doi: 10.1007/s00190-011-0467-x.

Panet I., G. Pajot-Métivier, M. Greff-Lefftz, L. Métivier, M. Diament & M. Mandea 2014. Mapping the mass distribution of Earth’s mantle using satellite-derived gravity gradients, Nature Geoscience 7, 131–135, doi:10.1038/ngeo2063.

Pavlis, N.K., Holmes, S.A., Kenyon, S.C., Factor, J.K., 2008. An Earth Gravitational Model to Degree 2160: EGM2008. In: Proceedings of the European Geosciences Union General Assembly, April 13–18, Vienna, Austria.

Pavlis, N.K., Holmes, S.A., Kenyon, S.C., Factor, J.K., 2012. The development and evaluation of the Earth Gravitational Model 2008 (EGM2008). Journal of Geophysical Research, 117, (B4), 2156 - 2202, doi: 10.1029/2011JB008916.

Prange, L., 2011. Global Gravity Field Determination Using the GPS Measurements Made Onboard the Low Earth Orbiting Satellite CHAMP. PhD Thesis, Geodätisch-geophysikalische Arbeiten in der Schweiz, vol. 81. http://www.sgc.ethz.ch/sgc-volumes/sgk-81.pdf

Reigber, C., Balmino, G., Schwintzer, P., Biancale, R., Bode, A., Lemoine, J.-M., Koenig, R., Loyer, S., Neumayer, H., Marty, J.C., Barthelmes, F., Perossanz, F., 2002. A high quality global gravity field model from CHAMP GPS tracking data and accelerometry (EIGEN-1S). Geophysical Research Letters, 29, 14, dx.doi.org/10.1029/2002GL015064

Reston, T.J., 2009. The structure, evolution and symmetry of the magma-poor rifted margins of the North and Central Atlantic: A synthesis. Tectonophysics 468, 6–27. doi:10.1016/j.tecto.2008.09.002.

Rudenko S., Dettmering D., Esselborn S., Schoene T., Foerste C., Lemoine J-M, Ablain M, Alexandre D, Neumayer K.-H., 2014. Influence of time variable geopotential models on precise orbits of altimetry satellites, global and regional mean sea level trends. Advances in Space Research, doi: 10.1016/j.asr.2014.03.010.

Salomon, A., Koehn, D., Passchier, C., Hackspacher, P.C. and Glasmacher, U.A., 2014. Contrasting stress fields on correlating margins of the South Atlantic, Gondwana Research, doi.org/10.1016/j.gr.2014.09.006.

Schaller. T., Andersen, J., Götze, H.-J., Koproch, N., Schmidt, S., Sobiesiak, M., Splettstößer,S., 2015. Segmentation of the Andean margin by isostatic models and gradients. Journal of South American Earth Sciences, 59, 69-85.

Scheck-Wenderoth, M., Maystrenko, Y., 2008. How warm are passive continental margins? A 3D lithosphere-scale study from the Norwegian margin. Geology, 36, (5), 419-422, DOI: 10.1130/G24545A.1.

Skogseid, J., Planke, S., Faleide, J.I., Pedersen, T., Eldholm, O., Neverdal, F., 2000. NE Atlantic continental rifting and volcanic margin formation, in Nottvedt, A.e.a., Ed., Dynamics of the Norwegian Margin, 167: London, Geological Society of London, Special Publications, p. 55–82.

Sobiesiak, M., Meyer U., Schmidt S., Götze H.-J., Krawczyk C.M., 2007. Asperity generating upper crustal sources revealed by b value and isostatic residual anomaly grids in the area of Antofagasta, Chile. Journal of Geophysical Research, v. 112, B12308, doi: 10.1029/2006JB004796.

Stadler, G., Gurnis,M., Burstedde, C., Wilcox, L.C., Alisic, L., Ghattas, O., 2010. The Dynamics of Plate Tectonics and Mantle Flow: From Local to Global Scales. Science, Vol. 329, Issue 5995, pp. 1033-1038, DOI: 10.1126/science.1191223.

Szwillus, W., Ebbing, J. and Holzrichter, N., 2016. Importance of far-field topographic and isostatic corrections for regional density modelling. Geo- physical Journal International, 207 (1), pp. 274-287, doi:10.1093/gji/ggw270

Szwillus, W., Götze, H.-J., 2016. Efficient mass correction using an adaptive method. In: R, Pasteka et al., Proceedings of the workshop on Bouguer Anomaly, Bratislava (Slowak Republic). Accepted.

Tapley, B.D., Bettadpur, S., Watkins, M., Reigber, C., 2004. The gravity recovery and climate experiment: mission overview and early results. Geophysical Research Letters, 31(9), L09607, AmericanGeophysical Union, http://dx.doi.org/10.1029/2004GL019920.

Tašárová, Z., 2007. Towards understanding the lithospheric structure of the southern Chilean subduction zone (36° S – 42° S) and its role in the gravity field. Geophysical Journal International, 170, (3), 995–1014. doi:10.1111/j.1365-246X.2007.03466.x

Torge W., 2001. Geodesy, 3rd edition, 416 pages. De Gruyter Berlin, ISBN 3-11-017072-8.

Torsvik, T. H., Rousse, S., Labails, C. and Smethurst, M.A., 2009. A new scheme for the opening of the South Atlantic Ocean and the dissection of an Aptian salt basin. Geophysical Journal International, 177, 3, pp. 1315-1333. doi: 10.1111/j.1365-246X.2009.04137.x.

Vine, F. J.; Matthews, D. H., 1963. Magnetic Anomalies Over Oceanic Ridges. Nature 199 (4897), 947–949.

Wadati, K., 1929. Shallow and deep earthquakes (2nd paper): Geophysical Magazine, 2, 1–36.

Wefer,G., Billet, D., Hebbeln, D., Barker Jorgensen, B., Schlüter, M., van Weering, T.C.E., 2003. Eds. Ocean Margin Systems. Springer, pp. 495. Doi.10.007/978/-3-662-05127-6

Wegener, A., 1920. Die Entstehung der Kontinente und Ozeane. In: E. Wiedemann (Herausgeber), Die Wissenschaft, Friedrich Vieweg und Sohn, Braunschweig, 2. Auflage, 66, 1-135.

Wenzel H., 1985: Hochauflösende Kugelfunktionsmodelle für das Gravitationspotential der Erde: Wissenschaftliche Arbeiten der Fachrichtung Vermessungswesen der Universität Hannover, 137, 1–155.White, R. S., Smith,L.K., 2009. Crustal structure of the Hatton and the conjugate east Greenland rifted volcanic continental margins, NE Atlantic. Journal of Geophysical Research, 114. B02305. DOI 10.1029/2008JB005856

Insights from recent gravity satellite missions in the density structure of continental margins – with focus on the passive margins of the South Atlantic

Abstract

We focus on new gravity and gravity gradient data sets from modern satellite missions GOCE, GRACE and CHAMP, and their geophysical interpretation at passive continental margins of the South Atlantic. Both sides, South Africa and South America, have been targets of hydrocarbon exploration and academic research of the German Priority Program SAMPLE (South Atlantic Margin Processes and Links with onshore Evolution). The achievable spatial resolution, driven by GOCE, is 70 - 80 km. Therefore, most of the geological structures, which cause a significant gravity effect (by both size and density contrast), can be resolved. However, one of the most important aspects is the evaluation of the omission error, which is not always in the focus of interpreters. It results from high-frequency signals of very rough topographic and bathymetric structures, which cannot be resolved by satellite gravimetry due to the exponential signal attenuation with altitude. The omission error is estimated from the difference of the combined gravity model EIGEN-6C4 and the satellite-only model GOCO05S. It can be significantly reduced by topographic reductions. Simple 2D density models and their related mathematical formulas provide insights in the magnitude of the gravity effect of masses that form a passive continental margin. They are contrasted with results from satellite-only and combined gravity models. Example geophysical interpretations are given for the western and eastern margin of the South Atlantic Ocean, where standard deviations vary from 25 – 16 mGal and 21 – 11 mGal, respectively. It could be demonstrated, that modern satellite gravity

data provide significant added value in the geophysical gravity data processing domain and in the validation of heterogeneous terrestrial data bases. Combined models derived from high-resolution terrestrial gravity and homogeneous satellite data will lead to more detailed and better constrained lithospheric density models, and hence will improve our knowledge about structure, evolution and state of stress in the lithosphere.

1. Motivation and the concept of Plate Tectonics

Geosciences are striving for an interdisciplinary perception to combine their basic findings in a world embracing synthesis to understand global processes in the Earth interior and at its surface. Most of these processes are generally geothermally driven, and it is easy to accept that their origin lies below the lithosphere, in the Earth's mantle (among others Stadler et al., 2010). Today, the theory of plate tectonics enables us to draw a coherent picture of the Earth´s lithosphere. Interactions between the plates at their plate boundaries are responsible for most of the earthquakes that occur here (among many other publications and websites: http://earthquake.usgs.gov/earthquakes/?source=sitenav, http://www.isc.ac.uk/about/ or http://geofon.gfz-potsdam.de/).
This paper will review the status of satellite gravity missions and terrestrial data, as well as global gravity models, fields and gradients derived from them. It will focus on their accuracy, resolution and the omission error – which is out of focus of many earth scientists. It is structured as follows: Section 1 defines continent-ocean transitions and recalls some basics in the context of Plate Tectonics concept and passive margins in particular. For those readers who

are not familiar with the interpretation of gravity anomalies at a continental margin in Section 2 the basic concepts are illustrated; this section can be skipped by experts. Further on the focus is set on the question how (satellite) gravity interpretations can help to explore these passive margins (Section 2.3). In the course of this paper we will notice later to what extent the new fields and gradients from recent satellite gravity missions can support research at the passive margins of the South Atlantic (Section 2.4).

In Section 3 we will demonstrate how this new information augmented our view on the density structures of the lithosphere particularly at passive margins of the South Atlantic. At last we describe the benefits for combined interpretations in Section 4, and merge information from both terrestrial and satellite gravity fields.

1.1 Short introduction to history of plate margins tectonics

Considering the history of the Plate Tectonic concepts in the early 1960s, Wegener´s view on the „the continental drift" (Wegener, 1920) began to be accepted after it was refined and confirmed by geophysical observations namely by early seismological studies on deep earthquakes (Wadati, 1929; Benioff, 1954), later by Isacks et al. (1968), Oliver and Isacks (1967) and paleo-magnetic shipborne observations (Hess, 1962; Vine and Matthews 1963 among others). Together with the techniques of radiometric dating (age determination) published first by Boltwood (1907) geophysicists were able to date the magnetic mid oceanic reversals by precise physical measurements. They helped to get the modern concept of “plate tectonics” fully accepted.

It provides the framework for the interpretation of structures, the history and composition of continental margins. Plate movements and the differences in density of oceanic and continental crust types led to the structural pattern of continental margins and result in a tectonic classification of coastlines as **active** or **passive** margins (among others Wefer et al., 2003). *Active margins* are typical units of the “Circum-Pacific Ring of Fire” in the Pacific where plates are converging and coincide with plate boundaries in a subduction zone. These margins are called *active* (e.g. Oncken et al., 2006; Lallemand, 2014) due to the big variety of tectonic, magmatic and metamorphic processes that occur here. If continental margins mark only the boundary to the oceanic portion of the same tectonic plate, they are called *passive margins*. Passive margins are typical of the Atlantic Ocean between Scandinavia and Greenland (Scheck-Wenderoth and Maystrenko 2008), Iberic peninsula and the East American coast or between Africa and South America (Blaich et al., 2011 and many papers within).

1.2 Passive Margins

Although we assume that most of the readers are familiar with the concept of plate tectonics we will recall briefly some basics. In particular *passive continental margins* are characterized by a transition of continental into oceanic crust within the same plate. It emerges from the splitting up of continents and the following divergent plate drift that forms new oceanic lithosphere by seafloor spreading at the divergent plate boundary. At the edges of the Atlantic geophysical investigations identify a laterally 10-15 km thick crustal transition between the thick crust of the continents and the thin oceanic crust. It is interpreted as relicts of thinned, mafic magmas which intruded into continental crust. In addition, passive continental margins are often stretched by intensive fault tectonics. They have a tectonically thinned continental crust, which is characterized by listric faults and tilted fault blocks. Tectonic crustal expansion starts at the time of installation of the continental drift rift system and refines the passive continental margin further (Blaich et al., 2011). These margins are marked by smooth relief due to tectonic inactivity and major sediment accumulation. This phenomenon is due to thermal cooling and sediment loading that led to conditions of subsidence and sediment accumulation, because the margins move away from the spreading center. Irregular subsidence and different sediment load often cause the accumulation of salt diapirs in the sediments of passive continental margins. The tectonic-sedimentary conditions are also favorable for the formation of hydrocarbon deposits and large salt deposits (Mohriak, 2014).

Modern passive margins (Fig. 1) border the oceans formed by the spreading caused by the break-up of the Gondwana supercontinent (e.g. Bond et al., 1984). From Figure 1 one can see that the margins of the South Atlantic Ocean (Cappelletti et al., 2011; Blaich et al., 2011; Mohriak, 2014), the western Indian Ocean, the Arctic and Norwegian seas (Scheck-Wenderoth and Maystrenko, 2008; Ebbing et al, 2006; Skogseid et al., 2000), the magma poor rifted margins of the North and Central Atlantic Ocean (Reston, 2009; Mohriak, 2014) and the margins of Antarctica are part of this system (Kalberg, 2016). A rising convection cell or a plume in the rifting area caused initial rifting and a regional uplift as well as volcanic activities above or below oceanic sea level after an initial period of crustal thinning and erosion. Basile (2015) describe another type of margin: “transform continental margins” by simple kinematic models of transform faulting which cause among two other types “passive transform margins”. The satellite gravity picture of the Equatorial Atlantic Ocean will be shown in Section 4.2, Fig. 20.

Figure 1: double column

Fig. 1. Continental margins on Earth. Blue lines mark passive continental margins mainly surrounding the Atlantic Ocean, the Antarctic Seas, and Indian Ocean; red lines indicate active margins (subduction zones). Continental margins were taken from from Frisch und Meschede (2005).The underlying gravity field is the map of “gravity disturbance” calculated on base of the EIGEN-6C4 model (Förste et al., 2014). Gravity was calculated on a grid of 0.5° x 0.5°.

1.3 Volcanic passive margins

These margins present distinctive genetic and structural features, e.g., high-rate extension of the lithosphere is associated with catastrophic mantle melting responsible for the accretion of a thick igneous crust (Geoffroy, 2005). Typical rifted “magma-dominated” margins are characterized by large volumes of flood basalts which flow across the continental hinterlands during continental breakup (among others refer to: Hopper et al., 2004; Eldholm et al., 2000; Gernigon et al., 2006; White and Smith, 2009; O´Connor et al., 2012). Underlying the extrusive lavas at the continent-ocean transition zone, these margins exhibit high seismic velocities in the lower crust of some The deeper crust is characterized by two areas of high seismic velocity (7.2 to 7.4 km/s; Franke et al., 2010)., which are associated with voluminous igneous rocks intruded into the lower crust.

In recent time the question arose in the context of fixing international boundaries offshore of the continents due to economic interests because e.g. hydrocarbon exploration moved further offshore e.g. to explore deep water resources. Toward the definition of this “continent-ocean-boundary, COB” at passive margins one of the crucial questions is how to define these boundaries. Torsvik et al. (2009) described how COB for the South Atlantic margins at both sides can be defined: by the interpretation of seismic, gravimetric, magnetic, bathymetric and geological information. Any identification of the COB is also important for the definition of plate boundaries at the time of break-up which allows the reconstruction of geometry and earlier position of former continents - e.g. in the reconstruction of Pangaea. It is not the aim of this paper to recalculate COBs. However we trust that the processing of gravity field and its second derivatives for recalculation of COB (Torsvik et al., 2009) will benefit from the increase of high resolution satellite derived gravity fields. Later we will return to this point in the conclusion (Section 5) suggesting calculating the 2nd derivative of satellite gravity (derivative of the gravity gradient).

2. Geophysical characteristics of margins

To investigate both active and passive continental margins almost all geophysical methods can help to discover their lithospheric structures: Seismic, potential, electro-magnetic and electrical fields. Recent studies (e.g. Torsvik et al. 2009) show that processes in the lithosphere are linked to the dynamic mantle and dynamic processes have an important influence on the evolution of lithospheric plates, which is manifested in the formation of dynamic topography (e.g. Flament et al., 2013; Colli et al., 2016). A key example for this interaction is the opening history of the Atlantic, where asthenospheric material reaches the surface at the mid-ocean spreading center. The uplift of hot material of the asthenosphere leads to seafloor spreading which manifests itself in the spreading anomalies in the magnetic field. The spreading axes are expressed either by topographic (heights above sea level, e.g. Iceland) or bathymetric heights (below sea level e.g. Atlantic ocean ridge). The worldwide offshore stripe pattern of magnetic anomalies which are located parallel to mid-ocean ridges allow a temporal classification of developed oceanic crust. The EMAG2 total magnetic field model has a reasonable resolution of two arc-minutes (Maus et al. 2009). The model was compiled from ship-, air-borne and satellite data (CHAMP). For the purpose of interpolation of magnetic field anomalies the oceanic crust ages of Müller et al. (2008) were employed (Maus et al. 2009). Hydro-carboniferous exploration targeted most of the passive margins of the world with both refraction and/or reflection seismic.

Seismic onshore-offshore investigations of a passive continental margin aim to investigate the transition zone between the oceans and continents, e.g. SE Atlantic and the African continent (Franke et al., 2006; 2010; Bauer et al., 2000; Hirsch et al., 2009; Schnabel et al., 2008). These studies reveal the history and mechanisms of the break-up and its relation to the driving magmatic processes (plume – crust interactions) in the underlying mantle and lithosphere. The South American side of the southern Atlantic was target of multiple seismic investigations since many years (Mohriak, 2014; Blaich et al., 2011; Franke et al. 2006; Heit et al. 2007; Hinz et al., 1999 and many more) to investigate the shelf areas offshore, the continent-ocean transition and the seaward dipping reflectors (SDR) which are characterized by high seismic velocities and related high densities.

2.1 The role of gravity field interpretations and prerequisites

Remark:

The units used for gravity field values and its gradients are given in mGal (Milligals) and E (Eötvös) – as it is still common use in Geophysics and Geodesy. Converting these units into SI-units, there are: 1 mGal = 10^{-5} m/s^2 and E = 10^{-9} s^{-2}.

Rock densities are always given in kg/m^3.

First, the situation will be analyzed which was typical before the era of satellite missions which started in the year 2000 with the launch of the CHAMP satellite (refer to Chapter 4). Modelling and interpretation of the Earth´s gravity field and its derivatives often had to deal with a merge of data sets with rather different resolution, different age and quality, coverage and wavelength content. This has been documented in a long list of papers (among many others: Schaller et al., 2015; Bouman et al., 2014; Hosse et al., 2014; Gutknecht et al., 2014; Köther et al., 2012; Tašárová, 2007). These papers have shown that lithospheric models of study regions suffer mainly from two facts:

(1) Nearly all information for constrained gravity field modelling of the lithospheric is based on irregularly distributed profiles and

(2) large data gaps and partly low data quality due to very limited access and infrastructure.

The global gravity model EGM2008 (Pavlis et al. 2012) inherited – and still inherits - these problems related with available terrestrial databases. Pavlis et al. (2008) described the compilation of the EGM2008 gravity which consists of different sources: up to a spatial resolution of approximately 140 km GRACE (Gravity Recovery and Climate Experiment) data have been used, data from 140 km to approx. 10 km spatial resolution are derived from terrestrial and satellite altimetry and so called “fill-in” data (Section 4.2). Today we know that the relative weighting of GRACE with respect to the other datasets was too low, leading to a dominance of terrestrial data errors in spectral regions where better GRACE data would already have been available.

Figure 2: double column

Fig. 2. This figure portrays the terrestrial data inconsistency which is rather typical for gravity surveys in remote areas (here across the South American continent at a swath between 36°S – 42°S from the passive margin in the East

to the active margin in the West). As an example the different sources of gravity data of the Southern Central American continent are shown together with the visualization of big data gaps (Tašárová, 2007). The green and red points in Chile (CH) and Argentina (AR) are stations in the ARANEDA I and II (University of Chile) datasets; black points in southern Chile and the Arauco Peninsula are ENAP data (Chilean oil industry); the gray dense network in Argentina (AR) show the YPF data (Argentine oil company); yellow points: stations of the MIGRA 2000 dataset, and the MIGRA 2002 data (both measured by the gravity group at the University Kiel) are shown in blue. The brown lines offshore denote the ship-borne gravity data profiles from the German research vessel “Sonne”.

Fig. 2 shows the situation some 20 years ago at the central South American subcontinent. For a continental gravity field study the field had to be compiled from very different data sources often without any meta data information - e.g. for gravity data which were measured on behalf of oil companies (grey area in Fig. 2). In other areas, e.g., in the eastern part of Argentina (yellow dots in Fig. 2) data are missing due to difficult or impossible access.

At the end of this Section we will pose the question how large lithospheric structures and how big density differences to their surrounding have to be in order to cause a detectable signal at orbit height of a satellite. This consideration describes the situation at active and passive margins in an analogues manner. In Fig. 3 the effects of gravity and gradients are shown for a simple model. For density contrasts between the values $\Delta\rho = 10^1 – 10^3$ kg/m^3 Gutknecht et al. (2011) calculated gravity and gradients at the GOCE satellite orbit height of 255 km resulting from a sphere with minimum diameters between d = 20 – 200 km (b = 10 – 100 km, refer to Fig. 3) to be tangent to the Earth surface). Within the range of the assumed parameters the minimum diameter required to produce signal differences of 1×10^{-5} ms^{-2} and 12×10^{-12} s^{-2} at orbit height. This is rather close to the expected accuracies of the gravity and vertical gravity gradient of the GOCE mission (recent values are: 0.45 mE for GOCE-only, 0.2 mE for GOCE+GRACE models, cf. also Fig. 13). Fig. 3 conveys that a structure with a diameter of some 45 km and a density contrast of 240 kg m^{-3} could be detected in satellite gravity at orbit height. If the diameter of the model sphere increases to 90 km, its density contrast should not be less than 33 kg m^{-3}.

The simple model described above fits rather well the dimension of the Jurassic arc batholiths at the Northern Chilean continental margin with diameters of roughly 60 – 120 km (Sobiesiak et al., 2007). This supports the idea that batholithic structures e.g. intrusions at continental margins, can be detected using data of the modern satellite missions– both gravity and gradients.

Figure 3: one and a half page width

Fig. 3. Gravity and gradient signal caused by a minimum diameter of a sphere with given density contrast in the orbit height of 255 km (Gutknecht et al., 2011). The thick solid and dotted lines represent gravity signals of 1 and 10 mGal at orbit height. The thin dashed and dash-dotted lines represent gradients of 12 and 1000 mE, respectively. The grey shaded area shows results which are based on a possible combination of geometry and density parameters of the causing mass anomaly.

2.2 Gravity anomalies and isostasy

A first look at Fig. 4 provides already helpful information on the gravity gradients of the Earth at the continental margins. The figure bases on the evaluation of gravity field maps from the recent gravity missions. A complete Bouguer anomaly (corrected by the effect of elevation, spherical slab, topography both on- and offshore) was used to calculate the first derivative of the field – the dip curvature of gravity.

Figure 4: Full page width

Fig 4. Global horizontal gravity gradients. Deep blueish colors mark regions on Earth where the dip curvature (horizontal gradient) of the worldwide Bouguer gravity field (EIGEN-6C4) is small or even zero. The more reddish the colors are the steeper the gradients. The strongest gradients are observed at the active continental margin of Central South America. On the contrary at most of the passive continental margins (Fig. 1) the gradients are rather small.

Dark blueish colors indicate rather weak dip curvature which means that horizontal gravity gradients are small, on the contrary reddish tones point to strong dip curvature and therefore strong gradients. The active continental margins in the area of the Circum-Pacific are generally marked by reddish colors – strong gradients – which are related with extended density variations in crust and mantle in the transition from oceanic to continental margins. Mostly low gradients – light blueish colors - are typical for passive continental margins. In order to understand this relationship two questions arise:

(1) How was the gravity *anomaly* calculated and how big is its magnitude of the anomaly caused by the mass distribution (both topography/bathymetry and densities) at continental margins and

(2) How was the *field* observed and what is known about accuracy and homogeneity of gravity field observations?

With regard to the first question one has to consider that gravity observations at the Earth´s surface and the Earth near space vary from the theoretical ”normal” field value. Their magnitude is caused not only by the latitude effect but by elevation of observational points, the density of cap beneath the station in the underground and the topographic masses in the neighborhood. After correction of earth tidal effects and air pressure variations the remaining time invariable parts of the measured signal are:

Normal gravity	γ_0
Effect of topographic masses	δg_{TOP}
Bouguer slab	δg_{BPL}
Elevation effect (free air term)	δg_{NIV}
Effect of the crustal root	δg_R
Known mass inhomogeneities	δg_{GEOL}

Common representations of gravity measurements in maps and profiles depend on what has been calculated as stated in the table above and added as corrections to the measured gravity field values. From all measured gravity values the normal gravity (in the height and position of the observable) is subtracted, and therefore the term “gravity anomaly” is defined. This is simply the difference between the observable values to “normal” gravity. In Geophysics we distinguish mainly between three anomalies Free air- (FA), Bouguer- (BA) and isostatic anomaly (ISA) which define gravity in the height of the observation (e.g. Li and Götze, 2001; Hackney and Featherstone, 2003; Naudy et al., 1965; LaFehr, 1991 and many others).

With δg_R we describe the effect of a mountain root and define Free Air, Bouguer and isostatic anomalies such as:

$$FA = \Delta g'_0 = g_{obs} + \delta g_{NIV} \left[+ \delta g_{TOP} \right] - \gamma_0$$

$$BA = \Delta g''_0 = g_{obs} + \delta g_{NIV} + \delta g_{TOP} + \delta g_{BPL} - \gamma_0$$

$$ISA = \Delta g_{ISA} = g_{obs} + \delta g_{NIV} + \delta g_{TOP} + \delta g_{BPL} + \delta g_R - \gamma_0$$

Calculations of the individual correction terms depend on the objective of the survey and are variously complicated to handle. g_{obs} denotes the measured gravity field value. The calculation of the topographical reduction (δg_{Top}) requires precise knowledge of the terrain and surface near densities and today it is most likely calculated by the aid of digital elevation models (DEM), among others refer to (Holzrichter, 2013 and Szwillus and Götze, 2016); it requires the use of a computer and digital elevation data. The effect of topographic masses is normally calculated in a surrounding circular area of 50 km up to 167 km (e.g. La Fehr, 1991; Hinze et al., 2006). However, Mikuška et al. (2006), Szwillus and Götze (2016), Szwillus et al., (2016) point to “long distant relief effects” and propose the calculation of *all* topographic masses on Earth. The gravity effect of a Bouguer slab with a thickness which is defined by the difference between the physical station height and the reference level (normally the geoid) should always be calculated by a spherical cap (e.g. Baeschlin, 1948). For smaller areas (with a reduction radius R < 20 km) and moderate terrain roughness the Bouguer slab can easily be calculated by:

$$\delta g_{BPL} = -2 \pi G \rho (H_S - H_B)$$

with:

G = Gravitational constant ($6.672 \cdot 10^{-11}$ m^3 s^{-2} kg^{-1}),

ρ = crustal density (2 670 kg/m^3); offshore: rock-equivalent density

H_S = station height; offshore: ocean depth H_D,

H_B = reference height (usually it is referred to the geoid).

In the last step the free air effect δg_{NIV} is calculated by use of the “normal gradient” (0.3085 mGal/m):

$$\delta g_{NIV} = 0.3085 \cdot (H_S - H_B) \text{ mGal/m}$$

It has to emphasized that the above used constant gravity gradient for large scale investigations has to be replaced by equivalent values of derivation of closed mathematical expression of the normal gravity which is always latitude and height dependent. It was also recommended to calculate an “atmospheric correction” (Wenzel, 1985) in order to eliminate long wavelengths errors from the observed gravity field.

Note: the terms of “flat” Bouguer slab in δg_{BPL} and the “constant vertical gradient” in δg_{NIV} are in the above formulas are used here for simplification only. Modern satellite gravity field processing at large spatial scales requires a spherical cap calculation and the consideration of latitude and height dependent calculation of the vertical gradient.

Special emphasis has to be put on the situation in oceanic regions. If we assume that station heights are equal to geoidal heights (h = 0 m) Bouguer and Free Air anomaly is equal due to:

$$BA = FA + \delta g_{BPL} = FA + [-2 \pi G \rho (H_S - H_B)]$$

with: $H_s - H_B = 0$ m;

it follows that BA = FA, in case the FA is already corrected by δg_{TOP} which contains gravity effect of masses at the ocean floor.

In oceanic areas the slab density in the Bouguer slab correction term must be modified due to the known water depth “D” and the difference in water- and rock density (Fig. 5). If we assume a crustal rock density of 2 670 kg/m^3 and a water density of 1030 kg/m^3 the resulting density for calculations of offshore Bouguer anomalies is $\rho^* = -1\,640$ kg/m^3.

This results in:

$$BA = FA + \delta g_{BPL} = FA + 2 \pi G \rho^* (H_S - H_D)$$

Figure 5: Full page width

Fig. 5. Illustration for describing the calculation of Bouguer anomalies on continents (A), at the ocean (B) and from satellite (C). (A): On land the reduction density ρ is commonly taken as 2 670 kg m^{-3}. The effect of

topography is already removed. The thickness of Bouguer slab equals the station height (H_s). (B): In contrast the reduction density at sea is – 1 640 kg m^{-3}. It is the difference between the sea water density of 1 030 kg m^{-3} and the rock density of 2 670 kg m^{-3}; thickness of the slab now is equal to the different water depths (D). (C): Calculating a Bouguer anomaly in case of satellite gravity a “mass correction” is calculated: $\delta g_{Mass} = \delta g_{Top} + \delta g_{BPL.}$

2.3 Gravity at passive continental margins

In Fig. 6 a very simple Airy-Isostasy model of a passive continental margin is shown. The continental crust is much thicker than the oceanic crust and above the oceanic crust there is the water cover of a few 1000 meters. The specific geometry of the „crust – mantle – water cover“ constellation plays an important role on the trend of the gravity field here. Because of the fact that in the example of Fig. 6 there is no topography, the continental margin remains in an isostatic equilibrium, and one can assume that no Free Air anomaly exists.

Figure 6: One and half page width

Fig. 6. Airy isostatic model at a continent – ocean transition. Notice the thick continental crust and the thin oceanic crust at a passive continental margin. Crust and mantle densities are simplified. Reasonable contrasts which cause large gravity anomalies are related to the water – continent density contrast

and crust – mantle density at the continent of approx. 430 kg m^{-3}. Refer to text for more information.

However, in Fig. 7 (A) strong gravity anomaly results from the same density model (Fig. 7C) which was shown in Fig. 6. The Fig. 7(A) shows the modelled anomaly only for water effect of gravity: related to a model of a “half-indefinite” plate the resulting anomaly is negative and is caused by a strong gradient. Fig. 7 (B) on the other side contains model results which have been done only for the oceanic mantle: now the anomaly is positive and it has a gentle increase because its position is far deeper. Finally Fig. 7(C) demonstrates how the total Free Air anomaly results from the superposition of both effects: the Free Air anomaly is zero in the continental area and over the ocean as well. However, exactly above the margin the gravity field is characterized by a maximum and a minimum that follows. This distribution is a so called „edge“ or boundary effect of the Free Air anomaly and is effected by the difference of the steep gradients in the model.

Figure 7: one and a half page width

Fig. 7. The principal effects on the gravity field at continental margins have equal gravity magnitudes but different gradients. In (A) the water effect causes a steep gradient and in (B) the density surplus of the oceanic mantle is a deeper seated effect which causes only a gentle gradient. In (C) it is explained that a Free Air anomaly at a continental margin is caused by both a negative

and positive “edge effect” due to the superposition of contributions that have equal magnitudes but different gradients.

The trends of a Free air and Bouguer anomalies are shown in Fig. 8. Here modelling again gets use of a „half indefinite“ thin plate for the offshore area (water). It is “zero” over the continent zero and over the oceanic area “positive” (ρ_w = 1030 kg/m^3). The half of the whole Free Air anomaly maximum is accomplished exactly over the edge of the continent.

Figure 8a-b: Full page width

Figure 8c: One and a half page width

Fig. 8. Free Air anomaly and Bouguer anomaly at continental margins which is also in an isostatic balance. (A) The absolute value of the excess mass |+Δm| is equal to the absolute value of the deficient mass|- Δ m|. Therefore the integral of gravity change with respect to the x-coordinate is zero: $\int \Delta g \, dx = 0$. (B) The Bouguer correction at the ocean (see Fig. 3) applied to the Free Air anomaly in (A) yields the general form of the Bouguer anomaly at passive continental margins. (C) The “geological” mass inhomogeneities at the continental margins (seaward dipping reflectors, magmatic remnants, salt structures etc.) cause rather local gravity anomalies which superimpose the regional gravity wavelengths – which are effected by the “simple” structures in (A) and (B).

The gravity fields in Figs. 7 and 8 are caused by the over simplified density structure at the “modelled margin” in Fig. 6. In the real world these margins show a rather complicated picture of gravity distribution due to mass inhomogeneities in the Earth´s crust and lithosphere (and even in the mantle) which are the results of the long-lasting history of the breakup of the Gondwana supercontinent. This becomes quite clear if looking at the processed gravity fields which are shown in the series of figures (Fig. 14 through 21) in Section 4. Their interpretation in terms of regional tectonic and distribution of rock densities will help to provide a rather detailed insight into the causing structure (geometry) and density distribution of the passive margins in the South Atlantic region.

Most aspects of the calculated anomalies, both Free Air and Bouguer, which were discussed before, are typical for nearly all of the continental passive and active margins on Earth. In the next Section the focus will be set on the situation in the Southern Atlantic between Africa and South America – the research area of the German Priority Program 1375 “SAMPLE” of the German Science Foundation – DFG (https://www.sample-spp.de/). The acronym stands for “**S**outh **A**tlantic **M**argin **P**rocesses and **L**inks with onshore **E**volution”. In this interdisciplinary project the primary research areas are the mantle dynamics and magmatic processes, the lithospheric structure, deformation processes and rifted margin formation, the post-rift topographic evolution and many more. In the following Section we will concentrate on this part of the world because a big variety of data and information is available to responds to one of the key questions – how modern satellite missions can contribute to the interpretations and to the understanding of the transition from continental to oceanic lithosphere.

2.4 Focus region: South Atlantic passive margins

To study deeper structures and the overall evolution of conjugate passive continental margins of the South African and South American continents 3D structural models have been designed and evaluated by SAMPLE scientists and their international partners: They constructed detailed density models at both sides of the Southern Atlantic Ocean and a rather preliminary density model for the oceanic part in course of a master thesis (Klinge, 2016). These models are constrained by information and data from boreholes, refraction and reflection seismic, seismological tomography and potential field data – mainly gravity field data. Geophysical fields and observations map geometry and distribution of physical properties of the transitional structures of both crust and lithospheric mantle. Model results (Fig. 9) show (Maystrenko et al., 2013; Autin et al., 2016) that basin centers at the western (Argentinean) side are oriented west-east and therefore oblique to the mid ocean rift axis while at the other (African) side basin centers extend parallel to the ocean rift in north-south direction.

Figure 9o: One and a half page width

Figure 9u: One and a half page width

Fig. 9. For illustration this figure portrays a 3D density model of the SW African continental margin (above, modified after Maystrenko et al., 2013), and the density structure at the Argentinean side (below, Autin et al., 2016).

Apart from these structural differences both sides of the Southern Atlantic reveal similar distributions in temperature and density. Small thicknesses and density modifications in the lithospheric mantle point to small lateral variations of heat transfer into the overlaying crust. However, more relevant for the crustal heat field are lateral thickness changes of the crystalline crust which produce the bigger part of radiogenic heat. This contrasts observations and modelling results at passive continental margins in the area of the Northern Atlantic (Scheck-Wenderoth and Maystrenko, 2008). They found that the oceanic part of lithospheric mantle is much thinner and characterized by smaller densities which cause higher temperatures in the upper crust of the ocean.

To contrasting large scale paleostress fields on the correlating margins of the South Atlantic Salomon et al. (2014) point to in their studies of the South Atlantic. They asked themselves “how passive” continental margins across the globe currently are. Following the results of several other studies these margins experience a variety of stress states and undergo significant vertical movements, as they were deduced from studies of paleo-stresses at both sides of the Southern Atlantic. Here, the bounding continents consist of very different recent geological histories: Africa experiencing continental rifting whereas South America is influenced by subduction on the Pacific side. It is not clear to what extent the Atlantic continental margins are subject to the same stresses and vertical motions as the main continents. Their results show that the tectonic evolution of the continental margins of the South Atlantic is not only passive and that both margins vary significantly in structural style and stress fields, indicating that variable plate boundary forces play a major role in margin evolution. In Fig. 10 we show the situation at the S-American and S-African margin with reference of the paleo-stress field, as it was published by Salomon et al. (2014). Their findings demand careful modelling of both continental margins and a geophysical database which is able to resolve even very small modifications of physical parameters and their structures; refer also to Fig 9 (a) and (b) and the 3D density modelling of lithospheric by Maystrenko et al. (2013) and Autin et al. (2016).

Figure 10: Faull page width

Fig. 10. The sketch (Salomon et al., 2014) portrays an E-W cross-Section between South Africa and South America which summarize the situation of their obtained paleo stresses. It shows that the African margin is controlled by extension while compression characterizes the situation at the South American side. Salomon et al. (2014) explained the extensional state in the east by the existing “African superplume” and the compression in the west by the Andean subduction zone.

Novel satellite gravity missions aim at a breakthrough in recovering the Earth´s gravity and magnetic fields, their gradients as well as their temporal variation. Static anomalies in potential fields (refer to Figs. 14 through 21) are caused by irregular mass distribution on and within the Earth, temporal variations of the gravity field are associated with mass transport processes in the Earth system, such as dynamic processes on the Earth's surface, in lithosphere and upper mantle.

3. Modern satellite gravity missions

The launch of the first generation of satellite gravity missions (Fig. 11) has revolutionized our knowledge of the global Earth's gravity field and its temporal changes. The German CHAMP (Challanging Minisatellite payload; mission period 2000-2010; Reigber et al., 2002; http://op.gfz-potsdam.de/champ/) mission, the US/German GRACE (Gravity Recovery and Climate Experiment; mission period 2002-ongoing; Tapley et al., 2004; http://www.csr.utexas.edu/grace/) mission, and the European GOCE (Gravity field and steady-state Ocean Circulation Explorer; mission period 2009-2013; Drinkwater et al., 2003; http://www.esa.int/Our_Activities/Observing_the_Earth/The_Living_Planet_Programme/Earth_Explorers/GOCE/ESA_s_gravity_mission_GOCE) operated by the European Space Agency (ESA), improved significantly the coverage and availability of high resolution and precisely measured data. These gravity missions are the only measurement technique that can directly observe mass changes on a global scale, and thus they provide a unique observation system for monitoring mass transport in the Earth system. For modern magnetic field observation, apart from the CHAMP mission (2000-2010), with ESA's three SWARM satellites that have been successfully launched in November 2013 also gradients observations have become available (http://esamultimedia.esa.int/multimedia/publications/BR-302/).

Figure 11: one and a half page width

Fig. 11. Satellite gravity missions CHAMP (left), GRACE (center) und GOCE (right). (Sources: CHAMP: GFZ Potsdam, GRACE: NASA, GOCE: ESA Medialab)

In these missions, three measurement concepts are implemented:

1. Observation of orbit perturbations of low-flying satellites due to the varying gravitational attraction, by Global Positioning System (GPS), with an accuracy of 2-3 cm. Non-gravitational forces acting on the satellite, such as drag of the residual atmosphere or solar radiation pressure, are measured by an accelerometer and corrected for in the frame of the gravity field modelling. This satellite tracking technique between a low Earth orbiter (LEO) and high-flying GPS satellites is called satellite-to-satellite tracking in high-low mode (SST-hl), and is implemented in all three missions CHAMP, GRACE and GOCE. It is the primary measurement technique of CHAMP.

2. Observation of orbit differences (ranges) and their temporal change (range rates) between two LEO satellites. This satellite-to-satellite tracking in low-low mode (SST-ll) concept is realized by the GRACE mission. It consists of two identical satellites following each other on the same orbit with an average distance of 200 km. The inter-satellite ranging is performed by means of a K-band microwave system with micrometer accuracy, and shall be done by laser interferometry in future gravity missions in order to further increase the ranging accuracy.

3. Observation of acceleration differences on very short baselines (satellite gravity gradiometry, SGG), representing second order derivatives of the gravitational potential V in all three spatial directions. This concept was

applied by the GOCE mission. Its core measurement, the gravity gradiometer, was composed of 6 accelerometers fixed on 3 orthogonal axes symmetrically around the center of mass of the satellite, measuring acceleration differences on very short baselines of only half a meter in all three spatial dimensions.

The achievable performance of satellite gravity missions depends mainly on the observation technique and the orbit altitude. Fig. 12 shows the performance of different mission concepts in terms of the degree error median, which describes the average signal or noise amplitude at a certain degree *n* of the spherical harmonic series expansion of the gravitational potential *V* in spherical coordinates (with radius *r*, co-latitude ϑ, longitude λ):

$$V(r,\vartheta,\lambda)=\frac{GM}{R}\sum_{n=0}^{N_{\max}}\left(\frac{R}{r}\right)^{n+1}\sum_{m=0}^{n}\bar{P}_{nm}(\cos\vartheta)\left[\bar{C}_{nm}\cos(m\lambda)+\bar{S}_{nm}\sin(m\lambda)\right]$$

where *G* is the gravitational constant, *M* the mass of the Earth*,* *R* the mean Earth radius, $\bar{P}_{nm}$ the fully normalized Legendre polynomials of degree *n* and order *m*, and $\{\bar{C}_{nm},\bar{S}_{nm}\}$ the corresponding (Stokes) coefficients (e.g Torge, 2001). Therefore, the degree error median describes the achievable gravity field accuracy at a certain spatial (half) wavelength λ. The wavelength λ is linked to the harmonic degree *n* by

λ = 20 000 km/*n*

As an example, a harmonic degree of n = 200, which was the minimum target resolution for the GOCE mission, corresponds to a spatial wavelength of λ = 20 000 km/*n* = 100 km.

As a reference, the stippled black curve in Fig. 12 shows the gravity field signal itself. Correspondingly, the cross-over point of a mission performance curve with the black stippled curve indicates at which harmonic degree the signal-to-noise ratio is ‘1’.

Figure 12: One and a half page width

Fig. 12. Absolute gravity signal and error estimates of different observation concepts as a function of the harmonic degree *n* (bottom axis) and spatial wavelength λ (top axis).

From the orbit information (SST-hl) only the long-wavelength features of the gravity field can be extracted. Although this observation type is not a direct gravity field functional, it can be interpreted as disturbing acceleration acting on the orbit, and thus the first order spatial derivative of the gravitational potential $\partial V/\partial x_i$. As a representative of this measurement concept, the grey dot-and-dashed line curve shows the performance of the CHAMP-only model AIUB-CHAMP 03S (Prange, 2011), which is based on 8 years of CHAMP kinematic orbit data.

The grey curve shows the performance of the recent GRACE-only model ITSG-Grace2014 (Mayer-Gürr et al., 2014), which is based on almost 11 years of K-band inter-satellite ranging data following the SST-ll concept (and supported by SST-hl in the very low degrees). Compared to CHAMP, the superior measurement principle of SST-ll results in a significantly better accuracy in the low to medium degree range as well as a higher spatial resolution. This can be explained by the fact that the SST-ll concept can be interpreted as a measurement of acceleration differences on long baselines of about 200 km. The excellent performance of GRACE in this spectral range makes this mission sensitive to the tiny temporal variations of the Earth’s gravity field, which are 4 - 5 magnitudes smaller than the static signal.

The black solid curve shows the performance of GOCE, represented by the GOCE-only model GOCE-TIM-R5 (Brockmann et al., 2014). It is mainly based on the measurement technique of SGG and again SST-hl in the low degrees, because SGG alone (green curve) is weak in this spectral range due to the specific noise characteristics of the gravity gradiometer instrument. Measuring acceleration differences on very short baselines of about half a meter, which approximate second order derivatives of the gravitational potential $\partial^2 V/(\partial x_i\, \partial x_j)$, enables a further increase of sensitivity for high-frequency signals. GOCE starts to become superior over GRACE approximately at degree n = 115.

3.1 Global Gravity Field Models

Gravity field models including GOCE data from the complete mission period are meanwhile available. While the model GOCE-TIM-R5, which is based on the time-wise approach (Pail et al., 2011), is based purely on GOCE data, GOCE-DIR-R5, which is based on the direct method (Bruinsma et al., 2014), contains also GRACE and satellite laser ranging (SLR) data. Further satellite-only models are, e.g., EIGEN-6S2 (Rudenko et al., 2014), or the S-models of the GOCO series (Pail et al., 2010). The maximum degree of expansion of these models is driven by the resolution of GOCE, and varies from n = 280 to 300, corresponding to about 70 km spatial wavelength. This makes clear that all medium scaled geological structures at continental margins and elsewhere in the world which cause a significant gravity effect can be detected (resolved) in the GOCE gravity field.

Combination models (notice the “C” in the field identifier) including also terrestrial, air- and shipborne as well as altimetric gravity are, e.g., the already mentioned pre-GOCE model EGM2008 (Pavlis et al. 2012), EIGEN-6C4 (Förste et al., 2014), and GOCO05C (Fecher et al., 2013, 2016). These models extend the spatial resolution beyond degree 2000 (which corresponds to 10 km wavelength). However, it should be noticed that there are many regions with sparse and/or low-quality terrestrial data, where it has to be questioned if such a high resolution is justified. This holds for many areas worldwide, e.g., the Central Andes in South America and also for the passive continental margins of the South Atlantic.

3.2 Products for use in Earth sciences interpretation

Specifically regarding GOCE-related data, modelers and other users have the choice among basically three representations of gravity field products:

3.2.1 Spherical harmonic coefficients

The most commonly used representation of the global gravitational potential *V* is its series expansion into spherical harmonics (Section 3). There corresponding fully normalized spherical harmonic (Stokes) coefficients $\{\bar{C}_{nm}, \bar{S}_{nm}\}$ represent the model parameters, and are usually the target quantity when deriving the model from the original gravity field data. The advantage of using this representation is that it can be considered as a weighted average of the original measurement data, so that the original noise level is significantly reduced due to this averaging. Based on the set of spherical harmonic coefficients any arbitrary gravity anomaly can be derived at the Earth's surface or at any height in outer space. All the global gravity models discussed above are given in this parametrization.

3.2.2 Original gravity gradients along the satellite's orbit

In principle, also the gravity gradient time series for all six tensor components measured along GOCE's satellite orbit can be used for geophysical modelling (refer e.g. to Fig. 3). They represent the most original measurements. However, it has to be considered that they are measured in a rotating reference frame, the so-called "gradiometer reference frame" (GRF), which means that tensor rotations of the base functions have to be applied to exploit them to the best possible extent. Additionally, they are affected by the colored noise characteristics of the GOCE gradiometer (Pail et al., 2011), so that a single point-wise gravity gradient observation is affected by large instrument noise, and therefore by itself has a low signal-to-noise ratio. All these drawbacks make it difficult to use this data type directly for geophysical modelling.

3.2.3 Gravity gradient grids

A reasonable compromise between the use of spherical harmonics and original gravity gradients (see above) results in the use of *gravity gradient grids*, which are usually defined in a well-oriented radial (North-East-up) frame at a constant altitude. They are computed from the original gravity gradients defined in the GRF by means of regional gravity processing methods. In fact, they are the spatial equivalent of the spherical harmonic representation, but much easier to use and interpret. Pure GOCE gravity gradient grids result from the space-wise method (Gatti and Reguzzoni, 2015). In the frame of the ESA project GEOExplore global grids of all six components of the gravity gradient tensor, based on a combination of GOCE and GRACE data, and defined in a radial Earth-fixed reference frame at two altitudes of 225 km and 255 km, have been derived (Bouman et al., 2015). Since these grid values are products of “averaging” original gradient data, the error level should be similar as that of gradients synthesized from global spherical harmonic models.

There is an ongoing discussion whether the gradient data contain more (high-frequency) signal than global gravity models that have been derived from them. The answer to this question lies in the constraints applied to these models. Constraints applied to global gravity models are usually designed to optimize the signal-to-noise ratio on a global scale. This means that in regions of very rough topography and therefore high-frequency gravity signals there is the tendency to constrain the system too strongly. Regional gravity solutions techniques, which are usually applied to generate gridded gravity gradient products, allow for regionally optimized constraints, but on the cost of global homogeneity. In Pail et al. (2015b) it could be shown, that compared to global models the gravity gradient grids are affected by a higher noise level.

The achievable accuracy and sensitivity of current gravity field models or corresponding gravity (gradient) grids can be expressed by cumulative quantities, which describe the estimated cumulative error at a certain harmonic degree (or the corresponding spatial wavelength). Fig. 13 shows cumulative gravity anomaly errors (a), as well as cumulative vertical gravity gradient errors at GOCE satellite altitude of 250 km (b), and ground level (c), for the GRACE models ITSG-GRACE2014s, the pure GOCE model GOCE-TIM-R5, the combined satellite-only model GOCO05S and the combined models EGM2008 (pre-GOCE) and GOCO05C (including GOCE data).

From Fig. 13 we can learn which geological structure at passive continental margins (or elsewhere) can be resolved by the different gravity model types. Assuming that the geological structure/mass anomaly generates a *gravity anomaly* with a certain spatial wavelength on the Earth’s surface, Fig. 13a then provides the accuracy in mGal with which this anomaly can been captured. (The connection from the size of a disturbing body to the resulting gravity signal is made in Fig. 3.). As an example, a gravity signal with 100 km spatial wavelength at the Earth’s surface could be measured by satellites with an accuracy of about 0.5 mGal (black dashed and solid grey curves). It can clearly be seen that the accuracy for shorter wavelength signals dramatically decreases, and is already larger than 2 mGal for gravity signals with approx. 80 km spatial wavelength. Beyond this resolution, satellites cannot significantly contribute anymore, and high-accuracy terrestrial information, as it was included, e.g., in

Figure 13: Full page width

Fig. 13. Cumulative gravity anomaly errors in (mGal) (a); vertical gravity gradient errors in (mE) at 250 km (b), and ground level (c). This figure shows the generally dramatic increase of the gravity gradient errors at ground level as a result of downward continuation.

GOCO05C (solid black curve), is necessary to resolve smaller-scale geological structures. This becomes immediately clear if looking at the series of Figs. 14 through 21: most of the anomaly sizes at the margins of the South Atlantic are smaller than 80 km. On the other hand we state that the regional gravity field caused at the ocean-continent transition can satisfyingly be resolved by satellite only models (S models). Fig. 13a also shows the major step forward due to satellite missions compared to pre-GOCE models such as EGM2008 (black dot-and-dashed line) especially in the long to medium wavelengths for gross interpretations at a continental scale.

Fig. 13b shows a similar representation when using *gravity gradients* at satellite altitude as basis information for geophysical modelling of geological structures. Pure GOCE-only models such as GOCE-TIM-R5 (dashed black curve) provide gravity gradients at satellite altitude with standard deviations of 0.45 mE for gravity signals with a spatial resolution of 100 km. These values can be decreased further to 0.25 mE by combination with GRACE information, as it was done, e.g., in the GOCO05S model (solid grey curve). Evidently, GRACE alone (dashed grey curve) results in very high error amplitudes in the higher degrees, demonstrating the dominant impact of GOCE at shorter wavelengths. Modern combined gravity models such as GOCO05C (solid black curve) further increase the performance in the short-wavelength range by complementing the satellite data by ground data over the continents and satellite altimetry over the oceans. Also here the improvement compared to pre-GOCE combined models such as EGM2008 (black dot-and-dashed line curve) is significant. Recently gradients of the satellite gravity field came into the focus for modelling purposes which can support interdisciplinary interpretations (Ebbing et al., 2013; Schaller et al., 2015; Götze, 2015).

In Fig. 13b a very interesting feature is the flat curve of the combined gravity model GOCO05C beyond degree 250. This results from the fact that beyond this degree the signal amplitude of gravity gradients is already below the mE level, i.e., due to signal attenuation with altitude there is no significant gradient signal left in orbit altitude beyond this degree, because most parts have been “filtered out” due to upward continuation. Inversely, this also means that GOCE has captured 97% of the amplitude of the gradient signal that exists in orbit altitude.

The picture changes completely (Fig. 13c) when continuing the gradient information down to ground level. Here the GOCE model (black dashed curve) and the GOCE+GRACE combination (solid grey curve) perform practically identical, again showing the dominance of GOCE compared to GRACE at shorter scales. However, also here for gravity signals with spatial scales below 80 - 100 km a combination with terrestrial/airborne gravity information is necessary to achieve acceptable accuracies (solid black curve), so that the gravity field information can be used for local geophysical modelling of short-scale density structures.

3.3 Not always in focus: the omission error

In order to perform a complete evaluation of the impact of modern satellite missions for deriving density structure of continental margins, one of the most important aspects is the evaluation of the *omission error*. It results from high-frequency signals, which cannot be resolved by satellite gravimetry due to the exponential signal attenuation with altitude. These missing signals of satellite-only models are an important issue for the determination of near-surface density variations, but also shallow lithospheric structures.

Fig. 14 shows gravity anomaly fields for the South Atlantic region. Fig. 14 a is based on the GOCO05S model resolved up to its maximum resolution of degree *n* = 280 (~ 70 km), while Fig. 14 b displays the free-air gravity anomalies based on EIGEN-6C4 with its maximum resolution of degree *n* = 2160 (10 km). Comparing these two figures, the current limits of satellite-only models regarding their spatial resolution becomes evident, and can only be coped with by combination with complementary data sources from terrestrial/airborne/shipborne gravimetry, and satellite altimetry over the oceans, as it was done in EIGEN-6C4. An estimate of the omission error (Fig. 14 c) for satellite gravity models is given by the difference of EIGEN-6C4 and GOCO05S, being equivalent to the difference of the Figs. 14 a and b. Evidently, very rough topographic and bathymetric structures, generating high-frequency gravity field anomalies and steep slopes, cannot be resolved by the satellite data. However, usually these topographic features are not the main focus of geophysical modelling and interpretation, but rather sub-surface lithospheric structures. Therefore, a topographic reduction was applied, using the RWI_TOPO_2015 topographic potential model (Grombein et al., 2015) and thus taking away the effect of topographic masses up to zero level: $\delta g_{TOP} + \delta g_{BPL}$. The so called “mass reduction effect” was already introduced in Fig. 6. The result is a significantly reduced omission error (Fig. 14 d).

This difference field in Figs. 14 c and d can be considered as errors made when computing Bouguer anomalies from pure satellite models, which are then further used for lithospheric modelling. Table 1 gives an overview of the main statistical parameters of the gravity anomaly fields shown in Fig. 14.

Figure 14: Full page width

Fig. 14. Free-air gravity anomalies (mGal) of the South Atlantic region based on satellite-only model GOCO05S (a) resolved up to degree 280 , combined gravity model EIGEN-6C4 (b) resolved up to degree 2160, omission error of a satellite-only model (c) and omission error after reduction of topographic signals (d).

Table 1: Main statistical parameters of gravity fields of the South Atlantic region.

Gravity field	Figure	min (mGal)	max (mGal)	std.dev. (mGal)
GOCO05S (d/o 280)	14 a	-199.8	116.1	18.8
EIGEN-6C4 (d/o 2160)	14 b	-227.7	453.8	21.3
GOCO05S omission error	14 c	-166.7	415.1	10.8
GOCO05S omission error, topo-reduced	14 d	-143.1	112.8	7.1

4. Benefits for combined interpretations

However, in relation with the two key questions asked in Section 2.3 (processing, quality and secondly availability for interpretations at continental margins) we have to respond to them in the light of interpretations of solid Earth structures. For example a precise geoid can be used to identify global and deep anomalies related to mantle lithosphere and deeper structures. Gravity anomalies, being first order radial derivatives of the gravitational potential, are sensitive to gravity effects of the entire lithosphere, and in particular to the crustal and upper crustal structures and density variations e.g. at active and passive continental margins. As it has been shown above (Fig. 14), each combination of satellite gravity data with terrestrial gravity data can be used for all interdisciplinary interpretations techniques, e.g., “back stripping” in basin modelling at the African continental margin (Dressel et al. 2015) which also includes thermal subsidence in the reconstruction of the passive margins through time or 3D modelling of Moho undulations. The new database was also used to reconstruct the Gondwana continent (Braitenberg, 2015). Fig. 15 refers to the isostatic residual anomaly in the Southern Atlantic. It was calculated by Klinge (2016) on base of the corresponding formula for “ISA” in Section 2.3 and the EIGEN-6C4 model also portrayed in Fig. 14 (b).

Both anomaly maps are rather similar and caused by the main tectonic features of the South Atlantic: the “highs” which are caused by the Mid Atlantic ridge, the extended “lows” of the four basins in front of South America (Argentinean and Brazilian basins) and South Africa (Cape and Angola basins). The hotspot trail (e.g. Torsvik et al., 2009 among others) is visible in the structure of the SW-NE trending Walvis Ridge offshore South Africa and the corresponding trace of the Rio Grande Rise at the western side. To the North of the Romanche Fracture Zone between Fortaleza in the west and Lagos in the East the Sierra Leone Rise is located. Even the regions of salt deposits offshore Brazil and West Africa (blueish colors indicating low gravity values) and the magmatic margins at both sides of the margins (reddish colors and high gravity values) can be distinguished in the satellite derived fields. The very short wavelengths in the gravity field correspond to masses that are located in the crust and lithosphere – they were already mentioned in the sketch of Fig. 8 and mark places of different density contrast at the margins. Other examples were given in Bouman et al. (2014), Gutknecht et al. (2014), and Hosse et al. (2014).

Figure 15: one and a half page width

Fig. 15. The isostatic residual field was calculated by Klinge (2016) in the framework of his MSc thesis. Reference depth T_0 = 30km and T_e = 20 km (elastic thickness

which was kept constant over the entire area). The figure shows the residual gravity field in the Southern Atlantic Ocean of the combined EIGEN-6C4 model (Förste et al., 2014). It correlates well with bathymetric/topographic structures e.g. the Mid Atlantic Rift (MAR) and portrays also the effect of geological bodies: the positive anomalies in the area of Windhoek and Buenos Aires. Along the Mid-ocean rift axes positive anomalies of up to 40 mGal exist. MAR = Mid Atlantic rift.

4.1 The continental margins of the South Atlantic

New light can be shed on the gravity structures of South Atlantic oceanic margins at regional (Figs. 16, 17, 19 and 20) and more local scales (Figs. 18 and 21). By the help of these new compiled maps we will show that modern satellite gravity fields described in Section 4 can support (1) interpretations of the lithospheric structures in the South Atlantic and its passive margins and (2) provide much more details in the gravity field than it was showed along the oversimplified profiles of Figs. 7 and 8.

With reference to the Fig. 14, the following sequence of Figs. (16 – 21) contains always the same information for comparative reasons: the two gravity fields based on the “satellite only” model GOCO05S (a) and the “combined model” EIGEN-6C4 (b), and additionally Figs. 18 and 19 include the omission errors *without* (c) and *with* (d) calculated topographic reductions.

Table 2 provides a summary of the standard deviations of the gravity fields shown in these figures. **d**/**o** refer to the spherical harmonic analysis: to **d**egree and **o**rder of the expansion.

Table 2: Standard deviations (mGal) of the gravity fields shown in Figures 16 to 21.

Region	Figure	GOCO05S	EIGEN-6C4	GOCO05S	GOCO05S

		(d/o 280)	(d/o 2160)	omission error	omission error, topo-reduced
Argentinean coast	16	22.4	24.6	9.8	7.1
Brazilian coast	17	15.9	18.8	10.8	6.3
Falkland Bank	18	24.4	25.3	7.3	5.9
African coast	19	19.3	21.5	10.6	7.3
Equatorial African margin	20	19.3	23.9	14.3	9.8
Tristan da Cunha isle	21	6.9	12.3	10.3	4.8

Continental gravity edge effects indicate a fast change from positive to negative anomalies as it is normal for the transition from oceanic to continental crust. In Fig. 16 the positive anomalies indicate in the offshore area the seaward dipping reflectors (SDR) which are of magmatic origin (e.g. Blaich, 2011; Franke et al. 2006; Section 2). The negative anomalies (greenish and blueish colors) offshore are caused by the sedimentary infill of the margin basins e.g. Colorado and Salado (e.g. Autin et al., 2013; 2016). Onshore positive anomalies follow W-E trending topographic features (Salado and Colorado Basin) and in the western continental part of the maps the topography of the Southern Central Andes.

Figure 16: Full page width

Fig. 16. Detailed picture of the free-air gravity field along the Argentinean coast compiled by the GOCO05S (a) and the EIGEN-6C4 (b) models. The lower two

figures indicate the omission errors without (c) and with topographic correction (d). For more information refer to manuscript. The continental areas are marked by transparent overlays.

In general the series of the following figures will portray similar gravity anomalies (both magnitude and trend of anomalies). It is no wonder that all EIGEN-6C4 compilations consist of more structural details than the GOCO05S models which base on data in the orbit height of some 250 km where small local gravity anomalies are not detectable.

Figs. 17 (a) and (b) shows that the “central Atlantic segment” is dominated by high density rocks which cause positive anomalies. The positive gravity offshore between 40° - 30° longitude is caused by the “Rio Grande High” which marks the most western edge of the hot spot trace which starts at the position of the Tristan da Cunha hotspot area. The negative gravity anomalies close to the Brazilian coast are caused by negative densities of salt accumulation here (Mohriak, 2014). The SDRs with their high rock densities (Section 2.2) of the southern segment are not documented here with high resolution; they are too small to be resolved *in detail* as we show already in Fig. 3. However, at a larger scale the belt of positive gravity marks the area of SRDs quite well.

Figure 17: Full page width

Fig. 17. The gravity fields (a) GOCO5S and (b) EIGEN6C4 along the Brazilian coast and offshore regions of the “central segment” of the southern Atlantic. Figures content is equal to Figs. 14 and 16. However the omission errors are not portrayed here.

The resolution of gravity anomaly in the off-shore area of the *Falkland Bank* and the Scotia Plate with the Eastern Sandwich trench allows the separation of subduction related trench lithosphere, the eastern border of the Sandwich Plate, and the southern rim with the Antarctic Plate (low gravity corresponding to blueish colors in Fig. 18) from high density rocks of the Scotia Plate and Sandwich Isles (yellow and reddish colors in Fig. 18 (a and b). Exactly here in a region with rather complex interplay of different plates the resolution of gravity fields before the era of the modern satellite missions was extremely low and often hindered a tectonic interpretation of lithosphere at medium scale. The Scotia Plate in the center (reddish colors in Fig. 18) is clearly separated from the other plates of the region (South American plate to the North, Antarctic plate to the South, Scotia plate to center.

Figure 18: One and a half page width

Fig. 18. The gravity field of the Falkland bank and the Scotia plate with the eastern South Sandwich trench after the processing of new satellite gravity (GOCO5S: (a) and EIGEN6C4: (b). Figures content is equal to Fig. 14.

Due to the symmetry of evolution of the South American and South African margins also the gravity field of the western African margin shows the same general features as it was exemplified for the South American margin: in the southern segment the magma dominated structures cause small positive gravity anomalies and North of the Walvis Ridge the area of salt layers is characterized by negative anomalies (blueish colors) in Fig. 19. The SW – NE trending Walvis Ridge separates the domains of magmatic material from salt layers. Positive gravity anomalies of the ridge clearly indicate the Tristan da Cunha hotspot trace – as it was already explained for the western part of the Southern Atlantic. More to the South at the South African tip of the Cape a second ridge (Agulhas Ridge) can be identified.

Onshore at the African continent close to the equator the extended gravity low (-50 mGal) of the Congo Basin with its thick sediments dominates the gravity picture.

Figure 19: full page width

Fig. 19. The gravity field of the African margin in the central and southern segment (Fig.15) after the GOCE gravity (a) and the EIGEN-6C4 data (b) processing. The series of maps correspond to the displayed formats of figures before; transparent overlay mark continental area.

One of the most spectacular fracture zones in the Equatorial and Northern South Atlantic connecting Africa and South America is illustrated in Fig. 20 (a and b). Fairhead and Wilson (2005) explain the formation of the fracture system with processes which were related with the opening of the Central and South Atlantic. They state that a differential motion between plate segments was absorbed in the Caribbean and West and Central African rift systems. The fracture system developed due to the temporal different opening phases of the northern and southern Atlantic. Then the two independent spreading centers joined a major shear zone developed between West Africa and the northern margin of Brazil. The maps of satellite gravity image impressively this major shear zone. The gravity map of the EIGEN6C4 model provides a clear and sharp picture of the fractures zones.

Figure 20: One a a half page width

Fig. 20. The two gravity fields (GOCO5S (a) and EIGEN (b)) of the Equatorial Atlantic Ocean map major transform structures offshore the African margin. Sequence of maps corresponds with displayed formats of figures before; transparent overlay mark continental area.

The limits of resolution of modern satellite only gravity fields (S models) can nicely be demonstrated by the gravity field of the Tristan da Cunha Isle, whose gravity field signal is at the edge of the spatial resolution of current satellite gravity missions. Fig. 21 shows that although GOCE is able to detect the gravity field signal of this island, it is significantly damped. It should be emphasized, that a constraint has been applied to the GOCO05S model in the frame of the gravity modelling procedure in order to improve the signal-to-noise ratio at higher degrees, i.e. noise is filtered out at the cost of damping also the signal. As already discussed in Section 3.2, the strength of constraining the solution was optimized on a global scale. Therefore, it is not tailored to small regions with strong gravity field signal, where a weaker constraint would be preferable due to a larger signal-to-noise ratio in this region compared to the global average. If the satellite gravity solution were optimized for this specific region, it can be expected that in such a regionally tailored solution slightly more signal could be retained. The series of Figs. 21 (a) – 21 (d) shows that the satellite gravity fields of both GOCE and EIGEN-6c4 are mainly caused by the topography of the island. Perfectly seen is the “ring” of negative anomalies in Fig. 21 (b) which can be explained by the flexure of oceanic lithosphere due to isostatic response of the loaded isle masses. After calculating a topographic correction (Fig. 21 (d)) an anomaly of some 20 mGal appears. One may speculate if this negative anomaly is caused by a mass deficit which is related to the hot spot or to crustal thickening..

The statistics in Table 2 shows that for such rather small-scale structures the amplitude of the omission error can be larger than the signal captured by GOCE. However, Fig. 21d shows that significant parts of this high-frequency gravity signal result from topography.

Figure 21: one a half page width

Fig. 21. The Free Air gravity field of the Tristan de Cunha area after the GOCE (a) gravity and EIGEN-6C4 (b) data processing. Sequence of the four maps corresponds with displayed formats of figures before; omission error without (c) and (d) with topographic correction. The limits of resolution of satellite observations can nicely be demonstrated by these gravity fields.

Figure 21a: Small column size

Fig. 21a. In addition to what we interpret in Fig. 21 this sketch can explain the typical negative ring around the positive anomaly in the last figure: the central mass causes the positive anomaly while the sediments around the central mass cause a symmetrical gravity low. The extent of deformed crust below the mass crust depends on the rigidity of the surrounding crust: the left situation (rigidity R1) demonstrates a case with extreme high rigidity, on the right a lower crustal rigidity R2 was assumed.

4.2 Validation of terrestrial gravity by GOCE data

The GOCE mission provided not only new geoid and gravity fields, but also gravity gradient data. Representing the second derivatives of the gravitational potential, they are more sensitive to the density structures of the upper crust than gravity data normally are. Additionally, gravity gradients provide a better resolution of flanks of geological structures, faults, lineaments or even large intrusions at continental margins. Gradient data from satellite missions have the potential to identify the extent of different structures with varying densities even in the lower crust (e.g. Ebbing et al., 2013). Panet et al. (2014) even identify correlations of certain components of the gravity gradient tensor with lower mantle structures.

For gravity interpretations at larger wavelengths the new satellite gravity database will help to identify a density zonation and segmentation in horizontal and vertical directions in the lithosphere. As shown in Section 3.2, GOCE satellite-only gradient data provide a spatial (horizontal) resolution in the range of less than 100 km. However, for many structures - in particular for offshore studies of Applied Geophysics - this spatial resolution is not yet sufficient, because smaller crustal structures cause anomalies with smaller spatial wavelengths. Therefore, terrestrial and airborne gravity measurements have not become obsolete even in the modern satellite era, but on the contrary they complement satellite observations on the short-wavelength scale where satellite data lack sensitivity.

In addition to their very high accuracy in the long to medium wavelength range, modern satellite gravity data definitely provide significant added value in the geophysical gravity fields processing domain, especially for:

a) Validation of heterogeneous terrestrial gravity data bases and identification of outliers;

b) Fill-in of regions with sparse terrestrial data coverage or even data gaps.

As an example of the first task (a), Fig. 22 a shows the difference between a terrestrial gravity data base of South America and GOCO05S, resolved up to degree 200. To bring them to the same spatial resolution, the terrestrial data have been expanded as part of a global 0.25° × 0.25° terrestrial gravity anomaly grid into a spherical harmonic series to degree 720, and then have been cut at degree 200. Fig. 22 a clearly indicates systematic differences, which can be attributed to errors of the terrestrial data, because of the globally homogeneous accuracy of less than 1 mGal for the satellite model. Based on this result, the terrestrial database can be further screened for outliers and suspicious observations (either of the gravity value itself or the attached height information, Hosse et al., 2014). This information can then be used to derive empirical error estimates of the terrestrial dataset, which can be further used for a spatially depending weighting scheme in the frame of a combined solution with satellite data (Fecher et al., 2013, 2016). The implicit assumption is that the data quality of a terrestrial observation is already reflected in its long-wavelength component. By means of this procedure, satellite data get a higher weight in regions where a lower accuracy of terrestrial data is suspected.

Figure 22: Full page width

Fig 22. (a) Gravity anomaly differences (mGal) between a South American terrestrial database (kindly provided by the US National Geospatial-Intelligence Agency) and GOCO05S, consistently resolved up to degree 200; b) empirical error estimates (mGal) derived from the difference field (after: Fecher et al. (2015), modified).

It should be emphasized, that this validation procedure can be applied in any region on Earth. Thereby, a globally uniform satellite gravity model provides the chance to estimate a-posteriori the accuracy and reliability even of historical gravity data bases (terrestrial, ship- and air-borne), for which only incomplete or even no meta-information about the measurement process and conditions is available.

Also Bomfim et al. (2013) describe how gradients of the GOCE mission can help to estimate systematic errors in terrestrial gravity data in the cratonal basins (e.g. Amazon and Parnaiba Basins) in Brazil. Here they calculate an average value of terrestrial gravity anomaly and compare its long- and medium-wavelength content of the terrestrial gravity with the GOCE gravity field. The analysis shows that where terrestrial data are sparse and therefore require an improvement in data coverage, satellite data can be substituted in order to represent the gravity field correctly. The method they proposed can be used directly to control other gravity databases and constitutes as a tool for the quality assessment of terrestrial gravity observations, both on- and offshore.

The second task (b) also addressed the heterogeneity of terrestrial gravity data. There are many regions worldwide where terrestrial data are of very bad quality or not available/accessible at all (refer to Fig. 2). In these regions, data from satellite gravity missions are the only available data source.

These examples demonstrate, that although satellite missions provide (only) long to medium wavelength gravity field data, they are able to provide new gravity field information especially in regions where up to now the gravity field has been practically unknown. This regional model can then been used as constraint for an improved lithospheric density model and the derivation of the state of stress of the subduction zone (Gutknecht et al., 2014), clearly demonstrating the added value of GOCE especially in these data-critical onshore regions.

5. Conclusions and outlook

The resolution of “satellite only data” up to now does not fall below a resolution of 80 - 100 km. This is still the borderline for studies presented in the above mentioned Sections. In summary we have to say that rather small complex structures related e.g. to the “seaward dipping reflectors at passive continental margins (SDR)” with small size and density contrast cannot be resolved as separated anomalies in the orbit heights of recent satellite missions (e.g. Schaller et al. 2015). For this purpose terrestrial gravity data have to be combined with satellite data in gravity models e.g. GOCO5C. The interpretations of Section 4.1. showed that gravity and its gradients from the modern satellite missions support interpretations at a medium scale – at passive continental margins and elsewhere.

Modelers of lithospheric structures at continental margins hope that medium scale gravity data from the recent and future satellite missions (GRACE and/or GOCE; GRACE follow on) can support combined interpretation together with seismological and gravity studies. For rather local models (wavelengths of gravity anomalies are smaller than 20 km) both resolution and quality of satellite only gravity data have to be seen still reluctant until today. However, there is no doubt that combinations with terrestrial gravity data bases and satellite gravity with a spatial resolution of 10 – 20 km can provide detailed insight in the structural behavior of continental margins.

For modelling at continental scales Fig. 2 demonstrated that terrestrial databases often are of inhomogeneous distribution (e.g. in South America), just if gravity data are sampled over long time-consuming field campaigns with big human efforts: there remain big gaps in the data base. They are mainly caused by limited access to the terrain in remote areas of the world – high mountains, deserts, swamps and jungle. Even more field procedures and technical instrumentation varied over time and together with missing other metadata a homogeneous data base can be established only with big effort and high costs. Here the new data bases already helped in a spectacular way: Hosse et al. (2014) and Gutknecht et al. (2014) replaced the incomplete terrestrial gravity data base by homogeneously measured satellite gravity and gravity gradient data for lithospheric modelling. New data were applied to the calculation of GPE (gravity potential energy), stress distributions and combined interpretation of complex geologic structures. Satellite gravity information was also used for validation and cleaning of inhomogeneous gravity databases taking the benefit of very homogeneous error characteristics and accuracy of global satellite gravity data (Hosse et. al, 2014; Bomfim et al., 2013). The high spatial resolution of terrestrial gravity *combined* with the homogeneous lower-orbit satellite data leads to more detailed and better-constrained lithospheric density models, and hence improves our knowledge about structure, evolution and state of stress in the lithosphere basing on the consistency in the long-to-medium wavelengths, down to 10 – 50 km.

At the beginning (Section 1.1) we mentioned the calculation/recalculation of the COB from an integrated interpretation of gravity, magnetic, seismic, electrical methods and geology (Torsvik et al., 2009). We did not deal with the calculation of COB, however, we think that the combined satellite fields can successfully replace the terrestrial gravity data which have to be used in former times. Because we analyzed Free Air gravity from the GOCE mission, in Fig. 23 topographic features on- and offshore are enhanced. These enhancements indicate clearly the slopes of the continental shelf regions of the Southern Atlantic.

Figure 23: Full page width

Fig. 23. The third derivations of the gravitational potential and the resulting total gradient of the vertical gravity gradient were calculated from the GOCO5C model (expansion to degree 720). It provides already good insight into local gravity field structures particularly at the margins by the derivations of the vertical gradient (V_{zz}).

In the near future complementary information from seismic and magnetics could be included in a joint inversion for lithospheric modelling also at passive continental margins. ESA's magnetic field mission *Swarm* was successfully launched in November 2013 and provides valuable information of the long to medium wavelength Earth's magnetic field and its temporal variations with an accuracy on the nT- (nano tesla) level (http://esamultimedia.esa.int/multimedia/publications/BR-302/). The value of the mission for the determination of the crustal remanent magnetic field will increase in the future, because the three satellites will continuously lower their orbit altitudes during mission lifetime, thus also increasing their sensitivity for detail magnetic field structures. However, a joint interpretation of remanent magnetic and gravity field is only possible in the case of common sources, i.e. similar contrasts in density and magnetization. In this case Poisson's equation can be applied, which links the magnetic and gravity potential fields. Swarm is already now a very valuable tool to determine the electric conductivity of the Earth's mantle and thus provides very important information on the thermochemical and compositional structure of the Earth.

Several concepts for future satellite mission constellations to explore the Earth’s potential fields are under development and investigation. A strong need by the user communities was expressed in terms of a joint IUGG resolution adopted at the IUGG General Assembly 2015 (IUGG, 2015). The science requirements and user needs for a future gravity field mission constellation were consolidated (Pail et al., 2015a) also under active participation of the geophysical user community. In addition to an improved temporal resolution for the detection of co- and post-seismic deformation, an increased spatial resolution together with an improved accuracy will shift the capabilities to use satellite-based gravity observations for geophysical interpretation in passive continental margins, and elsewhere, to even more small-scale structures.

Acknowledgements

The research partly described here in this paper was part of the Priority Program SAMPLE (**S**outh **A**tlantic **M**argin **P**rocesses and **L**inks with onshore **E**volution). It is financed by the Deutsche Forschungsgemeinschaft (DFG), Bonn which is thankfully acknowledged. HJG thanks M. Scheck-Wenderoth and members of her research team at GeoForschungsZentrum Potsdam for their continuous interest and many fruitful discussions over the last years. The satellite part of the paper was elaborated in a second DFG Priority Program “Mass Transport and Mass Distribution”. HJG and RP are deeply grateful to their research teams at the Christian Albrechts Universität Kiel, Technische Universität München and Friedrich-Schiller-Universität, Jena. We thank Reiner Rummel and Jörg Ebbing for their intensive “test reading” and fruitful suggestions. Carla Braitenberg, Bruno Meurers and an anonymous reviewer improved an earlier version of the paper by their careful reviews.

References

Autin, J., Scheck-Wenderoth, M., Loegering, M.J., Anka, Z., Vallejo, E., Rodriguez, J.F.,Dominguez, F., Marchal, D., Reichert, C., di Primio, R., Götze, H.-J., 2013. Colorado Basin 3D structure and evolution, Argentine passive margin. Tectonophysics 604, 264–279, doi:10.1016/j.tecto.2013.05.019

Autin, J., Scheck-Wenderoth, M., Götze, H.-J., Reichert, Ch., Marchal, D., 2016. Deep structure of the Argentine margin inferred from 3D gravity and temperature modelling, Colorado Basin. Tectonophysics 676, pp. 198-210, doi.org/10.1016/j.tecto.2015.11.023.

Baeschlin, C. F., 1948. Lehrbuch der Geodäsie. Verlag Orell Füssli, Zürich.

Bauer, K., Neben, S., Schreckenberger, B., Emmermann, R., Hinz, K., Fechner, N., Gohl, K., Schulze, A., Trumbull, R.B., Weber, K., 2000. Deep structure of the Namibia continental margin as derived from integrated geophysical studies. Journal of Geophysical Research 105, pp. 25 829 - 25,853.

Basile, C., 2015. Transform continental margins - Part 1: Concepts and models. Tectonophysics, Elsevier, no. 661, pp.1-10. 10.1016/j.tecto.2015.08.034

Benioff, H., 1954. Orogenesis and deep crustal structure – additional evidence from seismology, Bulletin of the Seismological Society of America, 66, 385–400.

Blaich, O. A., Faleide, J. I., Tsikalas, F., 2011. Crustal breakup and continent-ocean transition at South Atlantic conjugate margins, Journal of Geophysical Research. 116, B01402, doi:10.1029/2010JB007686.

Boltwood, B., 1907. The Ultimate Disintegration Products of the Radio-active Elements. Part II. The disintegration products of uranium. American Journal of Science series, 4, 23, 77–88. doi:10.2475/ajs.s4-23.134.78.

Bomfim, E.P., Braitenberg, C. and Molina, E.C., 2013. Mutual evaluation of global gravity models (EGM2008 and GOCE) and terrestrial data in Amazon Basin, Brazil. Geophysical Journal International, 14 pages, doi: 10.1093/gji/ggt283.

Bond, G.C., Nickelson, P.A., Kominz, M. A., 1984. Breakup of supercontinent between 625 Ma and 55 Ma, New evidence and implicationes for continental histories. Earth and Planetary Science Letters, 70, 325-345.

Bouman J., Ebbing J., Meekes S., Fattah R.A., Fuchs M., Gradmann S., Haagmans R., Lieb V., Schmidt M., Dettmering D., Bosch W., 2015. GOCE gravity gradient data for lithospheric modeling. International Journal of Applied Earth Observation and Geoinformation 35(A): 16-30, Elsevier, 10.1016/j.jag.2013.11.001.

Bouman, J., Fuchs, M., Lieb, V., Schmidt, M., Ebbing, J., Holzrichter, N., Gradmann, S., Abdul Fattah, R., Meekes, S., Novak, P., Sebera, J., 2014. GOCE+ GeoExolore - Final Report ESA, RP-GOCE+-DNT-11, 2.1, 1 – 443.

Braitenberg, C., 2015. Exploration of tectonic structures with GOCE in Africa and across continents. International Journal of Applied Earth Observation and Geoinformation, 35, pp. 88-95.

Brockmann, J.M., Zehentner, N., Höck, E., Pail, R., Loth, I., Mayer-Gürr, T., Schuh, W.-D., 2014. EGM_TIM_RL05: An independent Geoid with Centimeter Accuracy purely based on the GOCE Mission. Geophysical Research Letters, Wiley, doi: 10.1002/2014GL061904.

Bruinsma, S.L., C. Foerste, O. Abrikosov, J.M. Lemoine, J.C. Marty, S. Mulet, M.H. Rio und S. Bonvalot. 2014. ESA's satellite-only gravity field model via the direct approach based on all GOCE data. Geophysical Research Letters, 41(21), 7508–7514, DOI: 10.1002/2014GL062045.

Cappelletti, A., Salvi, F., Meda, M., Cavozzi, C., Chowdhury, B.R., Nestola, Y., Argnani, A., Tsikalas, F., Magistroni, M., Dalla, S., Roveri, M., Bevilacqua, N., 2011. Tectono-Stratigraphic Evolution of South Atlantic Extensional Rifted Margins: Constraints from Sandbox Analogue Modeling. Search and Discovery Article, no. 30204.

Colli, L., Ghelichkhan, S. and Bunge, H. -P., 2016. Geophysical Research Letters, Volume 43 Issue 6, pp. 2510-2516.

Dressel, I., Scheck-Wenderoth, M., Cacace, M., Lewerenz, B., Götze, H.-J., Reichert, Ch., 2015. Reconstruction of the southwestern African continental margin by backward modeling. Marine and Petroleum Geology, 67, DOI: 10.1016/j.marpetgeo.2015.06.006.

Drinkwater, M.R., Floberghagen, R., Haagmans, R., Muzi, D., Popescu, A., 2003. GOCE: ESA’s first Earth Explorer Core mission. In Beutler, G., Drinkwater, M.R., Rummel, R., von Steiger, R. (eds.), Earth Gravity Field from Space – From Sensors toEarth Sciences, Space Sciences Series of ISSI, vol. 17. Kluwer Academic Publishers,Dordrecht, The Netherlands, S. 419–432, ISBN: 1-4020-1408-2.

Ebbing J., Bouman J., Fuchs M., Lieb V., Haagmans R., Meekes J.A.C., Fattah R.A., 2013. Advancements in satellite gravity gradient data for crustal studies. Leading Edge, 32 (8), pp. 900-906.

Ebbing, J., Lundin, E., Olesen, O., Hansen, E.K., 2006. The mid-Norwegian margin: A discussion of crustal lineaments, mafic intrusions, and remnants of the Caledonian root by 3D density modelling and structural interpretation. Journal of the Geological Society, 163, 47-60.

Eldholm, O., Gladczenko, T.P, Skogseid, J., Planke, S., 2000. Atlantic volcanic margins: a comparative study. In: Nøttvedt, A., Larsen, B.T., Olaussen, S., Tørudbakken, B., Skogseid, J., Gabrielsen, R.H., Brekke, H.,Ø. Birkeland (eds.), Dynamics of the Norwegian Margin. Geological Society of London, Special Publication 167, 411-428.

Fairhead, J.D. and Wilson, M. 2005. Plate tectonic processes in the South Atlantic Ocean: do we need deep mantle plumes? In: G.R. Foulger, J.H. Natland, D.C. Presnall, D.L. Anderson (Eds.), Plates, Plumes, and Paradigms, Geological Society of America Special Paper, 388, pp. 537–553.

Fecher T., Pail R., Gruber T., 2013. Global gravity field modeling based on GOCE and complementary gravity data. International Journal of Applied Earth Observation and Geoinformation, doi: 10.1016/j.jag.2013.10.005.

Fecher T., Pail R., Gruber T. 2016. GOCO05c - A new combined gravity field model based on full normal equations and regionally varying weighting. Surveys in Geophysics, in review.

Fecher T., Pail R., Gruber Th., Holmes S., 2015. Validation of South American Terrestrial Gravity Anomalies by GOCE. Geophysical Research Abstracts, 17, EGU2015-4859-1 European Geosciences Union General Assembly 2015, Vienna, 14.04.2015.

Flament, N., Gurnis, M. and Müller, R.D., 2013. A review of observations and models of dynamic topography, Lithosphere, vol. 5, no. 2, pp. 189-210. doi: 10.1130/L245.1

Förste, C., Bruinsma, S. L., Abrikosov, O., Lemoine, J.-M., Marty, J. C., Flechtner, F., Balmino, G., Barthelmes, F., Biancale, R., 2014. EIGEN-6C4 The latest combined global gravity field model including GOCE data up to degree and order 2190 of GFZ Potsdam and GRGS Toulouse. GFZ Data Services. http://dx.doi.org/10.5880/icgem.2015.1

Franke, D., Neben, S., Schreckenberger, B., Schulze, A., Stiller, M., and Krawczyk, C.M., 2006. Crustal structure across the Colorado Basin, offshore Argentina. Geophys. J.Int., 165, 850 – 864.

Franke, D., Ladage, S., Schnabel, M., Schreckenberger, B., Reichert, C., Hinz, K.,Paterlini, M., de Abelleyra, J., Siciliano, M., 2010. Birth of a volcanic margin off Argentina, South Atlantic. Geochemistry, Geophysics, Geosystems 11,Q0AB04.

Frisch, W. und Meschede, M., 2005. Plattentektonik. Kontinentverschiebung und Gebirgsbildung. Primus Verlag GmbH, 208 Seiten. ISBN-10: 3896785257.

Gatti, A., Reguzzoni, M., 2015. Comparison of the space-wise grids with other GOCE solutions. Geophysical Research Abstracts, Vol. 17, EGU2015-11112, EGU General Assembly 2015.

Geoffroy, L.C.R., 2005. Volcanic passive margins. Geoscience 337, 1395 –1408. doi:10.1016/j.crte.2005.10.006.

Gernigon, L., Lucazeau, F., Brigaud, F., Ringenbach, J.-C., Planke, S., Le Gall, B., 2006. A moderate melting model for the Vøring margin (Norway) based on structural observations and a thermo-kinematical modelling: Implication for the meaning of the lower crustal bodies. Tectonophysics 412 (3-4), 255-278.

Götze, H.-J., 2015. Potential Methods and Geoinformation Systems. In: Freeden, W., Nashed, M.Z., Sonar, T. (Eds.): Handbook of Geo-Mathematics. Berlin, Heidelberg, Springer Verlag, S. 1-21. - ISBN 978-3-642-27793-1, (doi>10.1007/978-3-642-27793-1_52-2)

Grombein, T.; Seitz, K.; Heck, B. 2015. RWI_TOPO_2015: An update of the Rock-Water-Ice topographic gravity field model of the Earth, available from http://www.gik.kit.edu/rwi_model.php

Gutknecht, B.D., Götze, H.-J., Jahr, T., Jentzsch, G., Mahatsente, R., Zeumann, S., 2014. Surveys of Geophysics, 35, 1417–1440. DOI 10.1007/s10712-014-9296-9.

Gutknecht, B.D., Köther, N., Mahatsente, R., Götze, H.J., 2011. Utilisation of Gravity Gradients and Invariants for 3D Density Modelling. Proc. General Assembly of the International Union of Geodesy and Geophysics (IUGG), Melbourne, Australia.

Hackney, R. I. and Featherstone, W. E., 2003. Geodetic versus geophysical perspectives of the 'gravity anomaly'. Geophysical Journal International 154 (1), 35-43. doi: 10.1046/j.1365-246X.2003.01941.x

Heit, B., Sodoudi, f., Yuan, X., Bianchi, M., Kind, R., 2007. An S- Receiver Function Analysis of the Lithospheric Structure in South America, Geophyical. Resarch Letters, 34, L14307, doi:10.1029/2007GL030317.

Hess, H. H., 1962. History of Ocean Basins. In A. E. J. Engel, Harold L. James, and B. F. Leonard. Petrologic studies: a volume in honor of A. F. Buddington. Boulder, CO: Geological Society of America. pp. 599–620.

Hinz, K., Neben, S., Schreckenberger, B., Roeser, H.A., Block, M., Goncalves de Souza, K., Meyer, H., 1999. The Argentine continental margin north of 48°S: sedimentary successions, volcanic activity during break-up. Mar. & Petrol. Geol.,16, 1 - 25.

Hinze, W.J., Aiken, C., Brozena, J., Coakley, B., Dater, D., Flanagan, G., Forsberg, R., Hildenbrand, T., Keller, G.R., Kellogg, J., Kucks, R., Li, X., Mainville, A., Morin, R., Pilkington, M., Plouff, D., Ravat, D., Roman, D., Urrutia-Fucugauchi, J., Véronneau, M., Webring, M., Winester, D., 2006. New standards for reducing gravity observations: The Revised North American Gravity Database: http://paces.geo.utep.edu/research/gravmag/PDF/Final%20NAGDB%20Report%20091403.pdf

Hirsch, K.K., Bauer, K., Scheck-Wenderoth, M., 2009. Deep structure of the western South African passive margin e results of a combined approach of seismic, gravity and isostatic investigations. Tectonophysics 470, 57 - 70. http://dx.doi.org/10.1016/j.tecto.2008.04.028.

Holzrichter, N., 2013. Processing and interpretation of satellite and ground based gravity data at different lithospheric scales. Dissertation, 126 pages. Christian-Albrechts-Universität zu Kiel. Fakultät für Mathematik und Naturwissenschaften.

Hopper, J.R., Funck, T., Tucholke, B.E., Larsen, H.C., Holbrook, W.S., Louden, K.E., Shillington, D., Lau, H., 2004. Geological Society of America. Geology, 32, (1), 93 - 96. DOI 10.1130/G19694.1.

Hosse, M., Pail, R., Horwath, M., Holzrichter, N., Gutknecht, B.D., 2014. Combined Regional Gravity Model of the Andean Convergent Subduction Zone and Its Application to Crustal Density Modelling in Active Plate Margins. Surveys in Geophysics, 35, (6), 1393-1415.

Isacks, B., Oliver, J.,Sykes, L. R., 1968. Seismology and the New Global Tectonics. Journal of Geophysical Research, 73, (18), 5855.

IUGG, 2015. Resolutions adpoted by the IUGG Council at the XXVI General Assembly, Prague, Czech Republic, 22 June – 2 July 2015; http://www.iugg.org/resolutions/IUGGResolutions2015.pdf

Kalberg, T., 2016. Interpretation tektonomagmatischer Prozesse basierend auf 3D Potentialfeldmodellierungsergebnissen. Dissertation 185 pages. Fachbereich für Geowissenschaften, Universität Bremen.

Klinge, L., 2016. Gravitational potential energy (GPE) und Stress im südlichen Atlantik (in German). Master Arbeit, 89 pages. Institut für Geowissenschaften, Mathematisch-naturwissenschaftliche Fakultät der Christian-Albrechts-Universität Kiel.

Köther, N., Götze, H.-J., Gutknecht, B.G., Jahr, T., Jentzsch, G., Lücke, O.H., Mahatsentea, R., Sharma, R., Zeumann, S., 2012. The seismically active Andean and Central American margins: Can satellite gravity map lithospheric structures? Journal of Geodynamics, 59– 60, 207– 218.

LaFehr, T.R., 1991. An exact solution for the gravity curvature (Bullard B) correction: Geophysics, 56, (8), 1179–1184, doi: 10.1190/1.1443138.

Lallemand S., 2014. Active continental margin. In Encyclopedia of Marine Geosciences, Springer Science, Eds.: Harff, J., Meschede, M., Petersen, S. and Thiede, J., 7 pages, DOI 10.1007/978-94-007-6644-0_102-2.

Li, X. and Götze, H.-J., 2001. Ellipsoid, Geoid, Gravity, Geodesy, and Geophysics - A Tutorial. Geophysics, vol. 66, no. 6, 1660-1668.

Maus, S., Barckhausen, U., Berkenbosch, H., Bournas, N., Brozena, J., Childers, V., Dostaler, F., Fairhead, J.D., Finn, C., von Frese, R. R. B., Gaina, C., Golynsky, S., Kucks, R., Lühr, H., Milligan, P., Mogren, S., Müller, R.D., Olesen, O., Pilkington, M., Saltus, R., Schreckenberger, B., Thébault, E. and Caratori Tontini, F., 2009. EMAG2: A 2-arc min resolution Earth Magnetic Anomaly Grid compiled from satellite, airborne, and marine magnetic measurements. Geochemistry, Geophysics, Geosystems, vol. 10, no. 8. doi: 10.1029/2009GC002471.

Mayer-Gürr, T., Zehentner, N., Klinger, B., Kvas, A., 2014. ITSG-Grace2014: a new GRACE gravity field release computed in Graz. Presented at GRACE Science Team Meeting (GSTM), Potsdam, 29.09.2014.

Maystrenko, Y.P., Scheck-Wenderoth, M., Hartwig, A., Anka, Z., Watts, A.B., Hirsch, K.K, Fishwick, S. 2013. Salt as a 3D element in structural modeling – Example from the Central European Basin System. Tectonophysics, doi:10.1016/j.tecto.2012.06.030

Mikuška, J., Pašteka, R., Marušiak, I., 2006. Estimation of distant relief effect in gravimetry. GEOPHYSICS, 71, (6), J59–J69, doi: 10.1190/1.2338333.

Mohriak, W., 2014. Birth and development of continental margin basins: analogies from the South Atlantic, North Atlantic and the Red Sea. Search and Discovery article, http://www.searchanddiscovery.com/pdfz/documents /2014/41502mohriak/ndx_mohriak.pdf.html

Müller, R. D., Sdrolias, M., Gaina, C. and Roest, W.R., 2008. Age, spreading rates, and spreading asymmetry of the world's ocean crust. Geochemistry, Geophysics, Geosystems, vol. 9, no. 4., 19 pages, doi: 10.1029/2007GC001743.

Naudy, H. and Neumann R., 1965. Sur la définition de l'anomalie de Bouguer et ses

conséquences pratiques, Geophys. Prosp., vol 13, 1-11O'Connor, J.M., Jokat, W., le Roex, A.P., Class,C., Wijbrans,J.R., Keßling, S., Kuiper, K.F. and Nebel, O., 2012. Hotspot trails in the South Atlantic controlled by plume and plate tectonic processes. Nature Geoscience 5, pp. 735–738, doi:10.1038/ngeo1583.

Oliver, J., Isacks, B., 1967. Deep earthquake zones, anomalous structures in the upper mantle, and the lithosphere. Journal of Geophysical Research, 72 (16), pp. 4259-4275.

Oncken, O., Chong, G., Franz, G., Giese, P., Götze, H.-J., Ramos, V., Strecker, M. and Wigger, P., (Eds), 2006: The Andes - Active Subduction Orogeny., Frontiers in Earth Sciences, 1, Springer Verlag, pp. 570.

Pail R., Fecher T., Rexer M. 2015b. Validation of GOCE gravity gradient grids for geophysical applications. Geophysical Research Abstracts, Vol. 17, EGU2015-1652, Poster presented at EGU General Assembly 2015, Vienna.

Pail, R., Bingham, R., Braitenberg, C., Dobslaw, H., Eicker, A., Güntner, A., Horwath, M., Ivins, E., Longuevergne, L., Panet, I., Wouters, B. 2015a. Science and User Needs for Observing Global Mass Transport to Understand Global Change and to Benefit Society. Surveys in Geophysics, 36(6): 743-772, Springer Netherlands, doi: 10.1007/s10712-015-9348-9.

Pail, R., Goiginger, H., Schuh, W.-D., Höck, E., Brockmann, J. M., Fecher, T., Gruber, T., Mayer-Gürr, T., Kusche, J., Jäggi, A., Rieser, D. 2010. Combined satellite gravity field model GOCO01S derived from GOCE and GRACE. Geophysical Research Letters, Vol. 37, L20314, doi:10.1029/2010GL044906.

Pail, R., S. Bruinsma, F. Migliaccio, C. Förste, H. Goiginger, W.-D. Schuh, E. Höck, M. Reguzzoni, J. M. Brockmann, O. Abrikosov, M. Veicherts, T. Fecher, R. Mayrhofer, I. Krasbutter, F. Sansò, and C. C. Tscherning 2011. First GOCE gravity field models derived by three different approaches, Journal of Geodesy, 85(11), 819-843, doi: 10.1007/s00190-011-0467-x.

Panet I., G. Pajot-Métivier, M. Greff-Lefftz, L. Métivier, M. Diament & M. Mandea 2014. Mapping the mass distribution of Earth's mantle using satellite-derived gravity gradients, Nature Geoscience 7, 131–135, doi:10.1038/ngeo2063.

Pavlis, N.K., Holmes, S.A., Kenyon, S.C., Factor, J.K., 2008. An Earth Gravitational Model to Degree 2160: EGM2008. In: Proceedings of the European Geosciences Union General Assembly, April 13–18, Vienna, Austria.

Pavlis, N.K., Holmes, S.A., Kenyon, S.C., Factor, J.K., 2012. The development and evaluation of the Earth Gravitational Model 2008 (EGM2008). Journal of Geophysical Research, 117, (B4), 2156 - 2202, doi: 10.1029/2011JB008916.

Prange, L., 2011. Global Gravity Field Determination Using the GPS Measurements Made Onboard the Low Earth Orbiting Satellite CHAMP. PhD Thesis, Geodätisch-geophysikalische Arbeiten in der Schweiz, vol. 81. http://www.sgc.ethz.ch/sgc-volumes/sgk-81.pdf

Reigber, C., Balmino, G., Schwintzer, P., Biancale, R., Bode, A., Lemoine, J.-M., Koenig, R., Loyer, S., Neumayer, H., Marty, J.C., Barthelmes, F., Perossanz, F., 2002. A high quality global gravity field model from CHAMP GPS tracking data and accelerometry (EIGEN-1S). Geophysical Research Letters, 29, 14, dx.doi.org/10.1029/2002GL015064

Reston, T.J., 2009. The structure, evolution and symmetry of the magma-poor rifted margins of the North and Central Atlantic: A synthesis. Tectonophysics 468, 6–27. doi:10.1016/j.tecto.2008.09.002.

Rudenko S., Dettmering D., Esselborn S., Schoene T., Foerste C., Lemoine J-M, Ablain M, Alexandre D, Neumayer K.-H., 2014. Influence of time variable geopotential models on precise orbits of altimetry satellites, global and regional mean sea level trends. Advances in Space Research, doi: 10.1016/j.asr.2014.03.010.

Salomon, A., Koehn, D., Passchier, C., Hackspacher, P.C. and Glasmacher, U.A., 2014. Contrasting stress fields on correlating margins of the South Atlantic, Gondwana Research, doi.org/10.1016/j.gr.2014.09.006.

Schaller. T., Andersen, J., Götze, H.-J., Koproch, N., Schmidt, S., Sobiesiak, M., Splettstößer,S., 2015. Segmentation of the Andean margin by isostatic models and gradients. Journal of South American Earth Sciences, 59, 69-85.

Scheck-Wenderoth, M., Maystrenko, Y., 2008. How warm are passive continental margins? A 3D lithosphere-scale study from the Norwegian margin. Geology, 36, (5), 419-422, DOI: 10.1130/G24545A.1.

Skogseid, J., Planke, S., Faleide, J.I., Pedersen, T., Eldholm, O., Neverdal, F., 2000. NE Atlantic continental rifting and volcanic margin formation, in Nottvedt, A.e.a., Ed., Dynamics of the Norwegian Margin, 167: London, Geological Society of London, Special Publications, p. 55–82.

Sobiesiak, M., Meyer U., Schmidt S., Götze H.-J., Krawczyk C.M., 2007. Asperity generating upper crustal sources revealed by b value and isostatic residual anomaly grids in the area of Antofagasta, Chile. Journal of Geophysical Research, v. 112, B12308, doi: 10.1029/2006JB004796.

Stadler, G., Gurnis,M., Burstedde, C., Wilcox, L.C., Alisic, L., Ghattas, O., 2010. The Dynamics of Plate Tectonics and Mantle Flow: From Local to Global Scales. Science, Vol. 329, Issue 5995, pp. 1033-1038, DOI: 10.1126/science.1191223.

Szwillus, W., Ebbing, J. and Holzrichter, N., 2016. Importance of far-field topographic and isostatic corrections for regional density modelling. Geo- physical Journal International, 207 (1), pp. 274-287, doi:10.1093/gji/ggw270

Szwillus, W., Götze, H.-J., 2016. Efficient mass correction using an adaptive method. In: R, Pasteka et al., Proceedings of the workshop on Bouguer Anomaly, Bratislava (Slowak Republic). Accepted.

Tapley, B.D., Bettadpur, S., Watkins, M., Reigber, C., 2004. The gravity recovery and climate experiment: mission overview and early results. Geophysical Research Letters, 31(9), L09607, AmericanGeophysical Union, http://dx.doi.org/10.1029/2004GL019920.

Tašárová, Z., 2007. Towards understanding the lithospheric structure of the southern Chilean subduction zone (36° S – 42° S) and its role in the gravity field. Geophysical Journal International, 170, (3), 995–1014. doi:10.1111/j.1365-246X.2007.03466.x

Torge W., 2001. Geodesy, 3rd edition, 416 pages. De Gruyter Berlin, ISBN 3-11-017072-8.

Torsvik, T. H., Rousse, S., Labails, C. and Smethurst, M.A., 2009. A new scheme for the opening of the South Atlantic Ocean and the dissection of an Aptian salt basin. Geophysical Journal International, 177, 3, pp. 1315-1333. doi: 10.1111/j.1365-246X.2009.04137.x.

Vine, F. J.; Matthews, D. H., 1963. Magnetic Anomalies Over Oceanic Ridges. Nature 199 (4897), 947–949.

Wadati, K., 1929. Shallow and deep earthquakes (2nd paper): Geophysical Magazine, 2, 1–36.

Wefer,G., Billet, D., Hebbeln, D., Barker Jorgensen, B., Schlüter, M., van Weering, T.C.E., 2003. Eds. Ocean Margin Systems. Springer, pp. 495. Doi.10.007/978/-3-662-05127-6

Wegener, A., 1920. Die Entstehung der Kontinente und Ozeane. In: E. Wiedemann (Herausgeber), Die Wissenschaft, Friedrich Vieweg und Sohn, Braunschweig, 2. Auflage, 66, 1-135.

Wenzel H., 1985: Hochauflösende Kugelfunktionsmodelle für das Gravitationspotential der Erde: Wissenschaftliche Arbeiten der Fachrichtung Vermessungswesen der Universität Hannover, 137, 1–155.White, R. S., Smith,L.K., 2009. Crustal structure of the Hatton and the conjugate east Greenland rifted volcanic continental margins, NE Atlantic. Journal of Geophysical Research, 114. B02305. DOI 10.1029/2008JB005856

Cover Letter

CHRISTIAN-ALBRECHTS-UNIVERSITÄT ZU KIEL

INSTITUT FÜR GEOWISSENSCHAFTEN

Prof. Dr. H.-J. Götze

Abteilung Geophysik, Otto-Hahn-Platz 1, 24118 Kiel

Datum:March 24, 2017

Telefon: +49 (0)431 880-3805

FAX: +49 (0)431 880-1387

E-mail: hajo@geophysik.uni-kiel.de

http://www.gravity.uni-kiel.de

-

Ladies and Gentlemen,

This an invited manuscript by me and Roland Pail for the “Passive margin” issue.

Please, start with the review process.

Regards,

H.-J. Götze